The morphol

ana (R. pipiens

h the electron m

ermatogonia can b

ses of 20 to 25

ds that mitochon

ally there appea

ermatogonia of th

ermatogonia descr

the type A and B

ilar in both spe

phase of the firs

uld be positively

The early p

species. Howe

ation for acros

ABSTRACT

AN ULTRASTRUCTURAL STUDY
OF SPERMATOGENESIS IN
TWO SPECIES OF *RANA*

By

Gary Raymond Poirier

The morphology of spermatogenesis in two species of *Rana* (*R. pipiens* and *R. clamitans*) has been investigated with the electron microscope. Three distinct types of spermatogonia can be distinguished, one of which reaches sizes of 20 to 25 μm in diameter. It is in these large cells that mitochondrial multiplication occurs. Structurally there appears to be no difference between the spermatogonia of the two species. Certain of the spermatogonia described here have characteristics similar to the type A and B spermatogonia of mammals. Meiosis, similar in both species studied, is described through prophase of the first division. No secondary spermatocytes could be positively identified.

The early phases of spermiogenesis are similar in both species. However, each species has a different mechanism for acrosome formation. In *R. clamitans*, the

mucosa is form

derived from

piens, acro

mplet are fully

like eleme

formation.

Structura

different. The a

consist of homoge

the anterior port

piens sperma

portion of the mu

portion of the la

consist of a large

ndor vesicles of

The mid-pi

ype' type. The m

dividual organel

. claviformis spe

ristae, whereas i

ose mitochondria

s thought to be a

t present in both

ntinuous with the

e simple 9 + 2 ax

acrosome is formed by the fusion of vesicles thought to be derived from a Golgi-like cisternal apparatus. In R. pipiens, acrosomal formation occurs at the time when nuclei are fully elongated and condensed; no Golgi or Golgi-like elements appear to be associated with its formation.

Structurally the two acrosomes are completely different. The acrosomes of R. clamitans spermatozoa consist of homogeneous bag-like structures overlapping the anterior portion of the nuclei. The acrosomes of R. pipiens spermatozoa are situated at the most anterior portion of the nuclei, with no overlap at the anterior portion of the latter. The acrosomes of this species consist of a large PAS-positive granule, membrane stacks and/or vesicles of various sizes and densities.

The mid-pieces of both species are of the "primitive" type. The mitochondria are not fused but remain as individual organelles. The mitochondria in the mid-pieces of R. clamitans spermatozoa have many well developed cristae, whereas in R. pipiens the cristae in the mid-piece mitochondria are poorly developed and scarce. This is thought to be a true species variation. Two centrioles are present in both species, with the distal one being continuous with the axial filament. The tail consists of the simple 9 + 2 axial filament arrangement throughout its

ature length. R.

primitive type of c

as observed in R.

Various typ

ll packets of glyc

scribed in the sp

species.

The develop

ature Sertoli cell

ersist a common d

on this developm

Non-specif

located in the acr

Spermatozoa. Alka

ad-pieces and axi

nalizations of a

rried out for R.

entire length. R. clamitans spermatozoa also contain a primitive type of connecting piece. No similar structure was observed in R. pipiens spermatozoa.

Various types of intranuclear inclusions, including packets of glycogen and mitochondria-like bodies, are described in the spermatids and spermatozoa of both species.

The development of the follicle cell into the mature Sertoli cell is similar enough in both species to warrant a common description. Microtubules are associated with this development.

Non-specific acid and alkaline phosphatases are located in the acrosomal membranes of R. clamitans spermatozoa. Alkaline phosphatase is also found in the mid-pieces and axial filaments of R. clamitans spermatozoa. Localizations of alkaline and acid phosphatases were not carried out for R. pipiens spermatozoa.

AN ULTRASTRUCTURAL STUDY OF SPERMATOGENESIS IN TWO SPECIES OF *RANA*

By

Gary Raymond Poirier

A THESIS

Submitted to
Michigan State University
in partial fulfillment of the requirements
for the degree of

DOCTOR OF PHILOSOPHY

Department of Zoology

1970

I wish to
ggestions, patie
f this study. Hi
'p to bat" for me
ssful and enjoy
I am also
nselfish attitud
bilities availa
My thanks
ggestions on va
erving on my gra
s. Carola Wilso
s. Carola Wilso
discuss proble
r the line draw
A special
ose help in a m
I would a
s. Ralph A. Pol
aking the course

ACKNOWLEDGMENTS

I wish to thank Dr. John R. Shaver for his suggestions, patience and understanding during the course of this study. His confidence in me and willingness to "go to bat" for me has made my graduate studies both fruitful and enjoyable.

I am also grateful to Dr. Gordon Spink for his unselfish attitude in making his experience and laboratory facilities available for this study.

My thanks to Drs. N. Band and H. Ozaki for their suggestions on various portions of this work and for serving on my graduate committee; to Mrs. June Mack and Mrs. Carola Wilson for just being Mrs. June Mack and Mrs. Carola Wilson; to Robert Glick for being available to discuss problems as they arose and to Mrs. S. J. Rose for the line drawings.

A special word of thanks goes to "Mac" who and whose help in a multitude of ways will always be remembered.

I would also like to thank my parents, Mr. and Mrs. Ralph A. Poirer for their encouragement and aid during the course of my schooling.

Lastly, I w

gratitude and ap

ducation during t

Lastly, I would like to express to my wife, Judy, my gratitude and appreciation for her self-sacrifice and dedication during the years in graduate school.

TABLE OF CONTENTS

Type

1. Spermatogoni
2. Type 1 prima
3. Portions of
4. Type 2 prim
5. Portions of
6. Type 2 prim
7. Secondary s
8. Primary spe
9. Primary sp
R. Clari
10. Cytoplasm
R. clari
11. Primary sp
12. Cytoplasm
R. Clari
13. Primary sp
14. Primary s
R. Clar
14c. Cytoplasm
Pachyte
15. Primary s
16. Early spe
17. Early spe

LIST OF FIGURES

History

The first
1678 by Huygens
composed of a g
med of a transp
ry brisk and the
here their limbs
his discovery se
ployment to thos
mals." Howeve
ount is nothin
ld to him by Le
as Johan Ham (C
Spermatozoa hims
1677 that sem
malcules poss

The func
en debated for
ccepted as the
ne they were s

INTRODUCTION

History

The first description of spermatozoa was published in 1678 by Huygens (see Cole, 1930). He stated that semen is composed of a great quantity of animals. "They are formed of a transparent substance, their movements are very brisk and their shape is similar to that of frogs before their limbs are formed." He also mentions that "this discovery seems very important and should give employment to those interested in the generation of animals." However according to Cole, Huygen's published account is nothing more than a verification of a discovery told to him by Leeuwenhoek the previous year. Actually it was Johan Ham (Cole, 1930), who published nothing on spermatozoa himself, who brought the news to Leeuwenhoek in 1677 that semen contain animalcules and that these animalcules possess tails.

The functionality of the animalcules was discussed and debated for two centuries before they were finally accepted as the fertilizing agents in semen. During that time they were said to be found in many of the body

ammons. They

al and anal aper

ale men, little

ppropriate specie

me inanimate (se

parasites and w

e famille des Cer

e la classe des M

ppeared only in t

ers from other Ce

The criti

ther paper and

f both the filt

as performed by

1957) Spallanza

information, wa

ublished views

f C. Hertwig a

f the sperm an

nerally acce

ness in ferti

Mayr, 1967).

The f

roducts of t

d ovaries in

he first to

secretions. They were described as having intestines with oral and anal apertures and the more imaginative described little men, little horses, etc. in the animalcules of the appropriate species (see Cole, 1930). Linnaeus considered them inanimate (see Tyler, 1967). They also were described as parasites and were classified by Bory as "un genre de la famille des Cercarieés, dans l'ordre des Gymnodes et de la classe des Microscopiques." The fact that they appeared only in the semen of male animals distinguished them from other Cercariae (Cole, 1930).

The critical experiment, filtering semen through filter paper and testing separately the fertilizing powers of both the filtrate and material filtered (spermatozoa), was performed by Spallanzani in 1786. According to Tyler (1967) Spallanzani, a champion of the ovist theory of preformation, was not willing to change his earlier published views. It was not until 1875-1889 that the work of O. Hertwig and Fol showed actual penetration and union of the sperm and egg nuclei. After this time it was generally accepted that the sperm initiates and participates in fertilization and development of the egg (see Tyler, 1967).

The first clear report that spermatozoa were products of the male genital gland was made by Prevost and Dumas in 1824 (see Cole, 1930). Kolliker in 1841 was the first to actually trace the histogenesis of sperm from

lls of the teste
t. George in 1876
lowed each spe
ne Flemming, 18
ho introduced t
ondary sperma
n 1877 who firs
877).

No clea
e arrived at w
ni meiosis.
resent unders
an Beneden.
fertilizatio
f the offsp
ucleï of th
1878). Wei
discovery a
early 1890
plete pro
Wilson, 1
1881) des
n mitosi
described
see fi
n chro

cells of the testes (see Cole, 1930). La Valette St. George in 1876 introduced the term spermatocyte but believed each spermatocyte formed but one spermatozoön (see Flemming, 1880). According to Kingsbury (1902) he also introduced the terms spermatogonia, primary and secondary spermatocytes, and spermatid. It was von Baer in 1827 who first used the term spermatozoa (see Cole, 1930).

No clear understanding of spermatogenesis could be arrived at without the knowledge of Mendelian genetics and meiosis. One of the major discoveries leading to our present understanding of spermatogenesis was made by van Beneden. He demonstrated in 1887, while studying the fertilization processes in Ascaris, "that the chromosomes of the offsprings are derived in equal numbers from the nuclei of the two conjugating germ cells" (see Wilson, 1925). Weissman realized the importance of van Beneden's discovery and in a series of essays in the late 1880's and early 1890's made the first fruitful attempt to analyze gamete production in terms of reductional division (see Wilson, 1925). About the same time, Flemming (see Rugh, 1951) described longitudinal splitting of the chromosomes in mitosis. It was also Flemming, in 1879, who first described indirect cell division in testicular tubules (see Flemming, 1880) of vertebrates, although no reference to chromosomal reduction was made. In 1902, Sutton, while

ndying the chrom

ived that "the s

ning division re

omosomes which

nigration to diff

miliar with the

e formulated the

ple in heredity.

As far as

ns are concerned,

euwenhoek in 167

n the Seed of Fr

see van Oordt, 1

an organs and re

n the latter por

f the 20th, amph

d choice for st

ss and Flemming

ther investigat

tudy of spermat

Mlowitz, Meves

Wilson, 1925).

rely little ha

thesis in recen

blished on spe

Oscar, 1955) a

studying the chromosomes in the gametes of Brachystola showed that "the second postsynaptic division is a reducing division resulting in the separation of the chromosomes which have conjugated in synapis and their relegation to different cells." In 1903, after becoming familiar with the newly rediscovered Mendelian principles he formulated the connection between gametogenesis and its role in heredity.

As far as amphibian spermatozoa and spermatogenesis are concerned, the first published report was by Leeuwenhoek in 1678 (see Cole, 1930) entitled "The Animals in the Seed of Frogs." Jan Swanmerdam about the same time (see van Oordt, 1960) gave an accurate description of the sex organs and reproductive cycle of anuran amphibians. In the latter portion of the 19th century and first part of the 20th, amphibian material seemed to be the material of choice for studying cytogenetics. Champy, 1913; King, 1907 and Flemming, 1880 all worked on this material. Other investigators who used amphibian material for the study of spermatogenesis included Retius, Broman, Ballowitz, Meves, and Nussbaum (see Champy, 1913 and Wilson, 1925). Considering this earlier activity, relatively little has been done on anuran amphibian spermatogenesis in recent years. Nath and his students have published on spermatogenesis in Rana tigrina (Sharma and Sekhri, 1955) and Bufo stomaticus (Sharma and Dhindsa,

[illegible] Glass and
[illegible] (1957) have
[illegible]spermatogenesis in

At the ele
[illegible]mbian spermato
[illegible]spermatogenesis has
[illegible]ps and Fawcett
[illegible]1967) has publ
[illegible] and electron
[illegible] salamanders. S
[illegible] arenarum by
[illegible] temporaria by
[illegible]ultrastructure of
[illegible] Aoki et al.,
[illegible]chondrial de
[illegible]pecies of Rana

[illegible]hematogenetic

The pa
[illegible]ua in verteb
[illegible]ups; cystic
[illegible]. Fish a
[illegible]ptiles, bird

The f
[illegible]lled sperma
[illegible]mary sperma

1955). Glass and Rugh (1943), Rugh (1951) and Burgos and Ladman (1957) have published fragmentary reports on spermatogenesis in R. pipiens.

At the electron microscopic level observations of amphibian spermatogenesis are even scantier. Late spermiogenesis has been described in Bufo arenarum by Burgos and Fawcett (1956). Baker (1962, 1963, 1965, 1966 and 1967) has published a series of papers both at the light and electron microscopic levels on spermiogenesis in salamanders. Sertoli cells have been described in Bufo arenarum by Burgos and Vitale-Calpe (1967) and in R. temporaria by Brökelmann (1964). Two reports on the ultrastructure of interstitial cells (Brökelmann, 1964 and Aoki et al., 1969) and a single report on the inter-mitochondrial dense material in the spermatocytes of three species of Rana (Clerot, 1968) complete the list.

Spermatogenetic Cycle

The patterns followed in the formation of spermatozoa in vertebrates can be divided into two distinct groups; cystic and non-cystic spermatogenesis (Lofts, 1968). Fish and amphibians have the cystic type, while reptiles, birds and mammals exhibit the non-cystic pattern.

The first portion of any spermatogenetic cycle is called spermatocytogenesis. In amphibian testes each primary spermatogonium is surrounded by follicle or cyst

ells (Champy, 191
primary spermatogo
ry primary sperma
ondary spermato
main surrounded
me to divide.
Kushi (see Lofts
a eight division
ll. If the daug
parate and becom
ay remain primar
rangement insure
as been compared
ll cycle found i

The multip
condary sperma
nsformation of
ermatocytes.
hich occurs the
ding, first, se
econdary sperma
ot in mammals
ng, 1907; Shar
1951 and Rugh,
a process call

cells (Champy, 1913; Rugh, 1951 and van Oordt, 1960). The primary spermatogonia divide mitotically to form either new primary spermatogonia or secondary spermatogonia. If secondary spermatogonia are formed, the daughter cells will remain surrounded by the same follicle cells and will continue to divide. This is called the multiplication period. Witschi (see Lofts, 1968) found in R. temporaria as many as eight division stages during spermatogonial multiplication. If the daughter cells of the primary spermatogonium separate and become enclosed in separate follicle cells, they remain primary spermatogonia (van Oordt, 1960). This arrangement insures a continuous stem cell population and has been compared to the type A and B spermatogonial stem cell cycle found in mammals (Lofts, 1968).

The multiplication period produces a cluster of secondary spermatogonia. This period is followed by the transformation of the secondary spermatogonia into primary spermatocytes. This is followed by the growth period, in which occurs the first meiotic prophase. Meiosis follows, giving, first, secondary spermatocytes, then spermatids. Secondary spermatocytes have a short interphase period both in mammals (Gardner and Holyoke, 1964) and amphibians (King, 1907; Sharma and Sekhri, 1955; Sharma and Dhindsa, 1955; and Rugh, 1951). The spermatids then differentiate by a process called spermiogenesis (Bloom and Fawcett,

...ll., spermatohis...

...permatelecsis (Ba...

At the he...

...phibians, the te...

...ells in different ...

...over all the ce...

...n, although exce...

Amphibian ...

...e continuous or ...

...ous type, sper...

...ond of the yea...

...ughout the ye...

...temperature (...

...temperate cli...

...perature have ...

...s. Those in t...

...inuous type.

R. pipie...

...p., 1943 and ...

...ming this po...

...owever, from t...

...inuous spe...

The sp...

...piens (G...

...ed for othe...

...ual cycles,...

1968), spermatohistogenesis (van Oordt, 1960) or spermateleosis (Baker, 1966) into mature spermatozoa.

At the height of the spermatogenetic cycle of amphibians, the testes are filled with cysts of germinal cells in different stages of development. Within each cluster all the cells are at the same stage of development, although exceptions do exist (Champy, 1913).

Amphibian spermatogenesis can be further divided into continuous or discontinuous types. In the discontinuous type, spermatogenesis is confined to a certain period of the year while in the continuous type it occurs throughout the year. The basic reason for this difference is temperature (van Oordt, 1960). Generally, amphibians in temperate climates with large seasonal variations in temperature have the discontinuous type of spermatogenesis. Those in the tropical or sub-tropical possess the continuous type.

R. pipiens is of the discontinuous type (Glass and Rugh, 1943 and Rugh, 1951). No data on R. clamitans concerning this point were available in the literature; however, from this study, they also appear to have discontinuous spermatogenesis.

The spermatogenetic cycle has been described for R. pipiens (Glass and Rugh, 1943). It is similar to that seen for other amphibians with discontinuous spermatogenetic cycles, e.g. R. temporaria (Brökelmann, 1964) and

esculenta, livi

ivan Dordt, 196

ycle into three m

tive spermatogen

um. The breedin

ust April to Jun

re filled with ma

ma. Only a few

served. The pe

ther spermiation

ring this perio

mber of sperma

mber of sperma

creases until

reeding season

mber of sperm

eak about the

e breeding se

tober. Sper

September and

October. A

s also seen

ermiation i

Sperm they wi

following sp

is similar

R. esculenta, living in the temperate zone (Champy, 1913 and van Oordt, 1960). Glass and Rugh (1943) divided the cycle into three major periods: the breeding season, the active spermatogenetic period and preparation for hibernation. The breeding season for R. pipiens extends from about April to June. At this time the seminiferous tubules are filled with mature spermatozoa and primary spermatogonia. Only a few spermatocytes and spermatids are observed. The period of active spermatogenesis starts after spermiation around June and ends in mid-October. During this period there is a decrease in the relative number of spermatogonia followed by a sharp rise in the number of spermatocytes. The number of spermatocytes increases until about mid-July, then declines to the breeding season level sometime in October. The relative number of spermatids begins to increase about mid-July and peak about the first of September. Then it declines to the breeding season level reaching their low in mid-October. Spermatozoa begin to form around the first of September and increase in number until the first part of November. A rise in the relative number of spermatogonia is also seen during this period. As the animals go into hibernation in early November they contain all the mature sperm they will need for the next breeding season, the following spring. It is assumed that these relationships are similar for R. clamitans spermatogonesis though the

ycle may be a mon

period of this spe

The mating

es of short durat

es of maximum dim

mmal fertiliza

minates the need f

e released at a

n Bordt, 1960;

s well suited fo

In non-cy

rds and mammal

ones throughout

n this type tha

an be determine

he basement me

developing germ

relationship ex

Induction of P

The ult

he fine struct

been investiga

d Fawcett, 1

Accetti et al

Hagmann, 196

cycle may be a month or two later, since the breeding period of this species is not until early summer.

The mating periods of R. pipiens and R. clamitans are of short duration. Just before amplexsus, the testes are of maximum dimensions (Lofts, 1968). The type of external fertilization practiced by these animals necessitates the need for a large quantity of spermatozoa to be released at a specific time of the year. It is thought (van Oordt, 1960) that the cystic type of spermatogenesis is well suited for this type of breeding habit.

In non-cystic testes, characteristic of reptiles, birds and mammals, spermatozoa are produced in successive waves throughout extended periods (Lofts, 1968). It is in this type that the specific stage of spermatogenesis can be determined by the position of the cell relative to the basement membrane and their relationships to other developing germinal cells. In amphibian testes no such relationship exist.

Definition of Problem

The ultrastructural aspects of spermiogenesis and the fine structural features of mature spermatozoa have been investigated in a wide variety of species (Burgos and Fawcett, 1955 and 1956; Longo and Anderson, 1969 A&B; Baccetti et al., 1970; Clark, 1967; Reger, 1963 and 1967; Horstmann, 1961 and Nicander and Bane, 1966. Also see

mews by Dan, 19

Bnett, 1970). A

ere as a guide t

opic.

Relatively

ructural aspects

mmals (see Ni

this topic).

Only three

pects of spermio

d Fawcett (1956,

ther two on the

56 and 1967).

ved. For exam

ws a typical lo

milar to that

ther hand, no c

ytosome forms b

No anal

Spermatocytogen

Sertolian mater

Thus, c

ll the gap in

pects of spe

pecies. The

tudies on the

reviews by Dan, 1967; Hadek, 1969A; Austin, 1968 and Fawcett, 1970). Although this list is incomplete, it will serve as a guide to the comparative literature on this topic.

Relatively little has been done on the ultrastructural aspects of earlier spermatogenesis in any group of animals (see Nicander and Plöem, 1969A for a discussion of this topic).

Only three papers exist on the ultrastructural aspects of spermiogenesis in amphibians; one by Burgos and Fawcett (1956) on the toad Bufo arenarum and the other two on the salamander Amphiuma tridactylum (Baker, 1966 and 1967). Even so, interesting differences can be noted. For example, in the salamander the acrosome forms from a typical looking Golgi-element in a manner somewhat similar to that seen in mammals. In the toad, on the other hand, no conspicuous Golgi element is seen and the acrosome forms by fusion of two or more vesicles.

No analysis of the ultrastructural aspects of spermatocytogenesis or meiosis have been published for amphibian material.

Thus, one of the purposes of this report is to fill the gap in comparative studies on the ultrastructural aspects of spermatogenesis that exists for the amphibian species. The second purpose of this report is to initiate studies on the fine structure of the spermatozoa of some

f these species,

ans for future

rmilization in

ower, 1966 and

To keep t

ews from Pawcet

little that c
microscope es
era of cytolo
with vastly g
command, is f
but rediscove
were clearly
published ha

of these species, in the hope that it will serve as a basis for future experimental work on the mechanism of fertilization in amphibians (see Barch and Shaver, 1963; Shaver, 1966 and Metz, 1968).

To keep things in their proper perspective, a quote from Fawcett (1958) seems appropriate at this point.

> Little that could be resolved with the light microscope escaped detection in that fruitful era of cytology. Even the electron microscopist, with vastly greater resolving power at his command, is frequently humbled to find he has but rediscovered details of fine structure that were clearly depicted in excellent lithographs published half a century ago.

Mature R.

tained from com

e R. clamitans w

e the University

r. Christine Rich

Whole tes

ixed directly in

30%. The fixat

% paraformaldehy

sphate buffer

ut 1 to 2 mm cu

ng. The tissue

to 5 hours at r

ixed three time

ixed in 1% osmi

mperature in s

the R. pipiens

tone, according

After th

0 times in the

MATERIAL AND METHODS

Mature R. pipiens and R. clamitans males were obtained from commercial dealers in Wisconsin. A few of the R. clamitans were obtained from the amphibian facility at the University of Michigan through the courtesy of Dr. Christine Richards.

Whole testes were excised from pithed animals and placed directly into Karnovsky's fixative (Karnovsky, 1965). The fixative contained, in final concentrations, 4% paraformaldehyde and 5% gluteraldehyde in sodium phosphate buffer 0.1M, pH 7.0 to 7.2. The testes were cut into 1 to 2 mm cubes with new razor blades to avoid tearing. The tissue samples were kept in the fixative for 3 to 5 hours at room temperature. The samples were then rinsed three times with the phosphate buffer and post-fixed in 1% osmium tetroxide for 1 hour also at room temperature in sodium phosphate buffer (pH 7.2, 0.1M). Some R. pipiens testes were fixed with osmium tetroxide alone, according to the above post-fixation procedure.

After the fixation period the tissue was washed two times in the phosphate buffer and dehydrated through

graded series of

final concentrati

with EtOH for 10 mi

minutes each an

minutes each.

mixture of pi

then transferr

consisting of

ntained at 60°C u

Thin secti

silver gold, ap

ether glass or

ltramicrotome.

mesh uncoated

ained for 30 mi

concentrate-aque

ad citrate (Rey

The secti

transmission

ctures were ta

ns.

Cytochemical Pro

Glycogen

The deta

Other Proteinas

a graded series of ethyl alcohol. The series of increasing alcohol concentrations included steps at 25, 50, 75, and 95% EtOH for 10 minutes each, two changes of 100% for 15 minutes each and two changes of proplyene oxide for 30 minutes each. The tissue was left overnight in a 50/50 mixture of propylene oxide and Epon 812. The tissue was then transferred to gelatin capsules containing Epon 812 consisting of 7 parts A to 3 part B. The Epon was hardened at 60°C under vacuum for 48 hours.

Thin sections, with an interference color of silver to silver gold, approximately 75 to 90 m μ thick, were cut on either glass or diamond knives on a Porter-Blum MT-2 ultramicrotone. The sections were collected on 150 or 200 mesh uncoated copper ethene grids. The sections were stained for 30 minutes by floating them on uranyl-acetate (concentrate-aqueous) and then for 5 minutes on aqueous lead citrate (Reynolds, 1963).

The sections were observed in a Philips 100B or 300 transmission electron microscope operating at 60KV. Pictures were taken on 35 mm or 70 mm fine grain positive film.

Cytochemical Procedures

Glycogen

The details of the periodic acid-thiosemicarbazide-silver proteinate (PA-TSC-SP) procedure were worked out by

...ary (1967). In
...ed by Anderson a...
...ounts of parafo...
...oxide-fixed ti...
...ds. In some ca...
...formaldehyde-g...
...m sections were
...h periodic aci...
...as rinsed thoro...
...ersed for 30 m...
...mic acid. The
...%, 5%, 1% aceti...
...e sections were
...oteinate in dis...
...ther proteinate
...ally the secti...
...lled water.

Controls

...raction with p...
...ons with sali...
...ns prior to p...

...aline Phosph...

The lea...
...scribed by An...
...kaline phosph...

Thiery (1967). In this study, some of the modifications used by Anderson and Personne (1970) were followed. Thin sections of paraformaldehyde-gluteraldehyde-osmium tetroxide-fixed tissue were collected on 300-mesh gold grids. In some cases the tissues were fixed only with the paraformaldehyde-gluteraldehyde mixture. In either case the sections were immersed for 30 minutes in a solution of 1% periodic acid in distilled water. The grids were then rinsed thoroughly with distilled water and re-immersed for 30 minutes in 1% thiosemicarbazide in 10% acetic acid. The sections were subsequently washed in 10%, 5%, 1% acetic acid and then distilled water. Next the sections were immersed for 30 minutes in 1% silver proteinate in distilled water. The incubation in the silver proteinate solution was performed in the dark. Finally the sections were rinsed thoroughly with distilled water.

Controls consisted of either elimination of the oxidation with periodic acid or pretreatment of the sections with salivary amalyase for 4 hours at room temperature prior to PA-TSC-SP treatment.

Alkaline Phosphatase

The lead procedure according to the methods described by Anderson (1968) was used to demonstrate alkaline phosphatase activity. Spermatozoa were obtained

ncerating test

moving the clump

rough glass wool

re fixed accordi

taraldehyde pre

permatozoa were w

uffer pH 9.0, 0.2

minutes at 5°C

his buffer, 5 ml

ml of distil

ixtures consisted

-glycerolphosphat

after the incubat

ines in sodium p

ixed in osmium t

escribed above.

Acid Phosphatase

The acid

troduced by Go

permatozoa were

H 5.0, 0.05M).

ns in a solutio

% lead nitrate

.05M, to which

-glycerolphosphate

by macerating testes in 10% Holtfreter's solution and removing the clumped testicular tissue by filtration through glass wool. Centrifuged pelleted spermatozoa were fixed according to the above paraformaldehyde-gluteraldehyde procedure. Following the fixation the spermatozoa were washed three times with Tris-maleate buffer pH 9.0, 0.2M. The samples were then incubated for 30 minutes at 5°C in a solution containing 5 ml of the Tris buffer, 5 ml of 1.25% sodium β-glycerolphosphate, 11.7 ml of distilled water and 3.2 ml of 1% lead nitrate. Controls consisted of the above medium minus the sodium β-glycerolphosphate. All solutions were made fresh daily. After the incubation period the samples were washed two times in sodium phosphate buffer (pH 7.2, 0.2M) and post-fixed in osmium tetroxide according to the procedure described above.

Acid Phosphatase

The acid phosphatase procedure used was that introduced by Gomori (1956). Centrifuged pelleted spermatozoa were washed two times in sodium acetate buffer (pH 5.0, 0.05M). The samples were incubated for 1 hour at 37°C in a solution, made fresh daily, consisting of 0.6 gm of lead nitrate in 500 ml of sodium acetate buffer (pH 5.0, 0.05M) to which was added 50 ml of 3% sodium β-glycerolphosphate. The incubating medium was brought to

°C prior to use.

portion of the s

sium β-glycerolp

eroxide was carr

ight Microscopy

Sections a

e same paraforma

mples as those u

ption. The thi

lass knives with

ap of distilled

air dry. Once

ith solution of

hotographs were t

croscope.

Periodic Acid-Sch

The PAS p

M. O'Brien (196

ther Schiff-posi

ns the slides w

ne 2,4-dinitro

minutes. The

unning tap water

for 20 minutes.

37°C prior to use. The controls consisted of incubating a portion of the samples in the above medium without sodium β-glycerolphosphate. Post-fixation with osmium tetroxide was carried out as described above.

Light Microscopy

Sections approximately 1 mμ thick were taken from the same paraformaldehyde-gluteraldehyde-osmium fixed samples as those used for the electron microscopic investigation. The thick sections were taken dry from the glass knives with fine tapered forceps and placed on a drop of distilled water on a microscope slide and allowed to air dry. Once dried the sections were stained with a 0.05% solution of toluidine blue in distilled water. All photographs were taken on 35 mm film in a Zeiss or Wild photoscope.

Periodic Acid-Schiff (PAS)

The PAS procedure used was that described by Feder and O'Brien (1968). Aldehyde blockade was performed to cover Schiff-positive groups introduced by fixation. For this the slides were placed in a saturated solution of DNPH (2,4-dinitrophenylhydrazine) in 15% acetic acid for 10 minutes. The slides were washed for 10 minutes in running tap water, then were placed in Schiff's reagent for 20 minutes. Schiff's reagent was made according to

n procedure des

ff's treatment

directly into

.05% sodium me

used in running

ew counterstaine

ove.

the procedure described by Davenport (1960). After the Schiff's treatment the slides were transferred quickly and directly into three successive baths, 2 minutes each, of 0.05% sodium metabisulfate. Finally the slides were rinsed in running water for 5 minutes. Some sections were counterstained with toluidine blue as described above.

spermatocytogenes

Two types
ne light microsc
y Charpy (1913).
al Sekhri (1955)
rmations by Sha
khan (1957), br
ysia in R. pipie
ave briefly desc
f spermatogoniu
rimary spermtoc
entioned. The
f such low magn
o interpret.

In R. pi
three types of
light microgr
rimary sperma
rimary sperma
tion products o

OBSERVATIONS

Spermatocytogenesis

Two types of spermatogonia have been described at the light microscopic level in a large number of amphibians by Champy (1913). Three types were distinguished by Sharma and Sekhri (1955) in R. tigrina and three in Bufo stomaticus by Sharma and Dhindsa (1955). Burgos and Ladman (1957), briefly described two types of spermatogonia in R. pipiens. Glass and Rugh (1944) and Rugh (1951) have briefly described, also in R. pipiens, a single type of spermatogonium which appears to be similar to the primary spermtocytes described by the other authors mentioned. The photomicrographs of Glass and Rugh are of such low magnification that they are most difficult to interpret.

In R. pipiens and R. clamitans testes, at least three types of spermatogonia are present. Figure 1a is a light micrograph of what is called in this paper type 1 primary spermatogonium. Figure 1b represents type 2 primary spermatogonia. Type 2 spermatogonia are maturation products of type 1 with no intervening mitosis. The

Figure 1. Spermatogonial types-light micrographs.

a) R. pipiens

b) R. clamitans

c) R. pipiens

Note the type 1 primary spermatogonium (T1), groups of spermatocytes (Se), type 2 primary spermatogonia (T2) separated from each other by follicle cells (Fc) and a portion of a cluster of secondary spermatogonia (2nd). x 2,000.

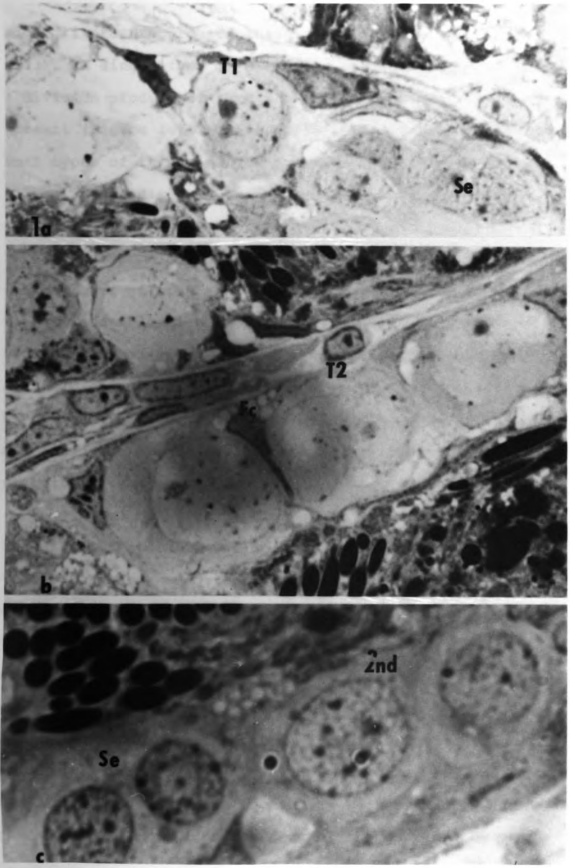
T1
Se
1a
T2
Fc
b
2nd
Se
c

the literature

III). A single

division produc

sent (Figure 1

ll types of the

d cells not dir

ells.

In mamma

n the basis of s

n the identifica

rious classes

nd 3 (Clermont

phibians, alth

mals, also e

lassifying spe

Three t

he ultrastruct

ates. Howeve

be evident to

he specific t

escription wi

Type

ype 1 primar

elatively la

circular a

ellum is is

older literature grouped these two types together (Champy, 1913). A single type of secondary spermatogonium which is a division product of type 2 primary spermatogonia is also present (Figure 1c). These cells occur in clusters while both types of the primary spermatogonia appear as individual cells not directly associated with other germinal cells.

In mammals spermatogonial typing is usually done on the basis of size and nuclear structure. This has led to the identification at the light microscopic level of various classes of the two main spermatogonial types, A and B (Clermont and Leblond, 1959 and Roosen-Runge, 1962). Amphibians, although not studied in as much detail as mammals, also evince nuclear morphology that aids in classifying spermatogonia.

Three types of spermatogonia are also visible at the ultrastructural level in R. pipiens and R. clamitans testes. However no definite ultrastructural variations are evident to distinguish between the spermatogonia of the specific types in the two species, so the following description will suffice for both.

Type 1 Primary Spermatogonia--Figure 2 shows a type 1 primary spermatogonium. Primary spermatogonia are relatively large cells (10 to 15 μm in diameter) and have a circular appearance in sections. Each primary spermatogonium is isolated from the rest of the germinal cells by

Figure 2. Type 1 primary spermatogonia, R. pipiens. Note the nucleus (N), nucleoli (Nu), mitochondria (M) and the follicle cells (Fc) surrounding the spermatogonium. x 10,200.

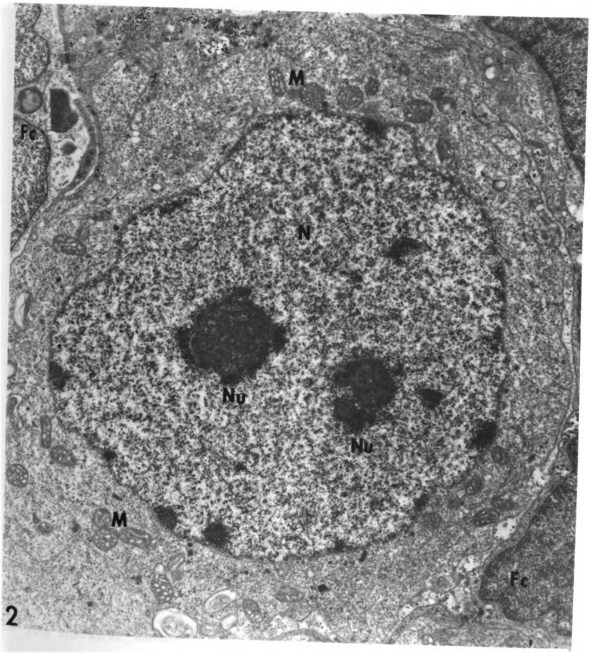
M
Fc
N
Nu
Nu
M
Fc
2

being completely surrounded by follicle cells. The nuclei are approximately circular in sections. The nuclear membrane is smooth and double walled. There are at least two nucleoli (Sharma and Sekhri, 1955) present. The nucleoplasm is finely granular with occasional clumps of moderately dense chromatin in association with the nuclear membrane.

The cytoplasm has many free ribosomes and a small amount of rough endoplasmic recticulum (Figure 3a). The mitochondria are circular to oblong in sections and distributed evenly throughout the cytoplasm. There is a tendency, however, for a small amount of mitochondrial clumping, similar to that observed by Nicander and Plöem (1969A) in rabbit type A spermatogonia. The mitochondrial cristae are dense and highly branched. The intercristal matrix has little electron density. Membrane scrolls are often seen (Figure 3b) in association with the mitochondria. In fact, what appears to be the beginning of scroll formation is often seen as a blebbing of the outer mitochondrial membrane (Figures 3a and b).

Small dense bodies are seen in the cytoplasm close to the nuclear membrane (Figures 3a and b). They have the same density and appearance as the chromatin condensations in the nucleus and in some cases are associated with mitochondria or membrane scrolls. (For further discussion

Figure 3. Portions of type 1 primary spermatogonia.

a) R. pipiens x 33,000.

b) R. clamitans. x 33,000.

Note the nuclei (N), rough endoplasmic recticulum (RER), ribosomes (R), membrane scrolls (S) and mitochondrial blebbing (MV). Arrows indicate the cytoplasmic dense bodies. A portion of surrounding follicle cells (FC) is also visible.

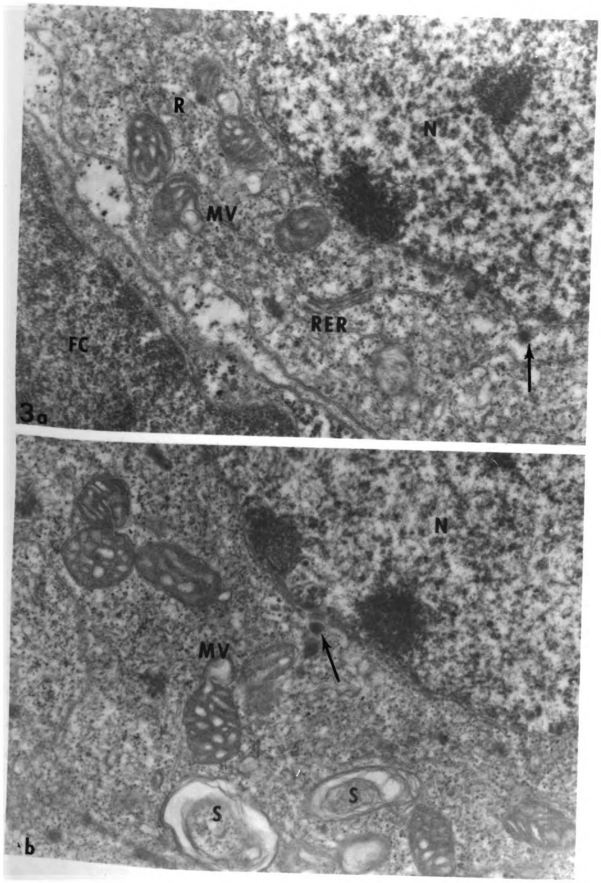
R
N
MV
RER
FC
3a
N
MV
S
S
b

the dense bo

gematogonia.)

The cha

gma are almo

ost describe

III. Simil

ase (Gardine

ller, 1969a,

ller, 1962).

mphology, b

ints in R.

Type

Hematogoni

Ehemer, th

ther micos

.e.: non

Hematogon

Th

Hematogo

Other app

All shape

Character

Although

Evidenc

Describing

of the dense bodies see the section on type 2 primary spermatogonia.)

The characteristics of type 1 primary spermatogonia are almost identical to the rat type A spermatogonia first described at the ultrastructural level by Watson (1952). Similar characteristics are also found in the mouse (Gardner and Holyoke, 1964), rabbit (Nicander and Plöem, 1969A), and human (Tres and Solari, 1968 and André, 1962). Brökelmann (1964) showed cells of similar morphology, both at the light and electron microscopic levels in R. temporaria.

Type 2 Primary Spermatogonia--Type 2 primary spermatogonia arise from type 1 primary spermatogonia. However, this change in cell type does not take place after mitosis for type 2 cells still appear individually (i.e.: not in clusters). Champy (1913) regarded type 2 spermatogonia as mature "gonia 1."

The most characteristic feature of type 2 primary spermatogonia are the polymorphic nuclei (Figure 4). The nuclei appear either as crescent-shaped, reniform, dumbbell shaped or multilobed. Polymorphic nuclei are characteristic of spermatogonia of many amphibian species, although much variation in the degree of lobing is evident (Champy, 1913).

Type 3 spermatogonia are much larger than type 1, measuring about 20 to 25 μm in diameter (Figure 6).

Figure 4. Type 2 primary spermatogonium, R. clamitans. Note the lobed nucleus (N), two nucleoli (Nu), clumped ribosomes (R), cytoplasmic dense bodies (DB), membranous scrolls (S) and mitochondria (M).
x 10,200.

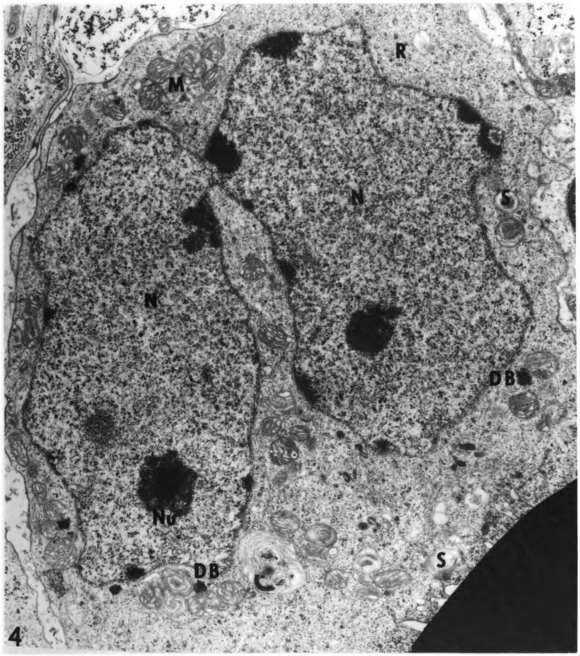
R
M
N
S
K
DB
Nu
DB
S
4

rust (1965) ha

protein and RNA

which occurs

in the increas

hyperphic and

figures 4 and 6

There

development as

al 5). The m

mation and th

by the crista

instead of be

ns now clump

the cases th

mitria to c

Aggre

these materi

ibers and H

Medley, 196

the amphibi

ed Piben (

chondri

It has been

mmalian s

ed Piben,

Hematocyt

Monesi (1965) has reported a very high synthesis of protein and RNA in type A mammalian spermatogonia which, if such occurs in amphibian spermatogonia, may account for the increase in size. Apparently the nuclei become polymorphic and then the cells increase in size (compare Figures 4 and 6).

There is an increase in the membraneous scroll development associated with the mitochondria (Figures 4 and 5). The mitochondria are still round to oblong in section and the matrix is clear. There is a tendency now for the cristae to become parallel with less branching. Instead of being randomly distributed the mitochondria are now clumped around the dense granular material. In some cases there is a partial polarization of the mitochondria to one portion of the cell (Figure 6).

Aggregation of mitochondria in clusters around dense material has been seen in growing oocytes of mammals (Adams and Hertwig, 1964; Hope, 1965; Odor, 1965 and Weakley, 1966) in some fishes (Zahnd and Porte, 1966) and some amphibians (Kessel, 1966, and Clerot, 1968). Nicander and Plöem (1969A) were the first to describe dense intermitochondrial material in mammalian type A spermatogonia. It has been described at the ultrastructural level in mammalian spermatocytes (André, 1962; Eddy, 1969; Nicander and Plöem, 1969B and Fawcett and Philips, 1967) and in spermatocytes of three species of Rana (Clerot, 1968).

Figure 5. Portions of type 2 primary spermatogonia.

a) R. clamitans. x 25,000.

b) R. pipiens. x 33,000.

Note dense bodies (DB) in close association with the nucleus (N) and the associated mitochondria. Arrows in 5a indicate membranous scroll-like bodies that may be forming mitochondria. In 5b the arrows indicate the close association of the dense bodies with the mitochondria. Membranous scrolls (S) are also seen.

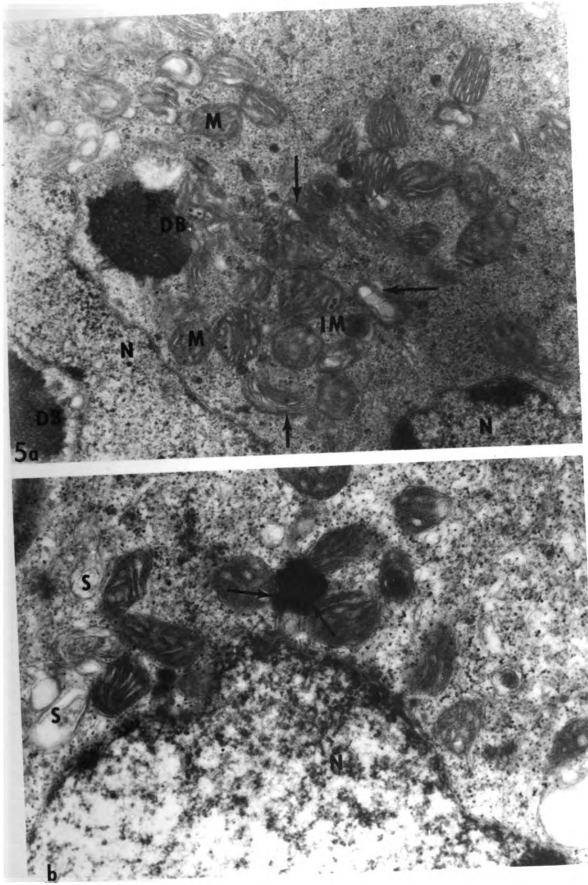
M
DB
N
M
IM
DB
N
5a
S
S
N
b

Figure 6. Type 2 primary spermatogonia, R. pipiens. Note the intermitochondrial dense bodies (DB) with the associated mitochondria (M), follicle cell (Fc) membranous scrolls (S) and the nucleus (N) and nucleolus (Nu) of the spermatogonium.
x 12,600.

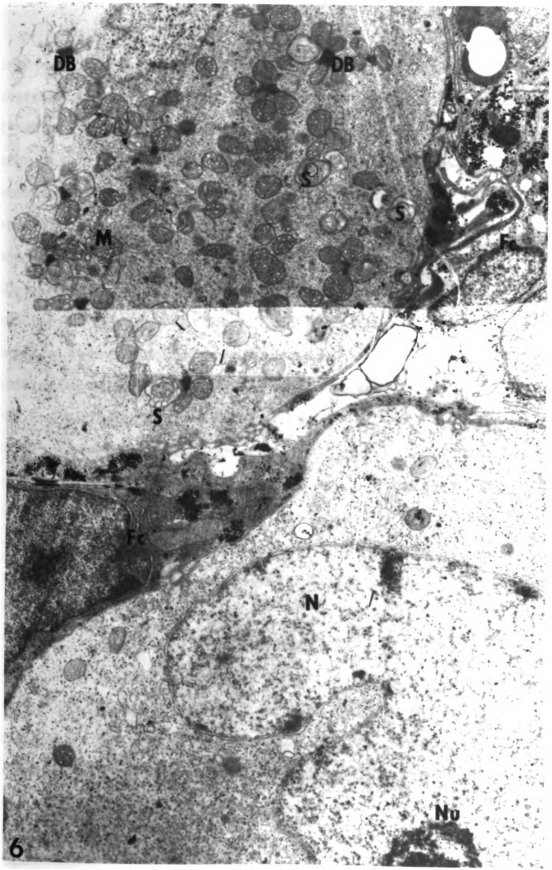
DB
DB
S
S
M
F
S
Fc
N
Nu
6

There

tension and

istance. F

nuclear or

ormation f

nterpret th

ined from

nsidered t

ribosomes.

tension in

mplete out

ssociation

30S and An

ed some de

bacco and

ggest tha

d section.

hromatoid

tivity.

In

Klem, 1969

ion of the

Fluorescence

hromatoid

ions the m

bacco et

There has been much debate about the origin, function and final fate of the dense intermitochonrial substance. Kessel (1966) suggests that the material is of nuclear origin and that it may function in transfer of information to the mitochondria. Zahnd and Porte (1966) interpret the dense material as ribonucleoprotein transported from nucleoli to the cytoplasm. André (1963) considered the dense material to be aggregations of ribosomes. Odor (1965) suggested that this material may function in de novo mitochondrial formation. The incomplete outer mitochondrial membrane often seen in association with the dense material (Kessel, 1966; Odor, 1965 and André, 1962) (also see Figure 5b) was thought to add some degree of credence to this supposition. However Fawcett and Phillips (1967) and Nicander and Plöem (1969A) suggest that the incomplete membrane is due to obliquity of section. Fawcett et al. (1970) suggest that the chromatoid body may be a product of mitochondrial synthetic activity.

In mammalian species (Eddy, 1969; Nicander and Plöem, 1969B, and Fawcett and Phillips, 1967), the formation of the chromatoid body has been described as a coalescence of the intermitochondrial dense material. The chromatoid body is then divided amongst the spermatids and forms the major component of the annulus. Recently Fawcett et al. (1970) have shown in a variety of mammalian

genes that

n zymlos

ymlos migr

Cyto

ggested t

lement, I

Inner Cle

mmcal In

ha is ser

May, 1969

ith RNase

Six

ee secti

ould have

hese spec

ucchondr

d not the

Al

ucchondr

ucchondr

t least,

chemica

ivision.

ncrease

The 2 pr

and 6/

species that the chromatoid body does not contribute to the annulus but seems to gradually disappear as the annulus migrates caudally.

Cytochemical studies on the chromatoid body have suggested the presence of ribonucleoprotein (Daoust and Clermont, 1955; Sud, 1961 and Fawcett and Phillips, 1967). However Clerot (1968) found that the intermitochondrial material in oocytes and spermatocyte of three species of Rana is sensitive to protease and not RNase. In mammals (Eddy, 1969 and 1970) the chromatoid body is resistant to both RNase and proteolytic enzymes.

Since amphibian spermatozoa do not have an annulus (see section entitled "Spermiogenesis"), another function would have to be suggested for the chromatoid body in these species. It is indeed possible that the intermitochondrial material found in amphibian germinal cells is not the same type of material as that found in mammals.

Although it seems improbable that the dense intermitochondrial material functions directly in de novo mitochondrial formation, it is still possible in amphibians at least, that André's (1962) other suggestion, that the intermitochondrial material may stimulate growth and/or division of mitochondria, is correct. There is a definite increase in the number of mitochondria from type 1 to type 2 primary spermatogonia (compare Figure 2 to Figures 4 and 6). This increase of mitochondria takes place in

mammals in the growing primary spermatocyte (Johnson and Hammond, 1963), where the intermitochondrial material is best demonstrated (Fawcett and Phillips, 1967 and Nicander and Plöem, 1969A). Figure 5 shows the association of membrane scrolls in association with dense material. The scrolls may be formed by blebbing of the outer mitochondrial membranes (Figure 3a and b). Figure 5b shows what may be the formation of new mitochondria from scroll-like material. It is equally possible that the membrane scrolls and mitochondrial blebbing may be fixation artifacts. These blebs and scrolls may also be the first indication of cell degeneration. Many spermatogonia do not develop further than this stage (Lofts, 1964 and Champy, 1913).

Some type A spermatogonia in mammals reproduce periodically to replace those spermatogonia which develop into spermatocytes (Roosen-Runge, 1962; Clermont, 1967 and Clermont and Bustos-Obregon, 1968). Although primary spermatogonia of R. clamitans and R. pipiens are similar in structure to type A stem cells of mammals, it is not known if they are functionally the same. Without triated thymidine-labeling experiments one can not be sure. However, it is assumed (Sharma and Sekhri, 1955 and Champy, 1913) that they do function as stem or reserve cells. The fact that primary spermatogonia are individual cells also adds some support to this idea.

Secc

nse by mit

ly worke

anism of

apy (191

nnse div

y to Cham

mary spe

Sec

e size of

pends on

e primary

Fig

ematogon

s neighbo

e whole

follicle

The

ot have

ikari, 19

he granu

apy (19

escriptio

eatures o

ristic o

Rycke, 19

Secondary Spermatogonia--Secondary spermatogonia arise by mitotic division of type 2 primary spermatogonia. Early workers (see Champy, 1913) suggested amitosis as a mechanism of division for type 2 primary spermatogonia. Champy (1913) and Sharma and Sekhri (1955) described mitotic division of type 2 primary spermatogonia. According to Champy (1913) amitotic division of the type 2 primary spermatogonia leads to cellular degeneration.

Secondary spermatogonia are found in clusters. The size of the individual cells and the number per cluster depends on the number of divisions which has occurred from the primary spermatogonia.

Figure 7 shows a portion of a cluster of secondary spermatogonia. Each cell in the cluster is separated from its neighboring germ cell by only its plasma membrane. The whole cluster of secondary spermatogonia is surrounded by follicle cells.

The nuclei have an increased number of thickenings that have been described as chromatin "flakes" (Sharma and Sekhri, 1955). The rest of the nucleoplasm still has the fine granular appearance. Sharma and Sekhri (1955) and Champy (1913) show similar nuclear features in their descriptions of secondary spermatogonia. These nuclear features of amphibian secondary spermatogonia are characteristic of mammalian type B spermatogonia (Gardner and Holyoke, 1964 and Nicander and Plöem, 1969A).

Figure 7. Secondary spermatogonia, R. pipiens. Note the nuclei (N) of the six secondary spermatogonia, intermitochondrial dense bodies (DB) surrounded by mitochondria (M), ribosomes (R) and the plasma membranes of the spermatogonia (PM). A portion of the surrounding follicle cell (Fc) is also visible. x 10,200.

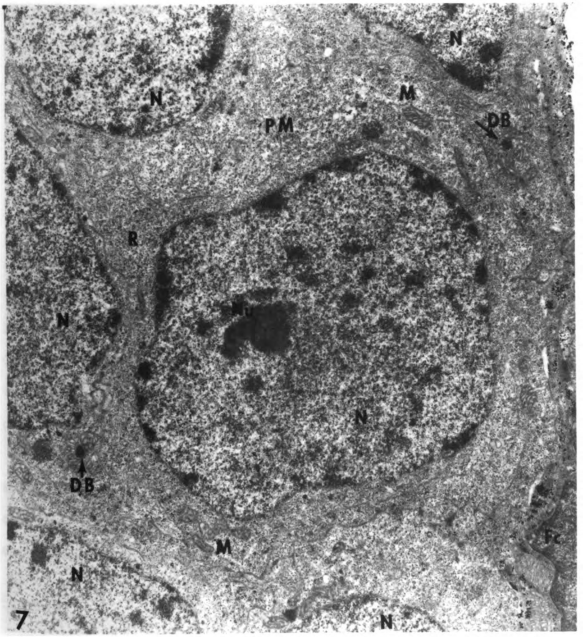
N
N
M
PM
DB
R
N
N
DB
M
N
7

The

nged cons

ius. The

mmitooh

ebranous

pearances

mering.

muscles.

No

ematogo

ules. N

ween ty

ether an

he last s

ning ris

No

ematogo

ly been

ntogonia

Nerves

I

f the ch

Nesting

ipoid va

tage is

The cytoplasm of secondary spermatogonia has changed considerably. There is a reduced amount of cytoplasm. The number of mitochondria are reduced. The dense intermitochondrial material is still present but the membranous scrolls are no longer evident. From all appearances mitochondrial multiplication is no longer occurring. There is however still a large amount of free ribosomes.

No intercellular bridges have been observed between spermatogonia of any stage in R. clamitans or R. pipiens testes. Nicander and Plöem (1969A) observed bridges between type B spermatogonia in the rabbit. However, Gardner and Holyoke (1964) and Fawcett (1961) suggest that the last spermatogonial division is incomplete thereby giving rise to conjoined primary spermatocytes.

No crystalloid bodies have been found in the spermatogonia. To the present, crystalloid bodies have only been observed in human and, possibly, chicken spermatogonia (Nagano, 1969).

Meiosis

In most sexually reproducing organisms the doubling of the chromosome number at fertilization is offset by reducing the chromosome number of the gametes to half their diploid value during a stage in their development. This change is brought about by a single chromosome duplication

llowed by

lled testes

d spermatog

Chro

are well d

ne Wilson

ften could

ividual

n when co

nalized

roscopic

lower, ev

escription

tance. Wi

d meiotic

ells but c

ny microg

spermatocy

ically i

aterial a

In

roscopic

eiotic pro

ropic obse

be observa

ld sharply

followed by two successive divisions. The process is called meiosis and occurs during the spermatocytic stages of spermatogenesis.

Chromosomal movements and behavior during meiosis were well documented by the early light microscopists (see Wilson, 1925). However, subtle changes in the cytoplasm could not be detected. At the ultrastructural level individual chromosomes are either too diffuse to be seen or, when compacted, need to be serially sectioned for full visualization (Solari and Tres, 1970). At the electron microscopic level cytoplasmic variations can be determined. However, even in well characterized mammalian cells, descriptions of morphological changes during meiosis are scarce. Nicander and Plöem (1969A) described the stages of meiotic prophase in rabbit showing micrographs of whole cells but only in the leptotene and pachytene stages. The only micrographs of the ultrastructure of amphibian spermatocytes were published by Clerot (1967). He was basically interested in the dense intermitochondrial material and not in the spermatocyte per se.

In this study an attempt was made at the electron microscopic level to classify the stages of the first meiotic prophase by relating the "typical" light microscopic observations of chromosome behavior in meiosis with the observations of Rugh (1951); Sharma and Sekhri (1955) and Champy (1913) on amphibian spermatogenesis.

No d

species in t

purpose wa

in both.

Fig

rimary spe

n section

ships are

rnational

ns seen in

mbed in

Sharma an

Th

aterial.

Fawcett

d in dis

Hematogo

ellular b

fusion,

ibes. Bo

Table in

he first

described,

Al Ribeh,

Sharma an

No distinguishing differences between the two species in the ultrastructural aspects of the first meiotic prophase was noted. The following description will suffice for both.

Figure 8 shows a portion of a cyst of interphase primary spermatocytes. The nuclei are circular to oblong in section with somewhat irregular outlines. Chromatin clumps are seen on the periphery of the nucleus with occasional condensations in the nucleoplasm. Two nucleoli are seen in some sections. Two nucleoli have been described in the primary spermatocytes of R. tigrina (Sharma and Sekhri, 1955).

The mitochondria are still clumped around dense material. Intercellular bridges are seen, which, according to Fawcett (1961) and Gardner and Holyoke (1964), are an aid in distinguishing primary spermatocytes from late spermatogonia. According to the above authors, intercellular bridges are formed at the last spermatogonial division, just prior to the transformation into spermatocytes. Rounded, swollen (active?) Golgi elements are visible in addition to the more flattened type. This is the first time Golgi elements are seen. They have been described, however, in mammalian spermatogonia (Nicander and Plöem, 1969A) and at the light microscopic level (Sharma and Sekhri, 1955 and Sharma and Dhindsa, 1955) in

Figure 8. Primary spermatocytes-interphase, R. pipiens. Note the mitochondria (M) still clumped around dense material, Golgi elements (GE) and intercellular bridge (IB) between spermatocytes. x 6,000.

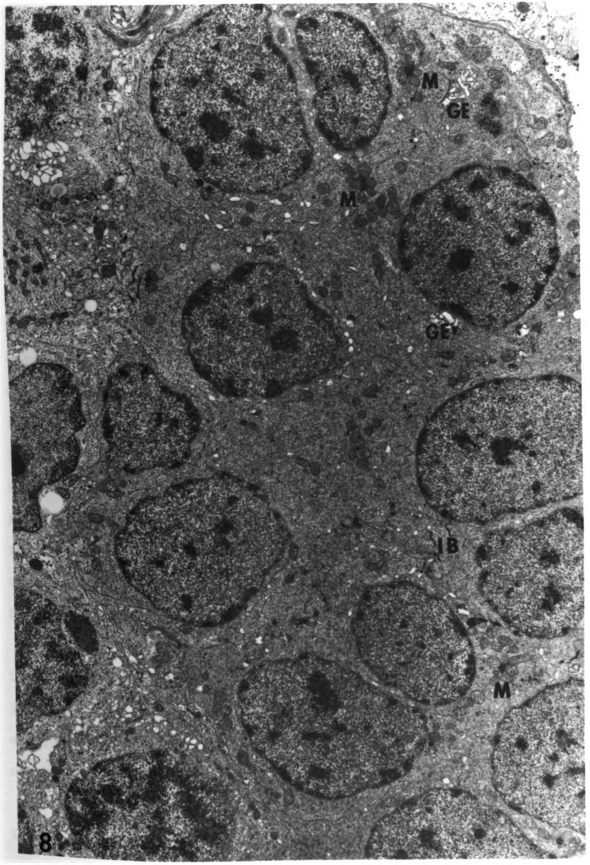
M
GE
M
GE
IB
M
8

amphibian spermatogonia. The rest of the cytoplasm is similar to that seen in the secondary spermatogonia.

Leptotene stage primary spermatocytes are shown in Figure 9. Most of the peripherally located chromatin clumps are no longer present. Instead, a large number of fine chromosome threads are visible in the internal nuclear area. It is thought that Figure 9 is a cross section through the so-called bouquet arrangement. The nucleoplasm is granular and the nucleoli are visible. In the cytoplasm the Golgi elements are circular in section with large vacuoles. Few distinct lamellar structures are associated with them. Clusters of free ribosomes fill the cytoplasm and a small amount of RER and SER are visible (Figure 10). Mitochondria are oblong in shape with distinct cristae. No membranous scrolls or mitochondrial blebbings are seen. Mitochondrial clumping is still visible. No definite relationship of the Golgi elements, centrioles and mitochondria, as described by Sharma and Sekhri (1955), could be distinguished.

By the zygotene stage the chromosomes are pairing. Notice the thicker, reduced number of chromosome threads in Figure 11. The nucleus is still oblong in section with an irregular outline. Solari (1969) finds synaptinemal complexes in mammalian spermatocytes of the zygotene stage.

Mitochondrial clusters are breaking down. According to Nicander and Plöem (1969A) this occurs in the late

Figure 9. Primary spermatocytes-leptotene, R. clamitans. Note the chromosome threads in the nuclei (N) the mitochondrial clumps and Golgi-elements (GE). x 5,000.

Figure 10. Cytoplasm of primary spermatocyte-leptotene R. clamitans.

Note the rough (RER) and smooth (SER) endoplasmic reticuli, portion of an intercellular bridge (IB), Golgi elements (GE), clumped ribosomes and dense intermitochondrial material (DB). Arrow indicates intramitochondrial material.

x 26,100.

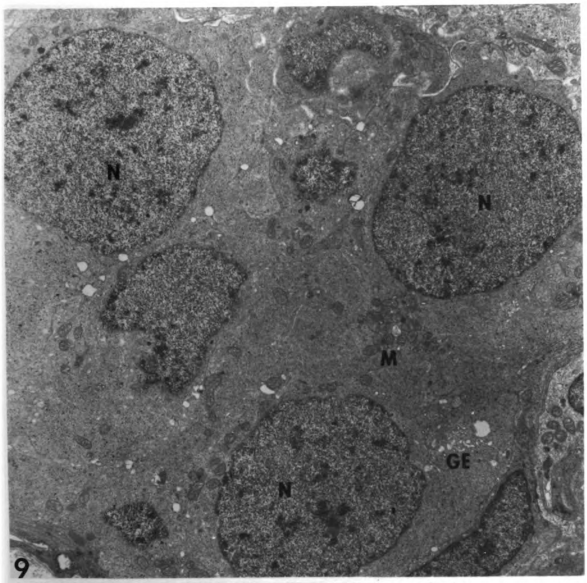
N
N
M
GE
N
9

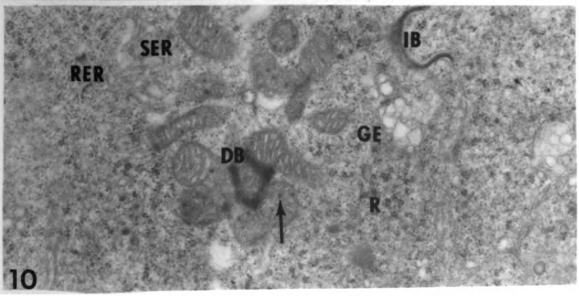
SER
IB
RER
GE
DB
R
10

Figure 11. Primary spermatocytes-zygotene, R. clamitans.
Note the thickened chromosomes (C), mitochondria (M) and Golgi-elements (GE).
x 10,200.

Figure 12. Cytoplasm of primary spermatocyte-zygotene, R. clamitans.
Note the smooth endoplasmic reticulum (SER), clumped or isolated ribosomes (R). Arrow indicates dense intramitochondrial material.
x 22,200.

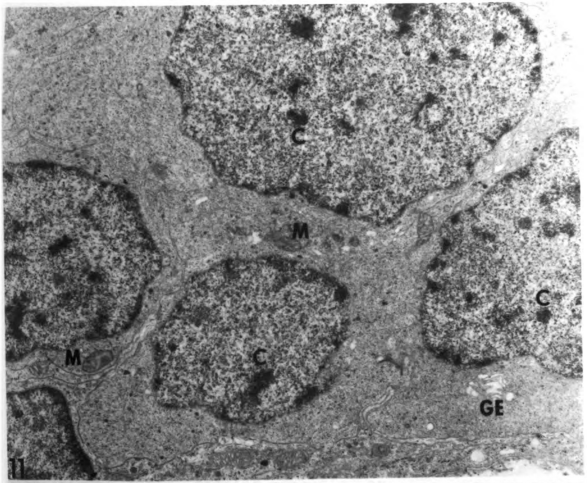
C
M
C
C
M
C
GE
11

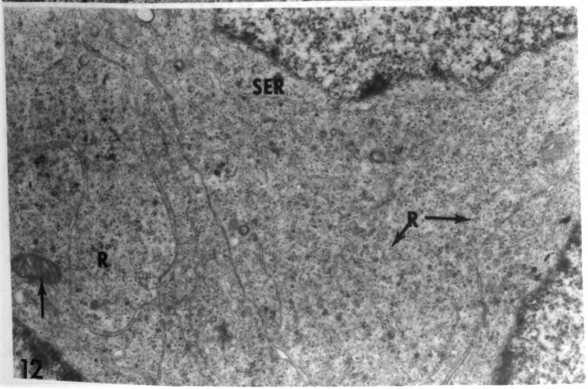
SER
R
R
12

pinytene s

re so long

ally throu

ytoplasmic

s no RER i

tubles can

The

n the long

ell. In

permatocyt

ures on a

ynaptonema

lateral com

m space

ule (Figur

Clark (196

permatocyt

The

haracteri

maller th

the body

hrough ou

Sertoli

By

the thicke

nucleus (a

pachytene stage in rabbit spermatocytes. The ribosomes are no longer arranged in clusters but are spread individually throughout the cytoplasm. Cisternae of smooth endoplasmic reticulum are becoming more numerous. Little or no RER is visible (Figure 12). Occasionally microtubules can be seen.

The next stage is called the pachytene stage and is the longest period of prophase (Swierstra and Foote, 1963). In the early pachytene nuclei of R. clamitans spermatocytes the chromosomes appear as thickened structures on a less dense nucleoplasmic background (Figure 13a). Synaptinemal complexes are seen for the first time. The lateral components of the complexes are separated by a 90 nm space and the central component is about 1.5 nm wide (Figure 13b). Similar measurements were given by Solari (1969) for synaptinemal complexes found in mice spermatocytes.

The Golgi elements have lost any similarity to the characteristic flattened form. The mitochondria appear smaller than in previous stages. A definite chromatoid-like body is present and the mitochondria are spread through out the cytoplasm. Occasionally some dense intermitochondrial material is still visible.

By late pachytene (Figure 14a) the chromosomes have thickened to such a degree that they fill the whole nucleus (also see Rugh, 1951). The nuclei appear circular

Figure 13. Primary spermatocytes-early pachtene.

a) R. pipiens. x 6,000.

b) R. clamitans. x 66,000.

Note the Golgi elements (GE), chromatoid-like body (Cb), synaptinemal complexes (Sp) and nucleolus (Nu).

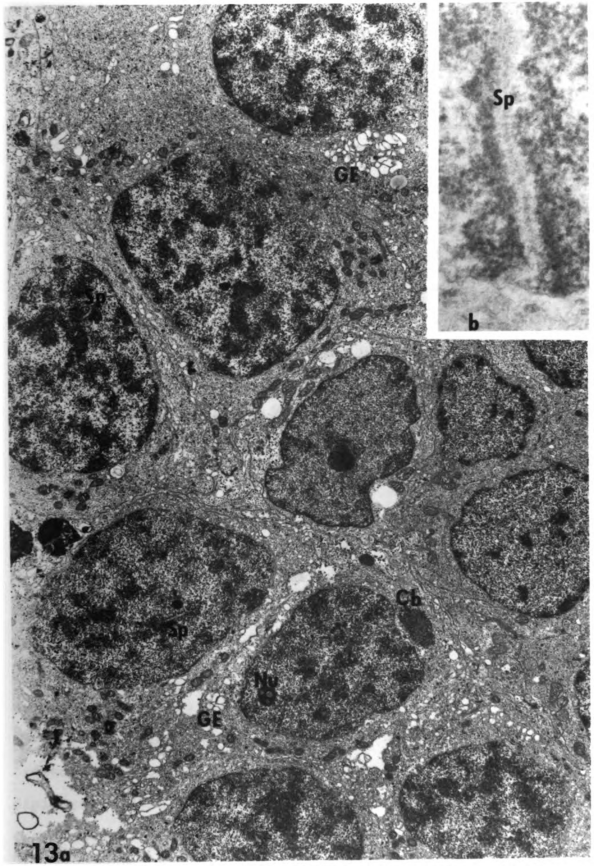
GE
Sp
Sp
b
Sp
Cb
Nu
GE
13a

section w

visible.

The

igure 14b)

ength, are

vascular S

liquid-fill

ber of r

remaining a

ribosome

mber of

ophas

ecopies.

ds (see

ytoplasm

ey seem

ich

ameter

he size

ormall

(365) s

recede

ipoten

correla

in section with a smooth outline. Synaptinemal complexes are visible.

The cytoplasm has changed considerably (Figure 14b). Mitochondria, although about the same length, are half the width of those seen in early prophase. Vesicular SER is very abundant and occasionally large liquid-filled vacuoles are seen. No RER is visible. The number of ribosomes appears to have decreased and those remaining are again arranged in clusters. The variations in ribosome arrangements may indicate a variation in the amount of protein synthesis during the different stages of prophase, as described by Monesi (1965) in mice spermatocytes. Dense bodies similar to those seen in spermatids (see page 80) are distributed throughout the cytoplasm. The number of microtubules has increased and they seem to have their origin or termination in association with the centrioles (Figure 14c).

The cells at this stage are about 10 μm in diameter with a nuclear diameter of approximately 7 μm. The size of an interphase nucleus measures about 5 μm.

During the diplotene stage one set of sister chromatids begin to separate from the other pair. Wilson (1925) states that spermatocyte nuclei of various species "recede or deconcentrate" in interphase nuclei in early diplotene. This sort of change, according to Wilson is correlated with the processes of cytoplasmic growth; in

Figure 14. Primary spermatocytes-late pachytene, R. clamitans.

a) x 5,000.

b) x 15,300.

Note the synaptinemal complexes (Sp) in the dense nuclei (N), smooth endoplasmic reticulum (SER), mitochondria (M), clumped ribosomes (R) and "fluid filled" vacuoles (VF).

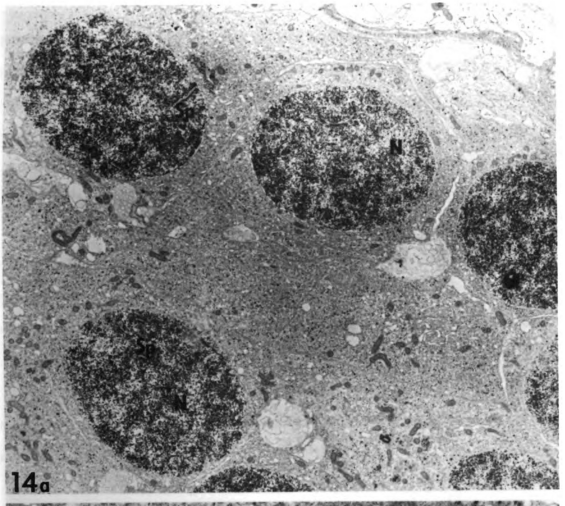

14a

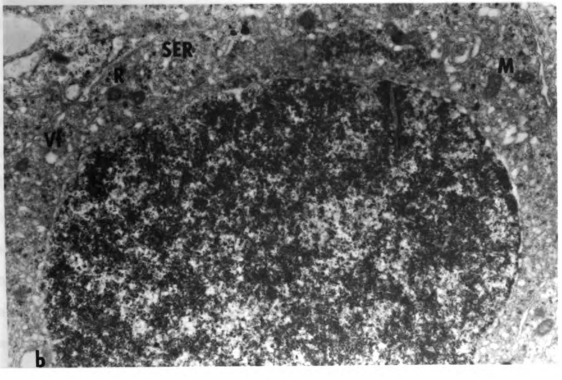

b

general the longer the growth period the greater the nuclear diffusion. However Solari (1969) states that condensation of chromatin material in the mouse spermatocyte increases up to early pachytene, then slow "uncondensation" takes place up to diplotene.

The diplotene nuclei of R. clamitans spermatocytes (Figure 15) are less dense than those of the late pachytene stage. Synaptinemal complexes are still visible. The cytoplasm is identical to that described for the late pachytene stage. The cell has increased in size to about 12 to 14 μm in diameter.

No definite sex vesicles, heterochromatic sex pair, were distinguished at any of the stages of meiotic prophase studied.

The remaining stages of the first division could not be identified.

Secondary spermatocytes arise from the first meiotic division. In R. pipiens they are said to be much smaller in size than primary spermatocytes (Burgos and Ladman, 1957 and Rugh, 1951). Burgos and Ladman (1957) described the nuclei of secondary spermatocytes as having peripherally located chromatin clumps. Rugh (1951) described the nuclei as uniformly stained. This of course may reflect different stages of the second division. Rugh also states that these cells are located towards the lumen and that the cytoplasm may be tapered at one end.

Figure 14c. Cytoplasm of primary spermatocyte-late pachytene, R. clamitans.

Note the centriole (C) with the associated microtubules (MT) and a Golgi element (GE).

x 26,100.

Figure 15. Primary spermatocyte-diplotene, R. clamitans.

x 10,200.

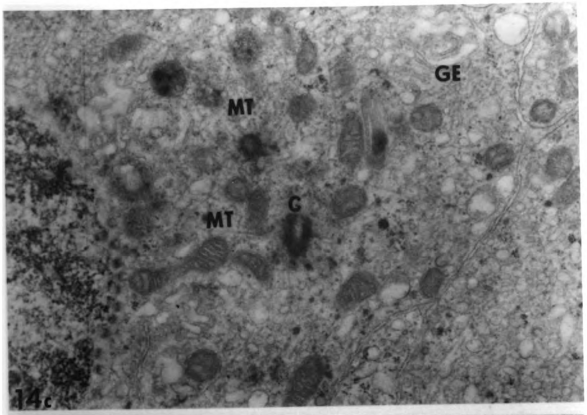

14c

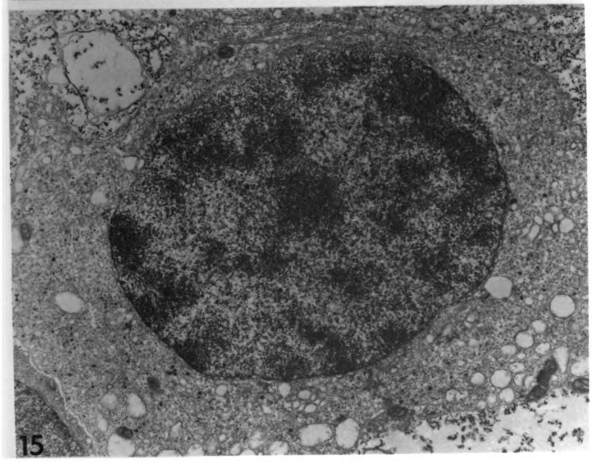

15

In

ne second

ny nuclei

Se

period, th

lusion.

ecific d

here is

he first

ymerapl

N

ypes co

hemolog

esult

ents a

hemolog

ino fou

ber of

Peptid

econd

h class

he proc

ibuta

In R. tigrina, Sharma and Sekhri (1955) described the secondary spermatocytes as having homogeneously staining nuclei. The mitochondria appear as "tiny particles."

Secondary spermatocytes have a short interphase period, that is, they rapidly go into the second meiotic division. In some insects, for example, the second meiotic division immediately follows the first so that there is no interphase and the telophase chromosomes of the first division are directly transferred into prometaphase of the second (Sharma and Parshad, 1955).

No positive identification of secondary spermatocytes could be made in this study.

Spermiogenesis

Spermatids arise from secondary spermatocytes as a result of the second meiotic division.

The series of developmental events by which spermatids are transformed into mature spermatozoa is called spermiogenesis. In mammals spermiogenesis can be divided into four general stages that are defined by the development of the acrosome (Bloom and Fawcett, 1968). More specifically, however, 19 stages were identified by Leblond and Clermont (1952). In R. pipiens and R. clamitans, spermiogenesis varies considerably from the process in mammals so no attempt will be made to fit amphibian spermiogenesis into this well defined system.

bever, du

pecies at

1) For

flag-ellate

nvolved w

ay be a u

ICH. T

structure,

ngure eq

ller, 1

hrvastav

d format

ysosome

ave been

2) C

terial

nuclear

change

ed Port

ion or

h chick

ellocal

known m

Borgos

d spec

ed elec

However, during development of the mature sperm, in most species at least, three major phases can be described:

1) Formation of the acrosome. In acrosome-bearing flag-ellated spermatozoa the Golgi element is usually involved with acrosome formation. That this association may be a universal occurrence was first suggested by Bowen (1920). The acrosome usually a membrane-bound bag-like structure, carries the enzymes needed to dissolve or rupture egg coverings so penetration can take place (Tyler, 1939; Berg, 1950; Wada et al., 1956; Dan, 1967 and Srivastava et al., 1965). Because of their similar mode of formation the acrosome has been called a specialized lysosome and indeed some of the enzymes found in lysosomes have been found in acrosomes (Anderson, 1968).

2) Condensation and elongation of the nuclear material. During spermiogenesis in the chicken the nuclear volume decreases from 110 μm^3 to about 2 μm^3 with a change in the axial ratio from 1:1 to 22:1 (McIntosh and Porter, 1967). There is thus a substantial condensation or elongation of the nucleus. The elongation process in chicken spermatids has been associated with elaborate helical microtubular formations. The manchette, a well known microtubular structure in mammalian spermatids (Burgos and Fawcett, 1955), is also thought to function in sperm shaping. Microtubular formations during spermatid elongation have been described in a wide variety of

species including the earthworm (Anderson et al., 1967), insects (Robison, 1966; Philips, 1966; Kessel, 1966 and 1967), and mammals and birds (Nicander, 1967). Condensation of nuclear material occurs in various ways in different species, varying from clumping of the chromatin to eventual fusion of condensing parallel thread-like structures (Fawcett, 1955). Karyolymph is eliminated during nuclear condensations and is expelled in clear membrane-bound pockets from the posterior portion of the nucleus (André, 1963; Franklin, 1968).

3) Mid-piece formation. The centrioles are first seen at the cell periphery in the early spermatid. From what will be the distal centriole the axial filament begins to grow. Axial filament formation is in itself not a universal criterion for the spermatid stage. Meves (see Wilson, 1925) has described four axial filaments in the primary spermatocytes of the butterfly Pygaera.

The centrioles with the elongating axial filament begin to migrate to a position close to the nucleus. Golgi elements are usually associated with the centrioles at this stage. The Golgi element and the centrioles then separate and take positions at opposite portions of the nucleus. Mitochondria become associated with the centrioles for mid-piece formation and the Golgi element functions in acrosome formation.

Ex

ase phas

ase vari

ion and

ed, pi

asis to

ater ev

ested.

ral e

ivesti

ions i

ble h

ach s

fecur

Secu

Clas

ze s

Clas

Base

The

Y L

Secu

Extreme variation occurs between species in these three phases of spermiogenesis. Detailed accounts of these variations are given by Wilson (1925), and Nath (1956 and 1965).

The early events of spermiogenesis in R. clamitans and R. pipiens are similar enough on a ultrastructural basis to be described together. Acrosome formation, a later event, is somewhat different and will be separately treated.

Of the two published accounts of the ultrastructural events of Amphibian spermiogenesis (Burgos and Fawcett, 1956 and Baker, 1967), both begin their descriptions in the mid-spermiogenic stages. An attempt will be made here to describe the early events which are common to both species of Rana, as well as the more specific later features of spermiogenesis.

Early Spermiogenic Events Characteristic of Both Species--Figure 16 shows a portion of two early spermatid clusters surrounded by follicle cells. Large desmosomes are seen along the apposing follicle cell membranes. The clusters and their associated follicle cells rest on the basement membrane which encircles the seminiferous tubule. The nuclei appear spherical in section, averaging about 10 µm in length by 6 µm wide. The nucleoplasm is heterogeneous and clumps of chromatin of various sizes are seen, a

Figure 16. Early spermatid cluster, R. pipiens.
Note the basement membrane, (BM) follicle cell cytoplasm (Fc), nuclei (N) and nucleoli (Nu) of the spermatids, chromatoid-like body (Cb), desmosomes (De) separating adjacent follicle cells and the lumen (L) of the seminiferous tubule. Centriole (C) close to the lumen, just prior to axial filament elongation and associated Golgi element (GE) (see insert) are also visible.
x 5,700.
Insert x 20,000.

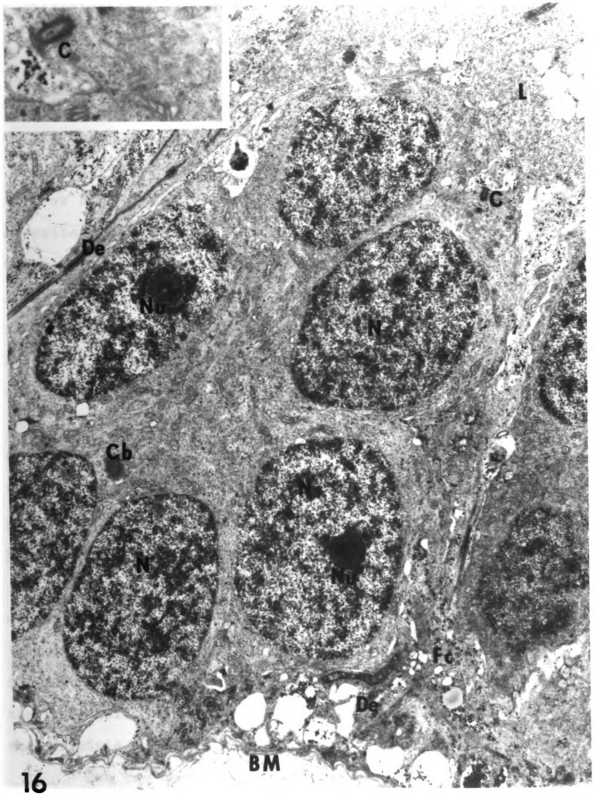

16

haracte

ample n

Ch

ation

eady ch

ith para

ee or d

ppsite

ight el

sert s

ture d

ual s

ecipla

e ch

kes

esen

ace

arly

ttac

f ch

e c

ttac

ose

a characteristic of condensing chromatin (Fawcett, 1958). A single nucleolus is visible in some sections.

The cytoplasm is dense and somewhat reduced in relation to the nuclear volume. The mitochondria, spread evenly through out the cytoplasm, are spherical in shape with parallel or branching cristae. The ribosomes are free or clustered in rosettes. In an area of the cytoplasm opposite the basement membrane, centrioles (Figure 16) and Golgi elements (Figure 16, insert) are seen. Figure 16 insert shows a thickened membrane at the extremity of the future distal centriole. This is the first indication of axial filament formation. A small amount of smooth endoplasmic reticular is also visible.

As chromatin condensation continues (Figure 17a) the chromatin clumps become larger and the nucleoplasm takes on a filamentous appearance. The nucleolus is still present and shows no sign of degeneration. In the cytoplasm most of the ribosomes are now in the rosette pattern.

Figure 17b is a similar picture of R. pipiens early spermatids showing early axial filament formation (arrow). The condensing chromatin and filamentous nature of the nucleoplasm are most striking. The cytoplasm shows the centrioles with the associated Golgi element, scattered mitochondria and rosetted ribosomes.

The two centrioles in the early spermatid are located close to the periphery of the cell (Figure 16).

Figure 17. Early spermatids.

a) R. clamitans. x 15,300.

b) R. pipiens x 17,400.

Note the nuclei (N), nucleolus (Nu), ribosomes (R), glycogen particles (G), the Golgi elements (GE) and the proximal (P) and (D) distal centrioles. Arrow indicates area of axial filament formation.

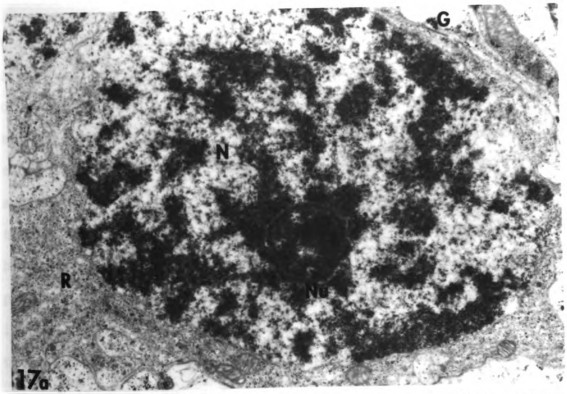
G
N
R
Nu
17a

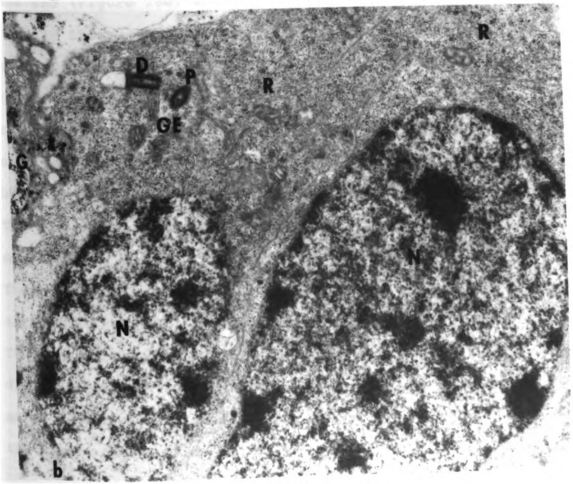
D
P
R
GE
G
R
N
N
b

small sac

mins at th

in Figure

mmial on

m. The s

n then i

enlarge

ening sl

rtion o

a notice

ins of

he sac

bably

mal ep

figure

een ea

ntrac

lands

he ce

hpas

he n

ttac

he d

ibra

Mal

he p

A small sac or invagination of the cell plasma membrane occurs at the distal portion of the future distal centriole (Figure 18a). There is an accumulation of dense material on the inner centriolar portion of the membrane sac. The sac expands first at the periphery (Figure 18b) and then in the center (Figure 18c). The sac continues to enlarge (Figure 18d), forming a cup-like structure bending slightly around the associated centriole. That portion of the membrane sac associated with the centriole is noticeably thicker or denser than the remaining portions of the membrane. The axial filament grows out into the sac (Figure 18e) and the sac begins to collapse. Finally the sac completely collapses around the extending axial filament, forming a sleeve-like arrangement (Figure 18f). It can be noted that the dense material seen earlier has remained at the distal portion of the centriole, in the region where the cell plasma membrane bends back to form the sleeve over the axial filament. The centrioles with the elongating axial filament then migrate to a position close to the nucleus (Figure 18g). The migration process further accentuates the sleeve-like arrangement of the plasma membrane over the axial filament. The dense material, still seen at the junction of the distal centriole (now, probably, the basal body) and the axial filament, may function as a zone of formation for the plasma membrane as it enlarges.

Figure 18. Axial filament formation.

a) R. pipiens. x 66,000.

b) R. clamitans. x 42,000.

c) R. pipiens. x 57,000.

d) R. pipiens. x 57,000.

e) R. clamitans. x 33,000.

f) R. pipiens. x 48,500.

g) R. pipiens. x 57,000.

Note the distal (D) and proximal (P) centrioles, axial filaments (AF) and Golgi elements (GE). Portion of a spermatid nucleus (N) can be seen in g. The dense material lining the inner aspect of the sperm plasma membrane at the point of axial filament elongation is marked with (-).

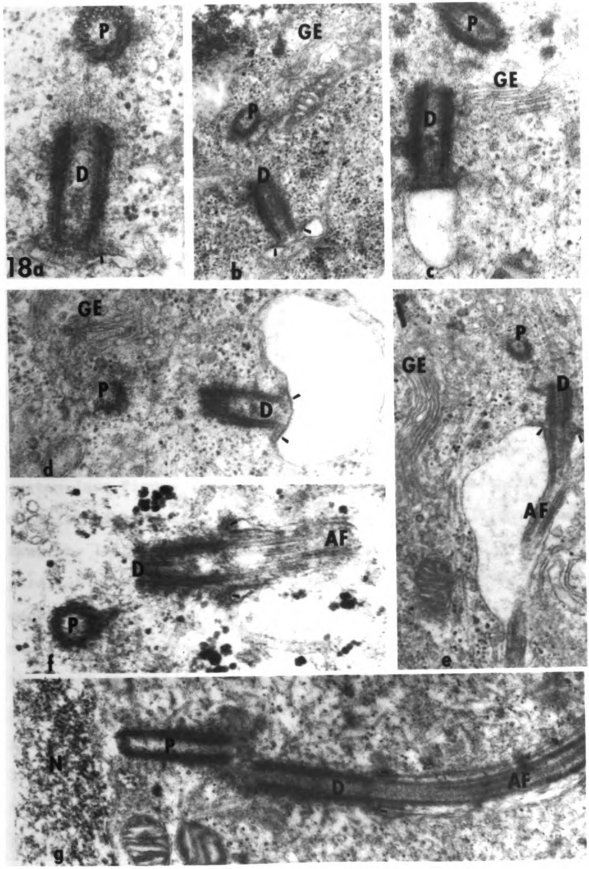
P
D
18a
GE
P
D
b
P
GE
D
c
GE
P
D
d
P
GE
D
AF
e
AF
D
P
f
N
P
D
AF
g

Th

species of

separate

F

Hemocoe

mber sh

figure

on the

muscles

ect ka

rmed

ached

he mu

ticke

ypes

mal

Paced

etail

descr

ow a

he e

Reco

he b

ther

his,

Rec

The remaining phases of spermiogenesis in the two species of Rana are significantly different to warrant separate descriptions.

Features Characteristic of Rana clamitans Spermiogenesis--Following axial filament formation the nuclei show a tendency to become round in section (Figure 19). Chromatin condensation is continuing but now the nucleoplasm has a fine granular appearance. Vesicles in close association with the nucleus may represent karyolymph and excess nuclear membrane which has been removed from the condensing nucleus. The centrioles have reached their final position at the posterior portion of the nucleus. The nuclear membranes in this region appear thicker and better defined than the remaining membrane system (see Figure 24b). This thickening, also seen in mammalian spermatids, is called the basal plate (Bloom and Fawcett, 1968). Mitochondria, circular in section and with parallel cristae, are beginning to associate with the centrioles for mid-piece formation. The Golgi elements, now a single element instead of multiple as observed in the early spermatid (Figure 20), have migrated to a position roughly half-way around the nucleus. Microtubules are becoming increasingly apparent (see Figure 23). Two intercellular bridges can be seen connecting three spermatids. The bridges are about 1 μm in diameter and are similar to those described in other species (Longo and

Figure 19. Cluster of spermatids, R. clamitans.
Note the Golgi elements (arrows), intercellular bridges (IB), granular condensing nuclei (N) centrioles (C) nuclear vesicles (Nv) axial filament (AF) and follicle cell cytoplasm (Fc).
x 10,200.

Figure 20. Golgi elements in spermatids, R. clamitans.
Note the spermatid nuclei (N) and the Golgi elements (GE).
x 17,400.

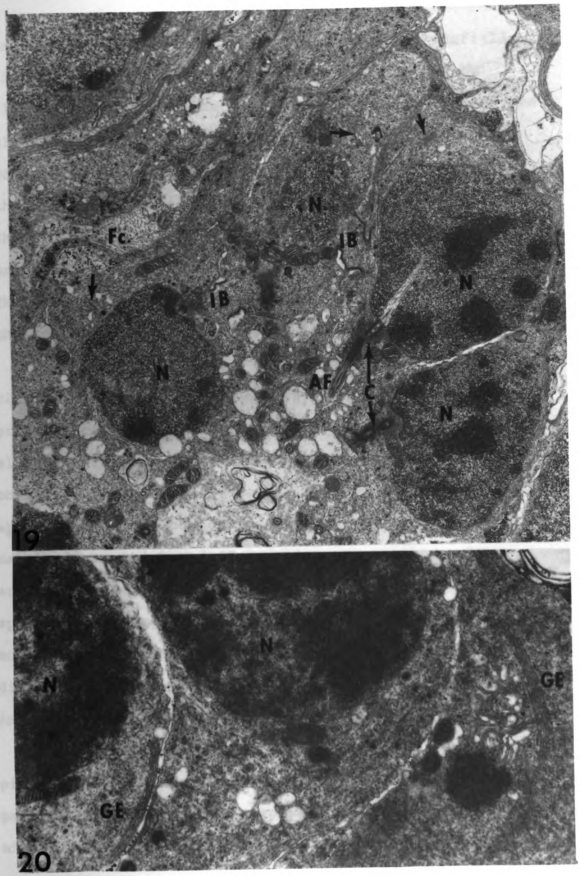
Fc
N
IB
IB
N
N
AF
C
N
19
N
N
GE
GE
20

Anderson, 1969 A&B; Fawcett, 1961; Longo and Dornfield, 1967; and Reger, 1963); that is, they are marked by electron dense thickenings on the cytoplasmic side of the plasma membrane. A rib-like structure similar to the connecting piece in mammalian spermatozoa has surrounded the centrioles (see Figure 21a and b). The extension of the proximal centriole into the nucleus may well be an artefact since this is the only time it was observed. The cytoplasm of the surrounding follicle cells is characterized by glycogen particles and microtubules.

Figure 21a shows a connecting piece. It is closely associated with the basal plate and "boxes in" the proximal centriole. Portions of the connecting piece are also seen in contact with the distal centriole. The obliquity of section is responsible for the incomplete appearance of the connecting piece. Nine ribs approximately 15 nm thick and 52 nm apart are visible. There are also nine ribs in the connecting piece of mammalian spermatids and spermatozoa. However in mammals it is a much more complicated structure, with quite different dimensions (Winstatt et al., 1966; Blom and Birch-Anderson, 1965 and Fawcett, 1965).

Figure 21b shows the relationship of the connecting piece to a centriole. The ribs appear to be extensions of part of a triplet. This very well may be the case since nine ribs can be counted in appropriate sections.

Figure 21. Sections through connecting pieces, R. clamitans.

a) x 33,000.

b) x 66,000.

Note the connecting pieces (CP), basal plate (BP), mid-piece mitochondria (M), proximal (P) and distal (D) centrioles. In (b) only a single centriole (c) is present.

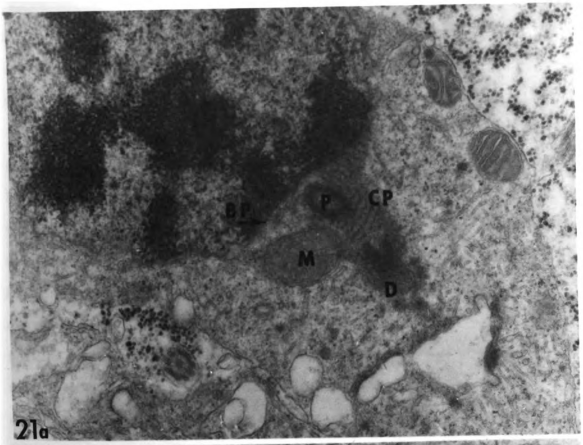

21a

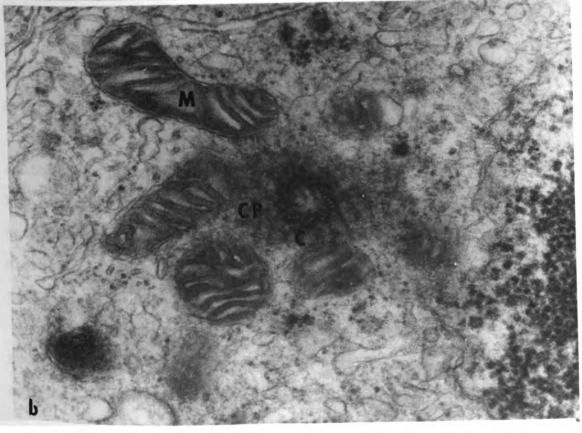

b

Extensions of the ribs are also visible in the interior of the centriole. Mitochondria are seen in association with the centriole for mid-piece formation.

Various types of dense bodies are seen in the cytoplasm of spermatids during this phase of development. Figure 22 shows two types of such bodies. It is not known what these inclusion bodies are, where they come from or what they do, but they appear frequently. Type 1 dense bodies are membrane bound with less dense cores. They average about 85 nm in diameter and are not seen in any future stages. Type 2 inclusions are smaller, about 50 to 70 nm in diameter and often appear in packets or scattered in the cytoplasm. They are not membrane-bound and appear to be made up of finely granular material. More will be seen of these as development proceeds. Note that the microtubules are arranged in a specific direction. A large amount of smooth endoplasmic reticulum is visible.

With the increase in nuclear condensation the first indications of nuclear elongation are occurring (Figure 23). The microtubules are arranging themselves along the future anterior-posterior axis of the developing sperm. These microtubules may be partially responsible for the elongation process.

By the time final nuclear condensation (but not nuclear compaction) has occurred, the first signs of acrosome formation are evident (Figure 24). The nucleus

Figure 22. Inclusion bodies in spermatid, R. clamitans.

Note the two types of cytoplasmic dense bodies (1 + 2), the mitochondria (M), microtubules (MT) and the smooth endoplasmic reticulum (SER).

x 26,100.

Figure 23. Microtubules in elongating spermatid, R. clamitans.

Note the microtubules (MT) and the centrioles (C).

x 17,400.

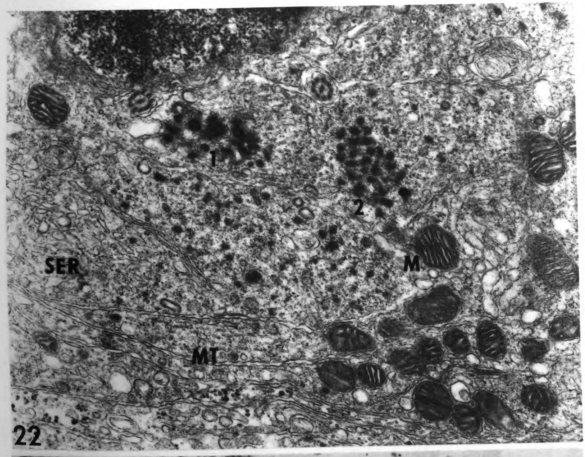

22

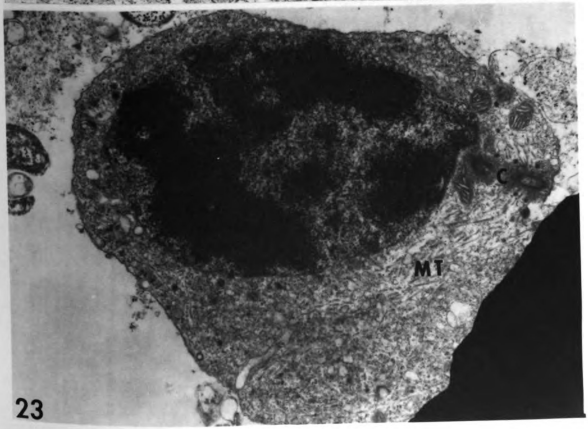

23

Figure 24. First signs of acrosome formation, R. clamitans.

a) x 15,300.

b) x 42,000.

Note the condensed but not yet compacted spermatid nuclei (N), what may be the remnant of the nucleolus (Nu), preacrosomal vesicles (arrow), type 2 cytoplasmic dense bodies (2), intercellular bridge (IB), basal plate (BP), mitochondria (M), axial filament (AF) and the Sertoli cell cytoplasm (Sc).

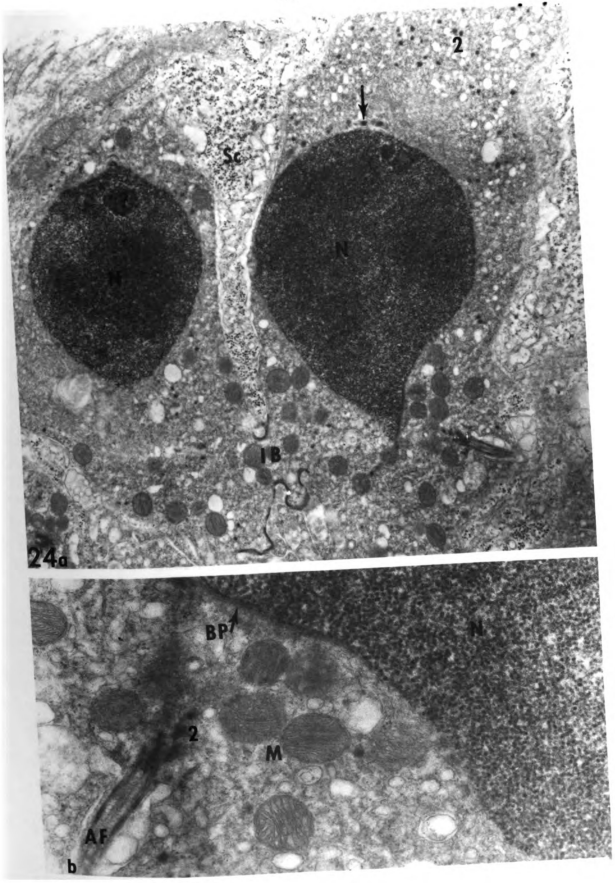
2
Sc
N
N
IB
24a
BP
N
2
M
AF
b

has a tightly packed dense granular appearance. The last remnants of the nucleolus are still evident. Large cisternal Golgi-like elements that may be rearrangement products of the smooth endoplasmic reticulum are seen (see Figure 25). No characteristic Golgi elements are seen at this stage and the origin of the cisternae and the fate of the Golgi seen in previous stages (Figures 17 and 19) are not known. Many vesicles are now seen in the cytoplasm and the mitochondria are circular in section (Figure 24b). The cristae are much thinner than in the mitochondria of previous stages and the matrix is denser (see Figure 21). Notice again the basal plate. Type 2 inclusion bodies are spread throughout the cytoplasm. Some, however, are in association with the centrioles. Dense preacrosomal vesicles are in close association with the anterior portion of the nucleus. The glycogen-rich Sertoli cell cytoplasm has separated the cells of the spermatid cluster. The intercellular bridges seem somewhat disarranged. This is due to the separation of the cells by the invading Sertoli cell cytoplasm.

Figure 25 shows the anterior portion of the nucleus prior to visible acrosome formation. The cisternal Golgi-like structure is clearly visible. Note the difference in size and density of the vesicles close to the anterior portion of the nucleus. The vesicles appear

somewhat smaller and more dense the closer they are to the nucleus.

Figure 26 shows the anterior portion of a spermatid which is actively engaged in acrosome formation. Note the large cisternal array and the membranous vesicles of various sizes and densities. Perhaps the vesicles arise from the cisternae in much the same way proacrosomal vesicles arise from the typical Golgi material in mammalian acrosome formation.

At least three phases of acrosome formation can be distinguished. 1) Forming phase: The cisternae give rise to the large clear vesicles. 2) Condensing phase: The large vesicles then move toward the nucleus, condensing as they go. 3) Acrosome phase: When the vesicles finally reach the anterior portion of the nucleus they are extremely dense and may now be called preacrosomal vesicles.

It is apparent that all the vesicles in the cytoplasm are not involved in acrosome formation. The type 2 dense bodies seen scattered throughout the cytoplasm do not appear to be associated with acrosome formation.

Figure 27 show progressive stages in the fusion of the preacrosomal vesicles. It is not known exactly when preacrosomal vesicles can be called acrosomes but by the time a membrane bound sac covering the anterior portion of the nucleus similar to that seen in Figure 27c is seen, the name immature acrosome may be appropriate.

Figure 25. Spermatid just prior to acrosome formation, R. clamitans.

Note the Golgi-like cisternal element (Cs) and the various type vesicles (V) around the nucleus (N).

x 42,000.

Figure 26. Forming acrosome, R. clamitans.

Note the cisternal element (Cs), preacrosomal vesicles (PA), and the type 2 cytoplasmic dense bodies (2). The three phases of acrosome formation; forming phase (Fp), condensing phase (Cp) and the acrosomal phase (Ap) are visible.

x 42,000.

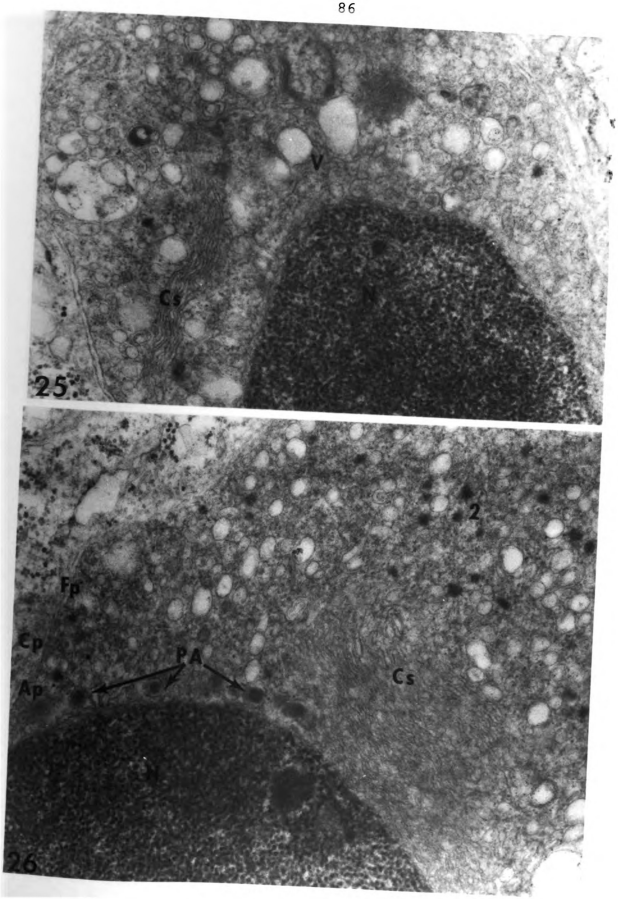
V
Cs
25
2
Fp
Cp
Ap
PA
Cs
26

Figure 27. Fusion of preacrosomal vesicles, R. clamitans.

a) x 26,000.

b) x 42,000.

c) x 33,000.

Note the fusing preacrosomal vesicles (Fa) at the tip of the spermatid nuclei (N), the cisternal element (Cs) and immature acrosome (IA).

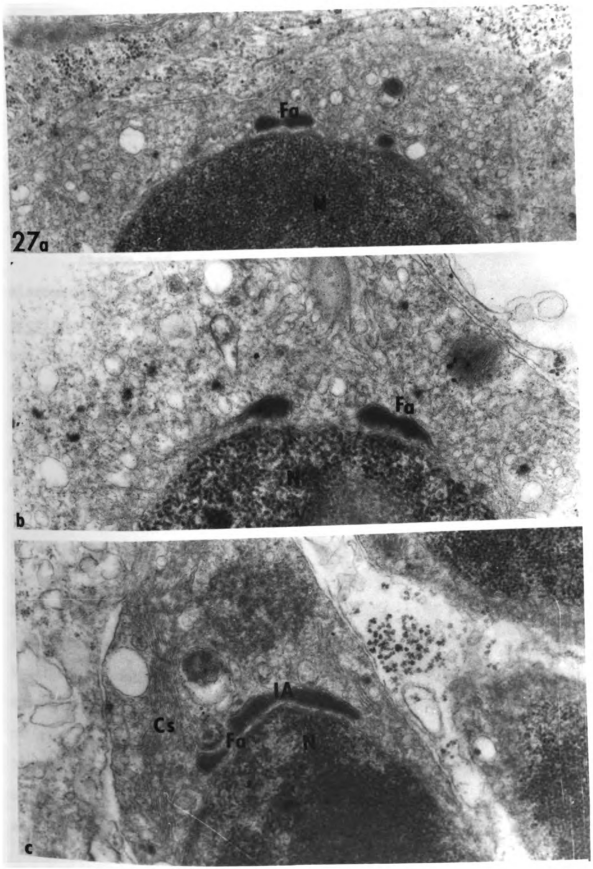
Fa
N
27a
Fa
N
b
IA
Cs
Fa
N
c

Burgos and Fawcett (1956) described acrosome formation in the toad at the electron microscopic level as a fusion of vesicles. They state that the spermatids lack conspicuous Golgi elements, but believe that the Golgi is represented by one or more very small aggregations of spherical vesicles of various sizes. No micrographs of this were shown.

Sharma and Sekhri (1955) describe at the light microscopic level Golgi elements in the spermatids of Rana tigrina as a few deeply staining granules scattered throughout the cytoplasm. These granules then coalesce near the centrioles to form what they call a proacrosome which migrates to a position at the anterior portion of the nucleus. This proacrosome increases in size to form the mature acrosome.

With acrosome formation, the nucleus continues to elongate (Figure 28). However, microtubules are no longer present; in fact, most have been displaced to the posterior portion of the cell in the residual cytoplasm which is now beginning to form. The invading Sertoli cell cytoplasm has completely separated the spermatids. The invasion of the cluster may also be responsible for the posterior movement of the spermatid cytoplasm. A small amount of cytoplasm is still visible at the anterior portion (acrosomal end) of the cell, very little being left in the lateral aspects and the remaining portion in the posterior region. Most

of the posterior portion will become the residual cytoplasm.

Figure 29 shows a section through a portion of the residual cytoplasm. It contains mitochondria, some of which seem to be deteriorating, microtubules, type 2 dense bodies, and vesicles of various sizes and densities. Notice that the axial filament is in the central portion of the residual cytoplasm. With further development the residual cytoplasm becomes extremely dense and organelles lose their identity.

Lipid droplets, mitochondria, ribosomes, endoplasmic reticulum, Golgi, multivesicular bodies, multigranular bodies and PAS-positive material have been described in the residual cytoplasm in a wide variety of mammalian species (Dauost and Clermont, 1955; Smith and Lacy, 1959; Lacy, 1960; Firlet and Davis, 1964 and Dietert, 1966).

By the time the nucleus has compacted, that is, has lost its granular appearance, the residual cytoplasm has reached the posterior portion of the nucleus (Figure 30). Intercellular bridges and mitochondria are the only structures still recognizable in the dense cytoplasm. Portions of the maturing acrosomes are visible on the elongating nuclei. Segments of the anterior excess cytoplasm are being eliminated into the Sertoli cell cytoplasm. The anterior excess cytoplasm may be analogous to the

Figure 28. Elongating spermatid, R. clamitans. Note the immature acrosome (A), spermatid nucleus (N), residual cytoplasm (Rc) and the Sertoli cell cytoplasm (Sc). x 17,400.

Figure 29. Residual cytoplasm, R. clamitans. Note the axial filament (AF), type 2 cytoplasmic dense bodies (2), vesicles (V), mitochondria (M) and microtubules (MT) in the residual cytoplasm (Rc). Portions of the Sertoli cell cytoplasm (Sc) and spermatid nuclei (N) can also be seen. x 17,400.

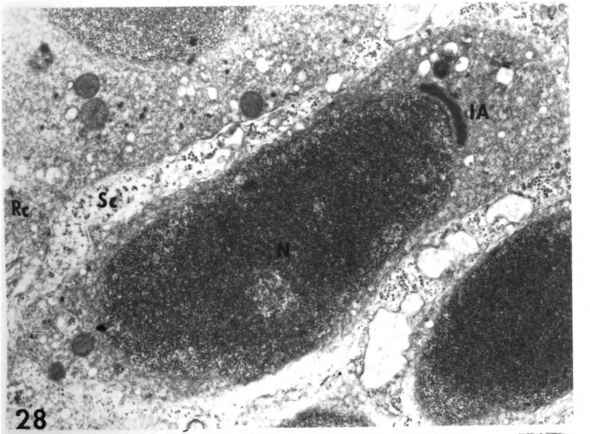

28

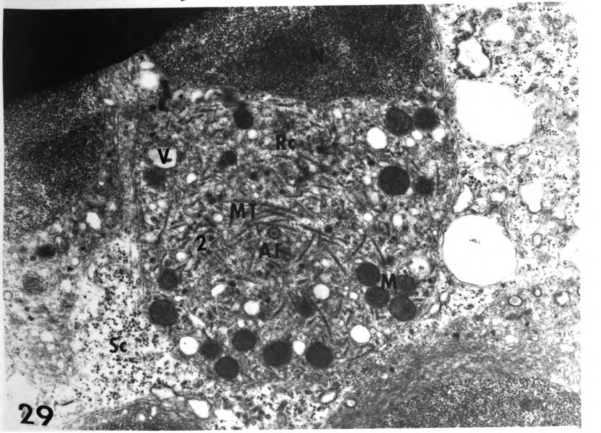

29

Figure 30. Nuclei in final stages of elongation, R. clamitans.

Note the anterior excess cytoplasm (Ac), intranuclear inclusions (I), immature acrosomes (IA), mid-pieces (MP), centrioles (C), and the residual cytoplasm (Rc) containing mitochondria (M) and intercellular bridges (IB). Portions of the Sertoli cell cytoplasm (Sc) are also visible.
x 10,200.

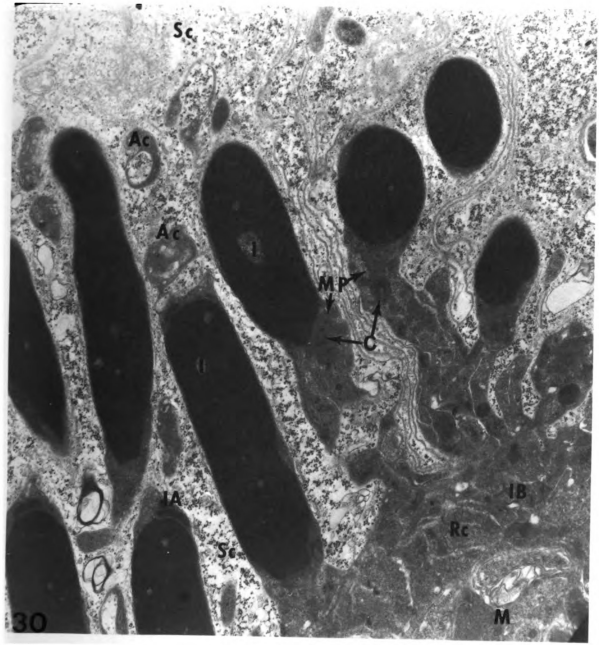
Sc
Ac
Ac
MP
C
IA
Sc
IB
Rc
M
30

cytoplasmic droplet seen in mammalian spermiogenesis. In mammals the residual cytoplasm and the cytoplasmic droplet are not the same. In mammals, final maturation occurs in the epididymis with the elimination of the cytoplasmic droplet. (See Bloom and Nicander, [1961] for an ultrastructural analysis of the cytoplasmic droplet in mammalian species.) Frog spermatozoa reach final maturity in the testes (Rugh, 1951 and van Oordt, 1960). Thus, similar processes may be occurring at different locales in the different species.

A large number of intranuclear inclusions are seen at this stage. For further discussion of this topic see the section entitled "Intranuclear Inclusions" p. 182.

With the final elongation of the nucleus the residual cytoplasm has proceeded over the mid-piece and has moved down the axial filament (Figure 31). While this is occurring, the anterior end of the nucleus elongates into a finger-like projection upon which the acrosome finishes its development by fusion of the remaining acrosomal vesicles (Figure 32).

Figure 33 is a diagramatic representation of nuclear elongation and residual body formation. (a) represents an early spermatid just after axial filament formation and just prior to nuclear elongation. The axial filament extends through the sleeve-like process of the spermatid cytoplasm. With the beginnings of nuclear

Figure 31. Mid-piece and tail with residual cytoplasm eliminated, R. clamitans.

Note the mid-piece, (MP), axial filament (AF) in the tail, glycogen (G) particles associated with the tail and portions of the residual cytoplasm (Rc). Microtubules (MT) in the Sertoli cell (Sc) are also visible.
x 10,200.

Figure 32. Maturing acrosome, R. clamitans.

Note the finger-like projection of the nucleus (F), the large, still immature, acrosomal vesicles (IA), anterior excess cytoplasm (Ac) and intranuclear inclusions (I).
x 33,000.

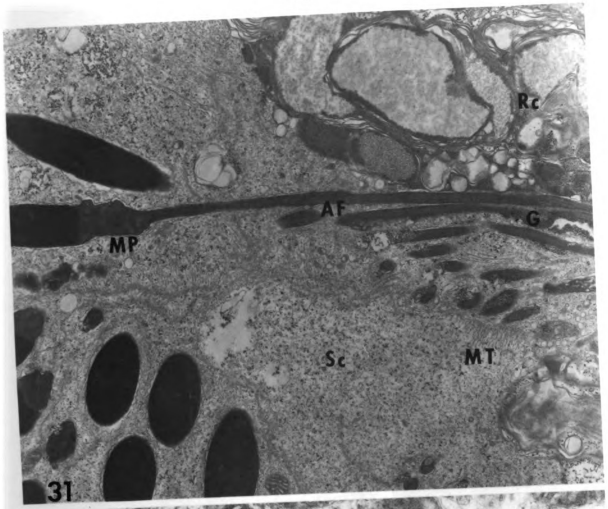
Rc
AF
G
MP
Sc
MT
31

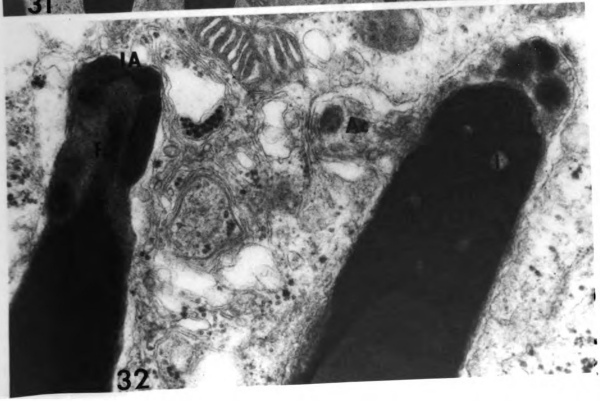
IA
32

Figure 33. Diagramatic representation of the elimination of the residual cytoplasm.

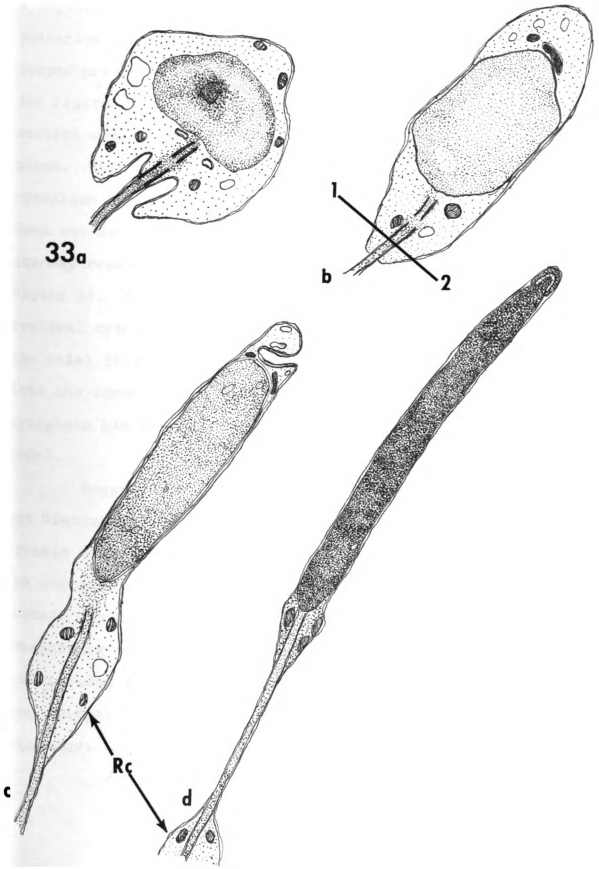
33a
1
2
b
c
Rc
d

elongation (b) the cytoplasm begins to collect in an area posterior to the nucleus. Note that the sleeve is no longer present. Line 1-2 is the proposed plane of section for Figure 29. Note that the axial filament in such a section would be represented in the middle of the cytoplasm. With continued nuclear elongation the residual cytoplasm begins to make its way past the mid-piece and down the axial filament. A longitudinal section through (c) may represent the section actually observed in Figure 30. Finally, in the fully elongated nucleus (d) the residual cytoplasm has made its way to the posterior end of the axial filament (see Figure 31) or has been eliminated into the lumen of the seminiferous tubule. Anterior excess cytoplasm has been eliminated in (d) of the diagramatic model.

Regaud (1901), Lacy (1960), Firlit and Davis (1965) and Dietert (1966) have described in mammals the phagocytosis of the residual cytoplasm by the Sertoli cell and its degradation as it migrates toward the basement membrane. Dietert (1966) and Brökelmann (1963) have demonstrated acid phosphatase activity in free granules and Golgi elements of the extruded residual cytoplasm. Dietert (1966) suggests that initial degradation occurs by lysosomal cytoplasmic autophagy.

No evidence of residual cytoplasmic phagocytosis by the Sertoli cells in either of the two species of Rana studied has been noted.

The final maturation product of spermiogenesis in R. clamitans can be seen in Figure 34. The nuclei are now long (15 to 17 μm), slender and very dense. The acrosomes have matured into bag-like structures at the anterior portion of the nucleus. The mid-pieces are formed and the residual cytoplasm has been eliminated.

Features Characteristic of Rana pipiens Spermiogenesis--The first noticeable difference in spermiogenesis between the two species concerns mid-piece formation. Figure 35 shows a portion of a spermatid cluster just after centriole migration and nuclear condensation. There is no indication of a connecting piece or basal plate as seen in R. clamitans spermatids of a similar stage of development (see Figure 21). The nuclear material condenses much earlier in R. pipiens spermatids. A similar stage of nuclear condensation is not reached in R. clamitans until the acrosomal formation stage (see Figure 24).

The cytoplasm has many free and rosetted ribosomes. Microtubules are randomly oriented. The mitochondria are oblong with parallel cristae. Those mitochondria not associated with the centrioles for mid-piece formation are located at the cell periphery. Few vesicles and no Golgi or Golgi-like elements are visible. Granular dense

Figure 34. Mature spermatozoa, R. clamitans.
Note the acrosomes (A) on the elongated nuclei, the mid-pieces (MP) and tails (T). Sertoli cell nucleus (Scn) and cytoplasm (Sc), along with residual cytoplasm (Rc) and degenerating spermatids (Ds) are also visible.
x 4,800.

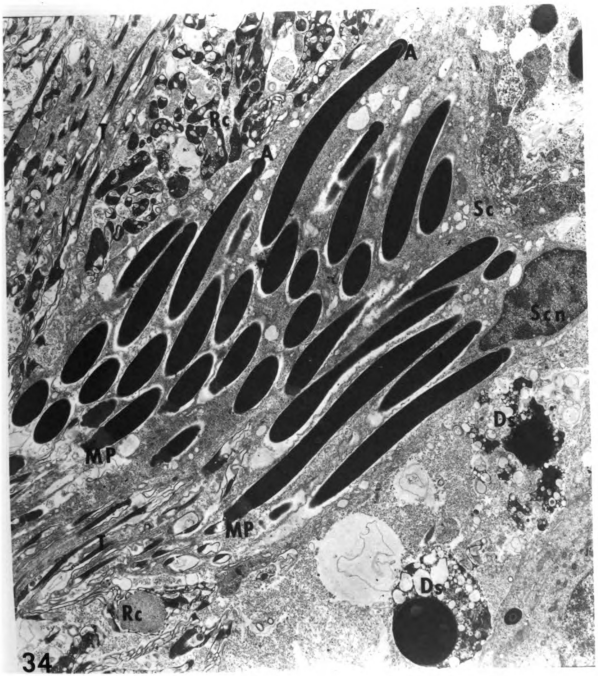
A
Rc
A
Sc
Scn
Ds
MP
MP
Ds
Rc
34

Figure 35. Spermatid, R. pipiens.

Note the condensed nucleus (N), proximal (P) and distal (D) centrioles, axial filament (AF), mitochondria (M), cytoplasmic inclusions (Ci), granular body (Gm) and microtubules (MT). Arrows indicate clumps of ribosomes. Glycogen (G) is visible in the Sertoli cell cytoplasm (Sc).

x 24,000.

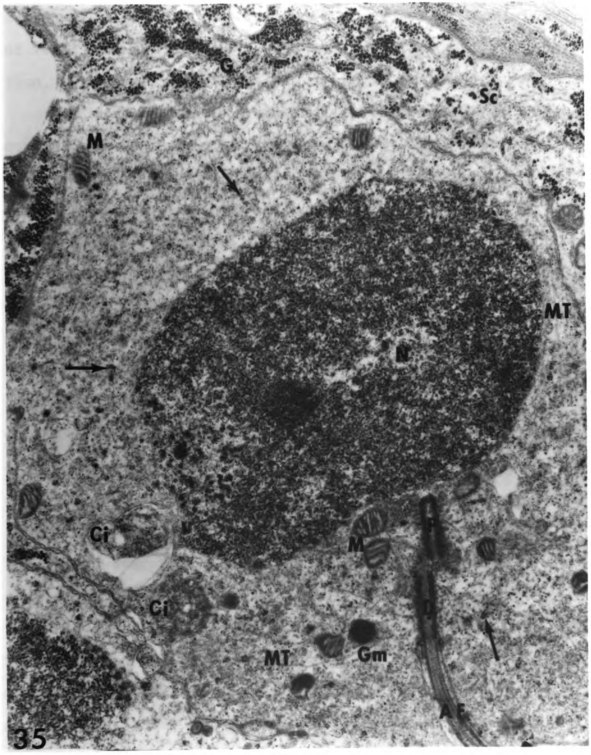
Sc
M
MT
N
Ci
Ci
M
MT
Gm
Ax
35

bodies about the size of mitochondria and inclusions, somewhat denser than the surrounding cytoplasm, consisting of vesicles and granular material, are visible. The function, origin and fate of these bodies is not known.

The Sertoli cell surrounding the spermatid cluster contains many α-type glycogen particles. There is a difference in density and size between the ribosome (18 nm) and the glycogen particles (28 nm).

Figure 36a shows a cell in the same cluster as that shown in Figure 35. The main purpose of this micrograph is to emphasize the apparent lack of Golgi-like material. The nuclear material shows signs of compacting and what may be a chromatoid body is present. Even with the beginning of elongation (Figure 36b) little or no change is observed in the cytoplasm. It may be noted that the spermatid cluster is retained, while in R. clamitans testes, clusters at similar stages are being broken up by the Sertoli cell cytoplasm (see Figure 24).

However by the time the nucleus is partially compacted, the cytoplasm has changed considerably (Figure 37). β-type glycogen particles become visible. There is also an increase in smooth endoplasmic reticulum. Smooth endoplasmic reticulum has been described (Coimbran and Leblond, 1966; and Millonig and Porter, 1960) as structural elements associated with glycogen production. Glycogen has not been observed in R. clamitans spermatids

Figure 36. Spermatids, R. pipiens.

a) x 17,400.

b) x 15,300.

Note the ribosomes (R), spermatid nuclei (N), chromatoid-like body (Cb) and axial filaments (AF).

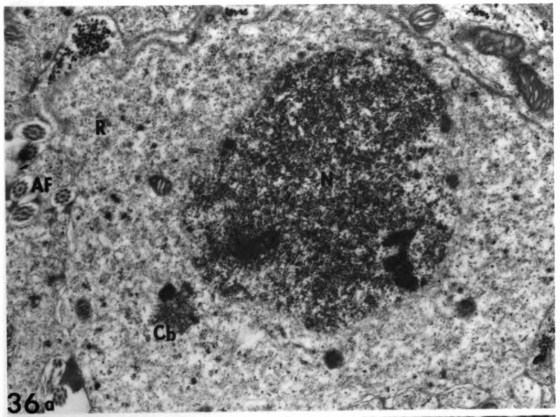

36a

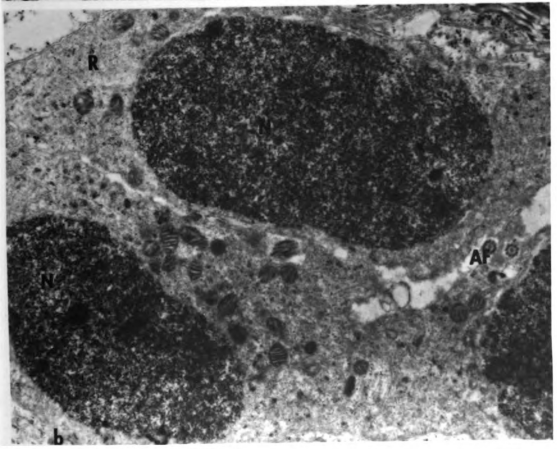

Figure 37. Condensing nucleus, R. pipiens. Note intranuclear inclusions (I), smooth endoplasmic reticulum (SER), glycogen particles (G), mitochondria (M), vesicles (V) and a Golgi-like element (GL). x 26,500.

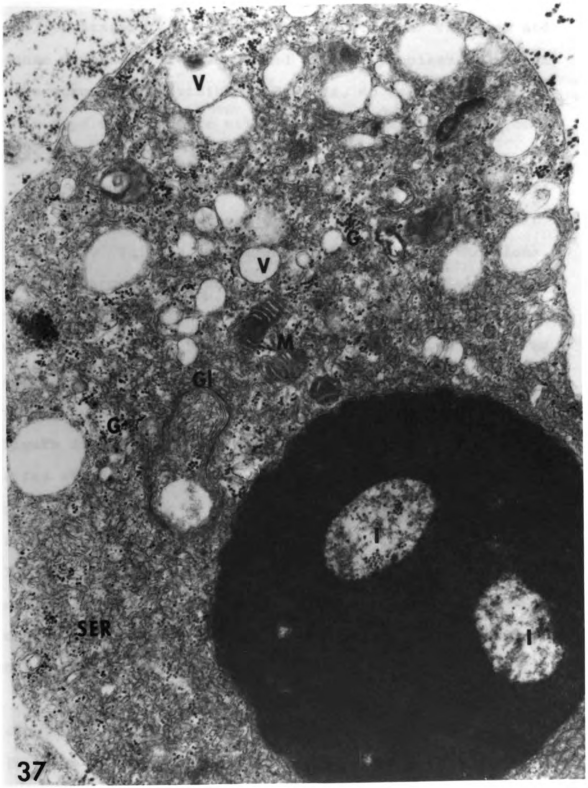
V
V
G
M
GI
G
I
I
SER
37

at this stage. Mitochondria resemble those described at earlier stages (see Figure 35). Large clear vacuoles and dense membranes are also found in the cytoplasm. A Golgi-like structure is visible. However, no association of this type of structure with acrosome formation could be made.

Figure 38 is a portion of a spermatid cluster at a stage in development somewhat later than that shown in Figure 37. This is an oblique section through the elongating spermatids. The amount of glycogen, which has substantially increased, is being formed in pockets, often associated with membranous scrolls. These scrolls may be excess nuclear membranes discarded during the compaction and elongation processes of nuclear development (see Figure 39). Numerous vesicles and vacuoles of various sizes and densities are visible in the cytoplasm. It is possible that some of these may function in acrosomal formation. However, no evidence for this is available. The mitochondria are clustered around the centrioles for mid-piece formation. Intracellular bridge, axial filament, microtubules and portions of the residual cytoplasm are all visible.

Figure 39a shows the membranous scrolls with their doubled membrane structure similar to nuclear membranes. Portions of the clustering glycogen particles are seen in association with these membranes.

Figure 38. Cluster of condensing nuclei, R. pipiens. Note centrioles (C), residual cytoplasm (Rc), intracellular bridge (IB), axial filaments (AF), glycogen particles (G), membranous scrolls (S) and vesicles (V).
x 12,500.

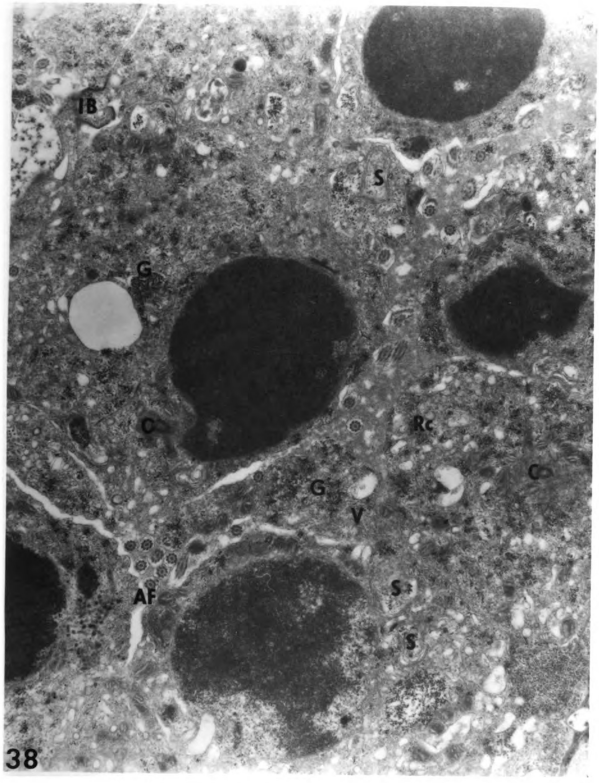
IB
S
G
C
Rc
G
V
C
AF
S
S
38

Figure 39. Membranous scrolls, R. pipiens.

a) x 44,000.

b) x 23,000.

Note membranous scrolls (S), glycogen particles (G), axial filaments (AF), and microtubules (MT).

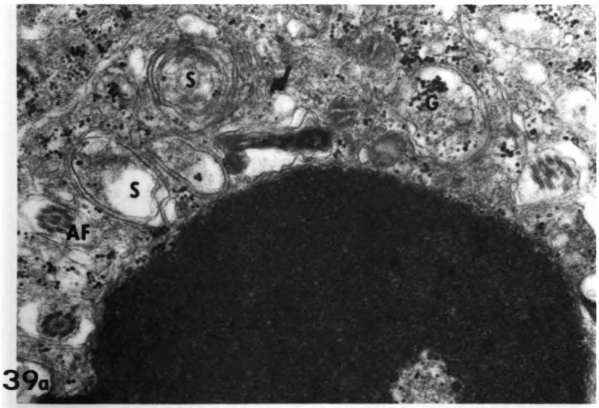

39a

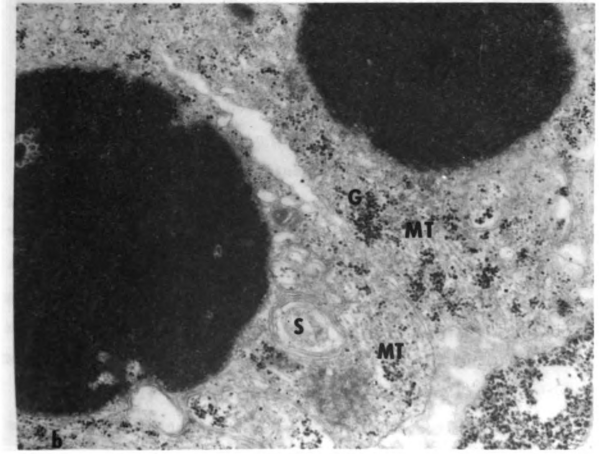

Figure 39b shows the orientated microtubules in the elongating spermatids. Membranous scrolls and clustering glycogen particles are also seen.

With the elongation and posterior migration of the residual cytoplasm, the spermatids appear to emerge out of the cluster. The glycogen particles are arranged in packets of varying densities. Portions of the membranous scrolls are seen in association with these packets. Mitochondria, intercellular bridges, axial filaments, and vesicles are still visible in the dense residual cytoplasm (Figure 40).

The residual cytoplasm with the massive amounts of glycogen is eliminated down the tail (Figure 41). In another portion of the cluster a partially elongated spermatid is seen with the residual cytoplasm at the area just posterior to the nucleus. Notice the size and density of the glycogen packets in the residual cytoplasm.

The "en masse" elimination of the residual cytoplasm and the process by which the Sertoli cell surrounds the individual sperm are different from what is observed in R. clamitans. In R. clamitans the Sertoli cell cytoplasm separates the spermatids at an early stage and the residual cytoplasm, is separately eliminated (see Figures 24 and 31).

Finally at maturation the spermatozoa are separately embedded in the Sertoli cell cytoplasm and

Figure 40. Emerging spermatid, R. pipiens.
Note the residual cytoplasm (Rc) containing packaged glycogen particles (G), intercellular bridges (IB), mitochondria (M) and axial filaments (AF). The emerging spermatid is surrounded by Sertoli cell cytoplasm (Sc). x 15,800.

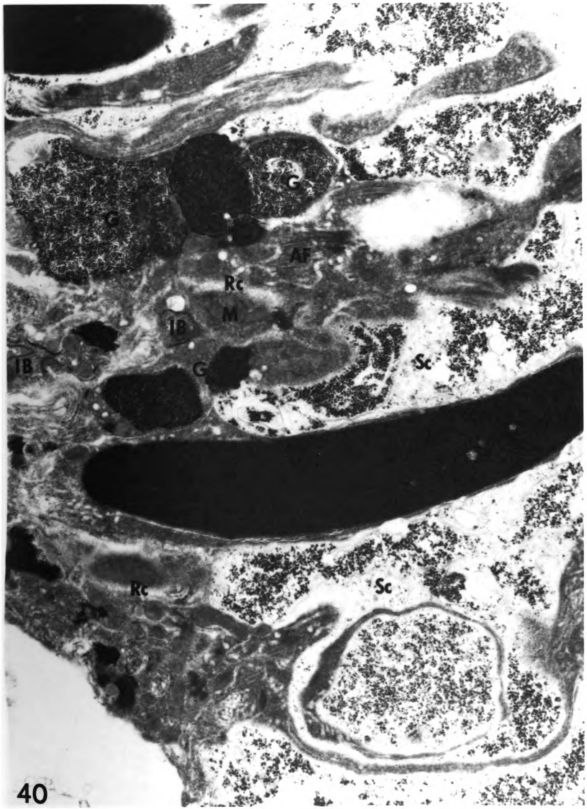
C
C
C
AF
Rc
M
IB
IB
C
Sc
Rc
Sc
40

Figure 41. Elimination of the residual cytoplasm, R. pipiens.

Note the Sertoli cell cytoplasm (Sc), sperm tails (T), mid-pieces (MP), residual cytoplasm (Rc), glycogen (G), intercellular bridge (IB) and microtubules (MT).

x 12,000.

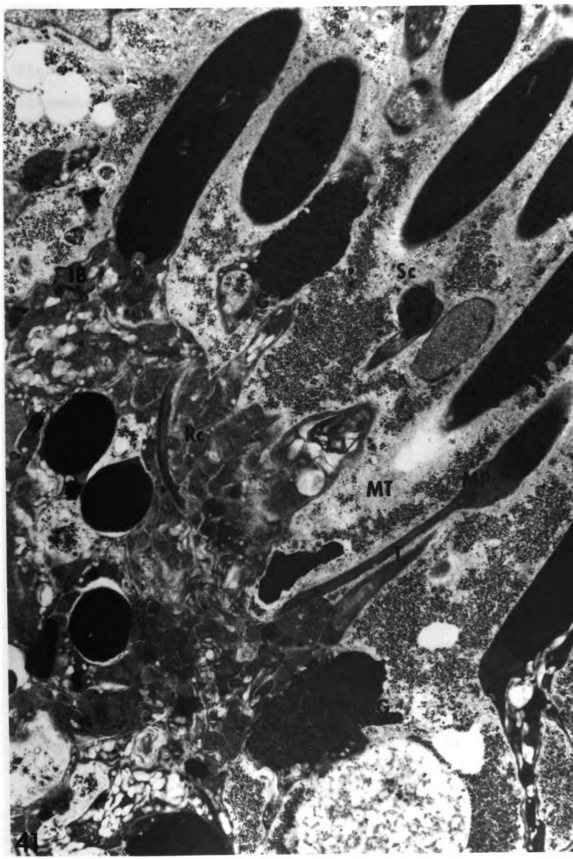
Sc
MT

the residual cytoplasm is for the most part eliminated (Figure 42). Acrosome, nuclei, mid-pieces and axial filaments are visible.

Acrosomal formation appears to take place in association with elongated nuclei. The progress is quite different from that observed in R. clamitans and from anything reported on in the literature. It will be discussed in the section entitled "Acrosomes of R. pipiens Spermatozoa" p. 145.

Figure 43 shows a portion of the residual cytoplasm still attached to axial filaments. At this stage the glycogen packets are dense and compacted and vacuoles appear in the cytoplasm. After the residual cytoplasm has been fully eliminated from the spermatozoa it becomes highly vacuolated and the dense packets of glycogen appear to swell (Figure 44a). Finally, vacuolization has honey combed the residual cytoplasm. The glycogen packets, still retaining some degree of orderliness, have reached sizes of 4 to 5 μm in diameter (Figure 44b).

This vacuolization of the residual cytoplasm may be an indication of degeneration. Since the vacuoles appear similar to lipid vacuoles it is possible that lipophanerosis (DeRobertis et al., 1960) may be involved.

Figure 42. Mature spermatozoa, R. pipiens.
Note acrosome (A) on the nuclei, mid-pieces (MP) and tails (T). Sertoli cell nuclei (Scn) and cytoplasm (Sc) are visible. Microtubules (MT) and residual cytoplasm (Rc) are also visible.
x 6,000.

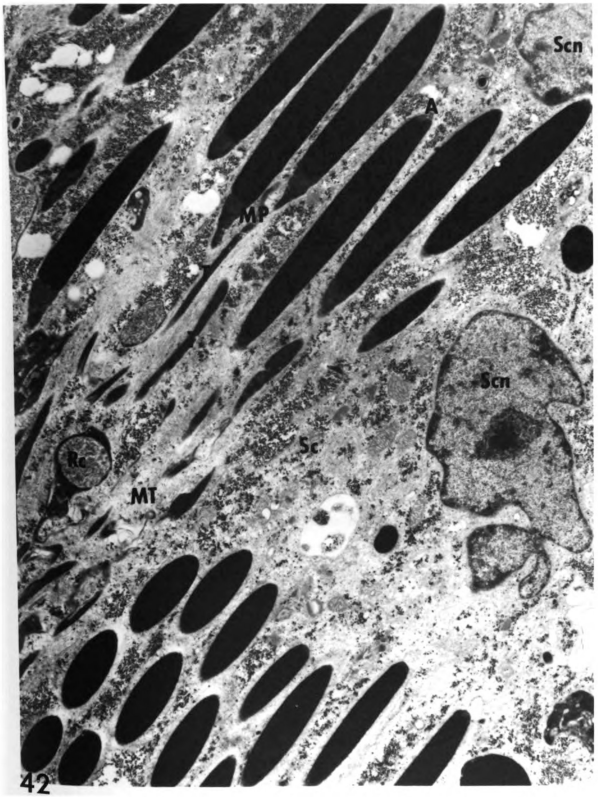

42

Figure 43. Residual cytoplasm, R. pipiens.
Note the glycogen packets (G) in the residual cytoplasm (Rc). The microtubules (MT) are in the Sertoli cell (Sc). The lumen (L) of the seminiferous tubules is also visible.
x 12,400.

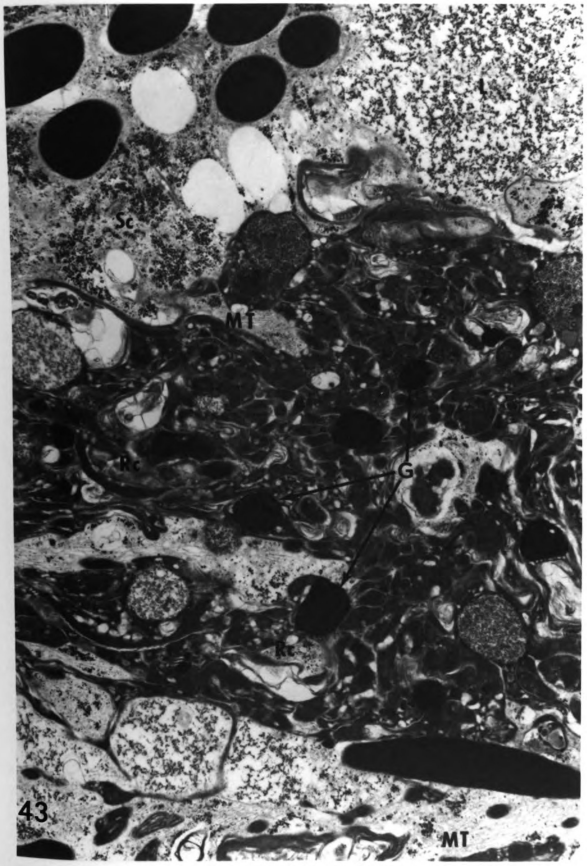

43

Figure 44. Eliminated residual cytoplasm, R. pipiens.

a) x 15,300.

b) x 17,400.

Note the vacuoles (V) and the glycogen packets (G) in the residual cytoplasm (Rc). Portions of the Sertoli cell (Sc) can also be seen.

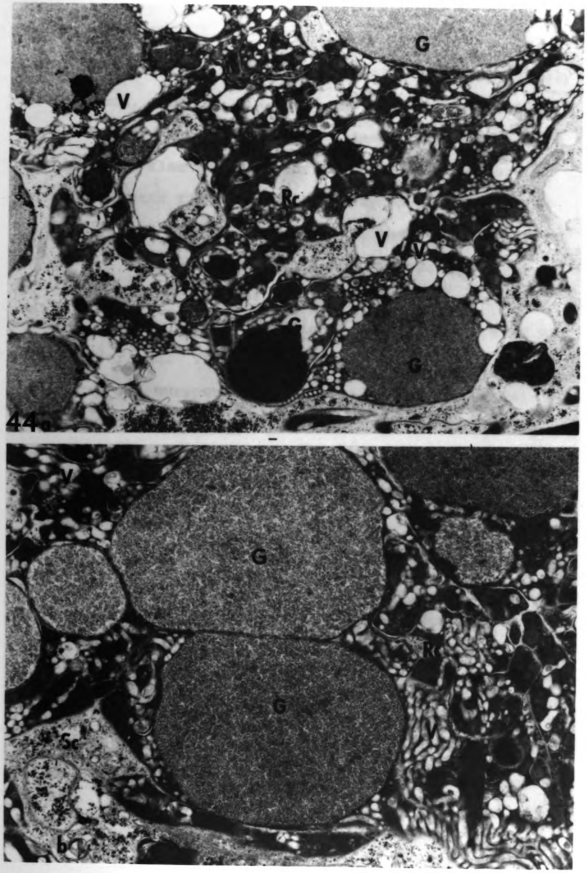
G
V
V
G
G
V
G
Sc

Mature Spermatozoa

All four principal spermatozoal structures, namely the acrosome, nucleus, mid-piece and tail are present in the mature spermatozoa of both species (see Figures 34 and 42). The fine structure of the acrosomes are so different in the two species that they will be discussed separately (see p. 140). The rest of the characteristics are similar enough to be described together.

Nuclei, Mid-Pieces and Tails--The spermatozoa of both species are elongated cylinders, slightly tapered at the anterior end. The nuclei of R. clamitans spermatozoa are longer and narrower (17 to 18 μm by 1.2 to 1.6 μm) than those of R. pipiens (12 to 13 μm by 1.7 to 2.0 μm).

A single plasma membrane surrounds the individual spermatozoa of both species while the nuclei are enclosed in a double membrane system (Figures 45 and 46b).

The nuclei are extremely dense and contain a variety of intranuclear inclusions including packets of glycogen particles and nuclear vacuoles. (For further discussion of these inclusions see the section entitled "Intranuclear Inclusions" p. 182). The anterior portion of R. clamitans spermatozoa is characterized by a finger-like projection of the nuclear material over which the acrosome forms (Figure 32). In R. pipiens spermatozoa the anterior portion of the nucleus forms a smooth curve with

Figure 45. Mid-pieces, R. clamitans.

a) x 33,000.

b) x 22,000.

Note the proximal (P) and distal (D) centrioles, mitochondria (M), axial filament (AF) with their associated glycogen (G) particles, connecting piece (CP), centriolar fossa (CF), double nuclear membrane (NM) and intranuclear inclusions (I). The surrounding Sertoli cell cytoplasm (Sc) is also evident.

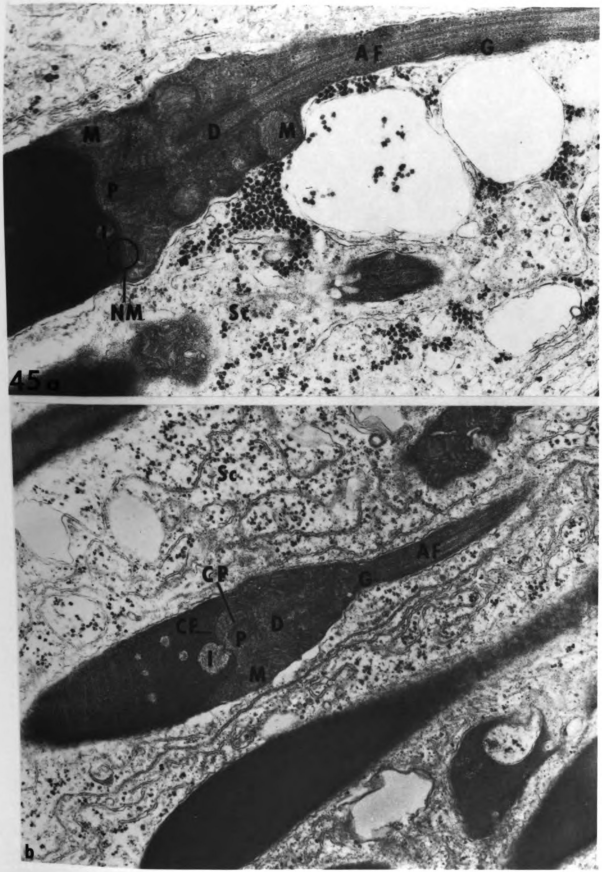
AF
G
M
D
M
P
NM
Sc
45
a
Sc
AF
CP
G
CE
P
D
M
b

Figure 46. Mid-pieces, R. pipiens.

a) osmium fixed. x 46,000.

b) osmium fixed. x 33,000.

c) x 22,000.

Note the mitochondria (M) with few cristae (Cr), the proximal (P) and distal (D) centrioles, axial filament (AF), double nuclear membrane (NM) and intranuclear inclusion (I).

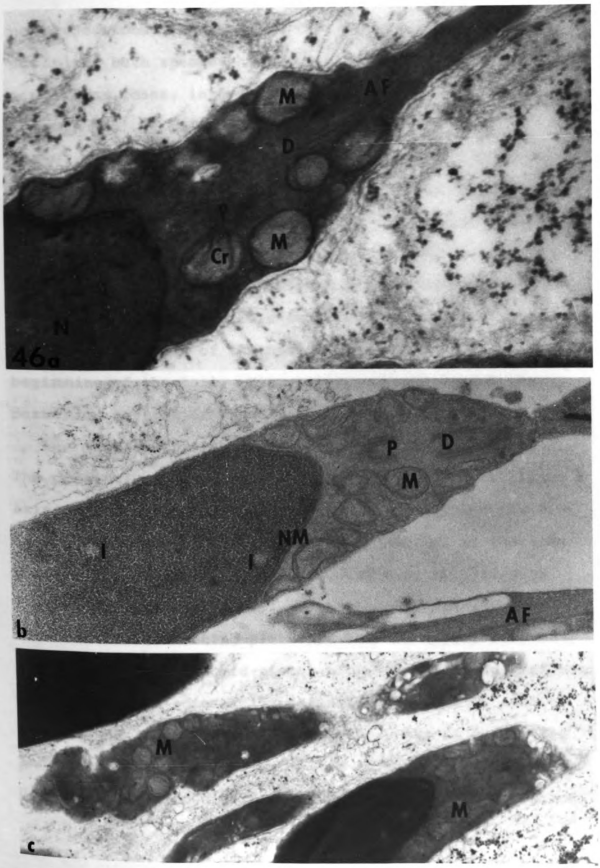
M
AF
D
P
Cr
M
N
46a
P
D
M
I
I
NM
AF
b
M
M
c

no projections (Figure 42). The posterior end of the nuclei of both species has a small indentation, called the centriolar fossa, into which the proximal centriole extends (Figure 45b).

The mid-pieces of both species are of the "primitive" type (André, 1962 and Nath, 1956); that is, they are short with the mitochondria clustered at the posterior end of the nucleus. The mid-pieces measure about 1.4 to 1.6 μm long from the centriolar fossa to the posterior end of the distal centriole and are tapered from about 1.3 μm at the base of the nucleus to about 0.3 μm at the beginning of the tail. Mitochondria extend beyond the posterior portion of the distal centriole.

Two centrioles are present (Figures 45 and 46). The proximal one lies at the 30 degree angle to the long axis of the sperm and extends into the centriolar fossa. The distal centriole lies in a plane parallel to the long axis. The basal plates, so distinctive in R. clamitans spermatids (see Figure 24), are no longer evident. Portions of the connecting piece are seen in appropriate sections through the mid-pieces of R. clamitans spermatozoa, but it has lost some of its definition as seen in earlier stages (see Figure 21). This, however, may be due to the increased density of the cytoplasm in the mature mid-piece. No connecting pieces were observed in R. pipiens mid-pieces.

The mitochondria of the mid-pieces are discrete (Figures 45 and 46), that is, not fused as they appear in mammalian species (Burgos and Fawcett, 1955 and André, 1962). The mitochondria bulge somewhat under the plasma membrane giving the mid-pieces a crenated appearance. Anderson and Personne (1969) described β-type glycogen particles only between the mitochondria in the mid-pieces of mature R. pipiens spermatozoa. Material fixed with Karnovsky's fixative shows β-type glycogen particles in the mid-pieces and in the tail of slightly immature spermatozoa of both R. pipiens and R. clamitans. With osmium fixation these particles have a "washed out" appearance. However glycogen-like particles were not observed in developing R. clamitans spermatids.

The mitochondria in the mid-pieces of the two species differ structurally. The cristae in the mitochondria of R. clamitans mid-pieces are parallel to each other and densely packed. The matrix is somewhat dense (Figure 45). Relatively few cristae are seen in R. pipiens mitochondria when compared (Figure 46) to those of R. clamitans. This difference does not appear to be due to the differences in the time of maturation since the testes of both species were fixed at approximately the same time in their spermatogenetic cycle. It is thought to be a true species variation.

The axial filaments arise from the distal centrioles (basal bodies) (Figure 45). Figure 47 shows a cross section through mid-pieces and centrioles. The typical array of nine triplets is seen. However, in three of the five distal centrioles visible in this section two additional tubules in the center of the triplets are visible. This may be the area of transition from the centriole to the axial filament. "Extra" tubules and glycogen are visible in some of the mid-pieces. Sections through the tail region still containing residual cytoplasm filled with vesicles and glycogen particles are also visible.

The axial filament complex in the tail of both species consists of the simple 9 + 2 pattern throughout its entire length (Figure 48). Figure 48a shows a section through a group of tails still enclosed in the Sertoli cell cytoplasm. This is an immature stage still containing dense residual cytoplasm, including "extra" tubules and glycogen particles. A double tail is also visible.

With final maturation the tail extends into the lumen of the seminiferous tubule (Figure 48b). The "extra" tubules and glycogen have been eliminated and the cytoplasm is less dense. Spokes connect the outer doublets with the inner pair of tubules. Occasionally arms are visible on the A tubule of the doublets.

Figure 47. Cross sections through nuclei, mid-pieces and tails, R. clamitans.

Note the centrioles (C) and the areas of transition between the centrioles and the axial filaments (IC), axial filament (AF), residual cytoplasm (Rc), mitochondria (M), intranuclear inclusions (I) and the Sertoli cell cytoplasm (Sc) with its glycogen (G) particles.

x 22,000.

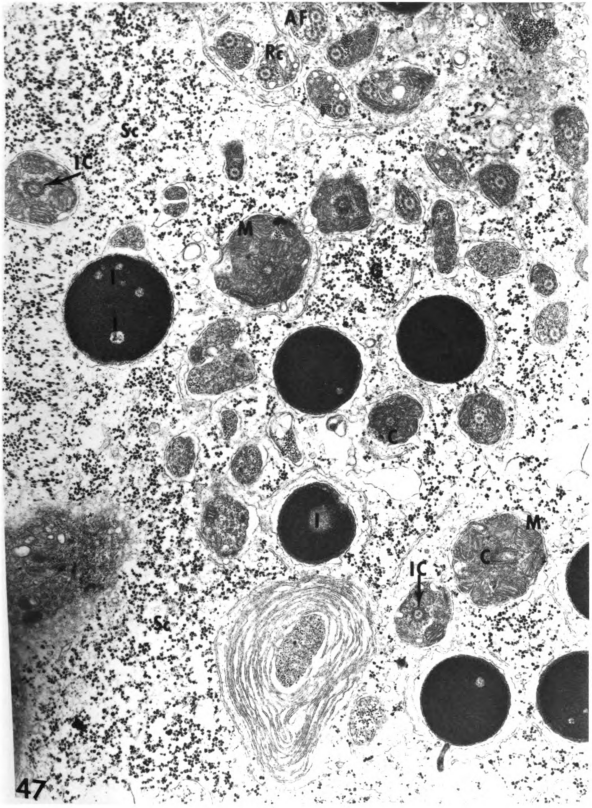
AF
Re
Sc
IC
M
L
L
C
L
M
C
IC
Sc
47

Figure 48. Cross sections through the tail region.

a) R. clamitans. x 66,000.

b) R. pipiens. x 66,000.

Note the sperm plasma membrane (SM), a "double" tail (DT), Sertoli cell cytoplasm (Sc), glycogen particles (G), portion of the lumen (L) of the seminiferous tubule and "extra" tubules (E).

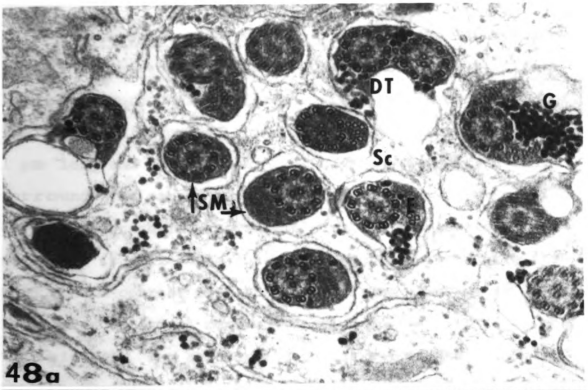
DT
G
Sc
SM
48a

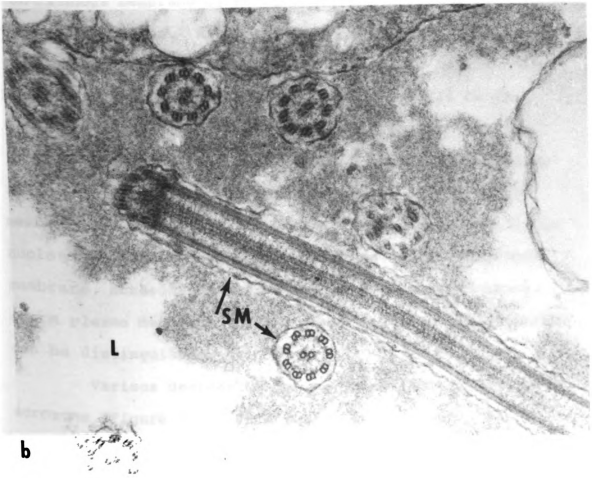
SM
L
b

Acrosomes of R. clamitans Spermatozoa--An acrosome of a R. clamitan spermatozoön consists of a sac(s)-like structure surrounding a finger-like anterior projection of the nucleus (Figure 49). An acrosome is approximately 1 μm long and 0.7 μm wide. The continuous membrane that surrounds the sac is divided into two parts. That portion of the membrane in association with the double nuclear membrane is called the inner acrosomal membrane while the portion in contact with the sperm plasma membrane is called the outer acrosomal membrane (arrows indicate the area of transition). The acrosomal material surrounded by the continuous membrane is homogeneous and slightly less dense than the nucleus. A sub-acrosomal space is visible between the inner acrosomal membrane and the double nuclear membrane. Excess sperm plasma membrane can still be seen; these membranes will be eliminated at final maturation.

Figure 50 is a cross section through an acrosome and nuclear projection showing the relationship of the membranes. Beginning at the center with the nucleus, the nuclear membranes, sub-acrosomal space, inner acrosomal membrane, acrosomal material, outer acrosomal membrane, sperm plasma membrane and the Sertoli cell plasma membrane can be distinguished.

Various degrees of lobing are evident in the mature acrosome (Figure 51). This lobing is apparently due to incomplete fusion of the preacrosomal vesicles.

Figure 49. Acrosome, R. clamitans.

Note the acrosome (A), the finger-like (F) projection of the nucleus (N), extra sperm plasma membranes (EM), nuclear membranes (NM), sub-acrosomal space (Ss), inner acrosomal membrane (Ia), outer acrosomal membrane (Oa), sperm plasma membrane (SM) and Sertoli cell membrane (Scm). Arrows indicate transition from inner to outer acrosomal membranes. x 125,000.

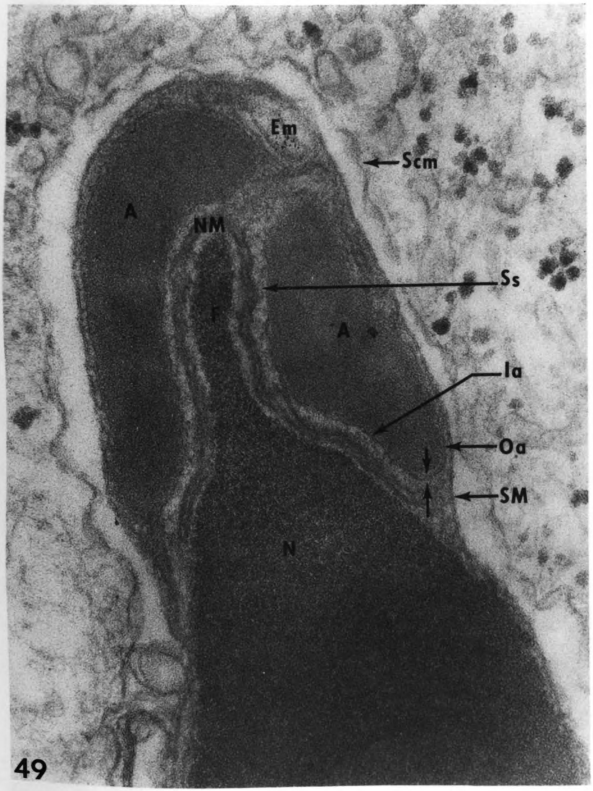

49

Figure 50. Cross section through acrosome, R. clamitans. Note the nucleus (N), nuclear membranes (NM), sub-acrosomal space (Ss), inner acrosomal membrane (Ia), outer acrosomal membrane (Oa), acrosome (A), sperm plasma membrane (SM) and Sertoli cell membrane (Scm). x 102,000.

Figure 51. Lobed acrosome, R. clamitans. Note the three lobes to the acrosomes (A). The sperm nuclei (N) and portions of the Sertoli cell cytoplasm are also visible. x 42,000.

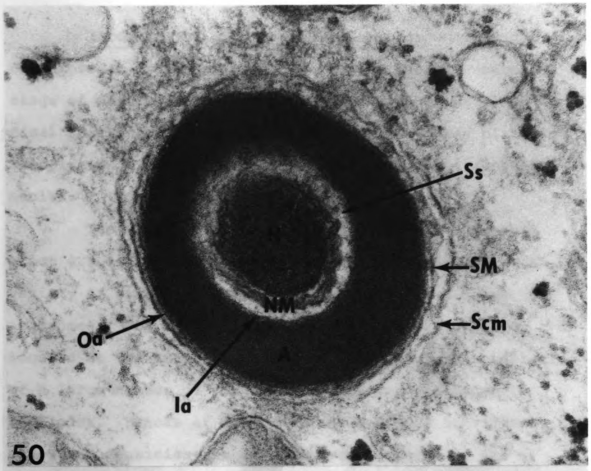

50

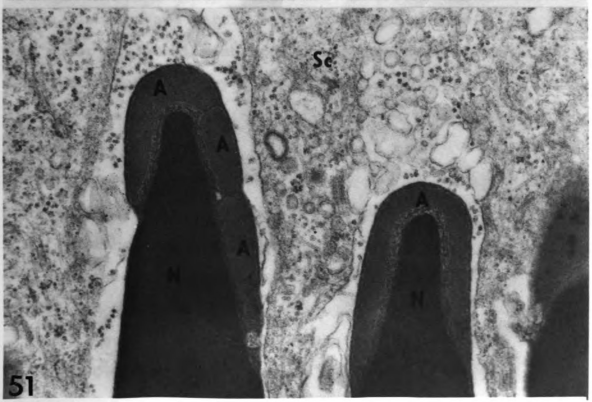

51

Acrosomes of R. pipiens Spermatozoa--No indications of acrosomal formation were observed in the mid-spermatid stage of development. Acrosomal formation or at least final rearrangement of acrosomal materials takes place in association with elongated, fully condensed and compacted nuclei.

The acrosomes of R. pipiens spermatozoa measure about 0.5 to 0.7 μm in length by 1.0 to 1.2 μm wide. A variety of structural elements are observed in these acrosomes. The most prominent is a acrosomal granule, located at the anterior portion of the acrosome, consisting of a large number of tightly packed β-type glycogen particles. Stacks of membranes and vesicles of various sizes and densities are also observed. However, all of these elements are rarely seen in any one acrosome. Inner and outer acrosomal membranes are not present. The whole structure is bounded by the sperm plasma membrane.

It should be pointed out that since ejaculated spermatozoa could not be fixed properly, using a wide variety of techniques and fixatives, the acrosomal structure of fully mature spermatozoa can not be described. The following describes, therefore, elements observed in the acrosomes of spermatozoa with fully elongated, condensed and compacted nuclei.

Figure 52 show acrosomal granules containing PAS and PA-TSC-SP-positive β-type glycogen particles (see

Figure 52. Acrosomal granules, R. pipiens.

a) x 26,100.

b) x 66,000.

c) x 33,000.

d) x 33,000.

e) x 33,000.

f) x 26,000.

Note the acrosomal granules (Ag). d, e, and f are fixed with osmium tetroxide alone.

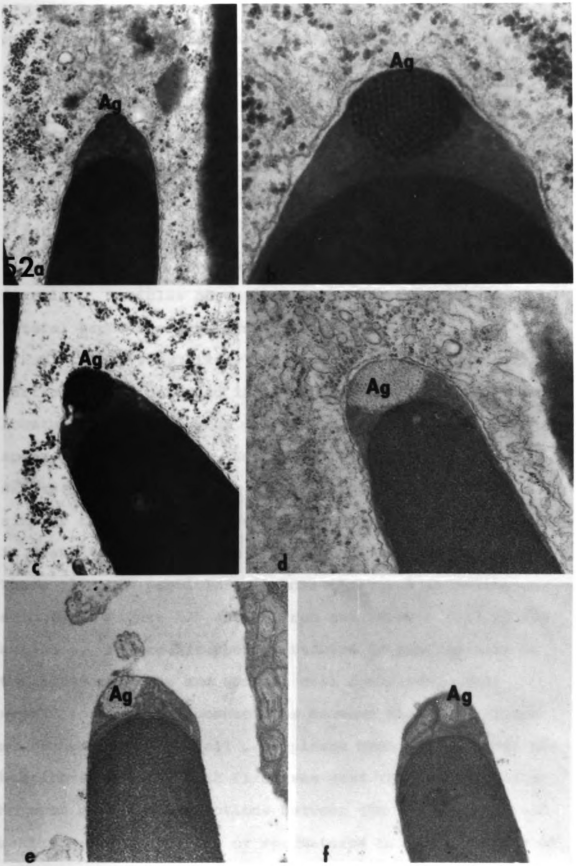

52a

e, and f

section entitled "Histochemistry" p. 186). Individual glycogen particles are about 20 nm in diameter and appear to be arranged in rows. This arrangement is similar to that seen in the residual cytoplasm (see Figure 41). The whole acrosomal granule measures about 0.5 μm in diameter. The granule has a "washed out" appearance with osmium fixation (Figure 52d, e, and f). The sperm plasma membrane surrounding the granule is more apparent after osmium fixation. Vesicles of various sizes are seen in the lateral aspects of the acrosome.

It is very likely that the constituent glycogen particles were produced in the spermatid stage and became located in the acrosomal granule by the collapsing of the sperm plasma membrane. However, another possibility exists. Figure 53a shows α-type glycogen particles similar to those in the Sertoli cell cytoplasm apparently in transition between the Sertoli cell and the acrosome. These glycogen particles may move through a tube-like structure (Figure 53b and c) from the Sertoli cell to the acrosome. Figure 53c shows particles of similar size in the acrosome, tube and Sertoli cell cytoplasm. What appear to be actual connections between the sperm plasma membrane and the Sertoli cell plasma membrane (arrows) has been observed with both fixatives used (Figure 53d and e). No such membrane connections between the Sertoli cell and membranes of spermatids or spermatozoa have been previously

Figure 53. Possible mechanism for acrosomal granule formation, R. pipiens.

a) x 33,000.

b) x 26,000.

c) x 26,000.

d) x 33,000.

e) x 33,000.

Note the acrosomal tube (At). The arrows indicate connections between the sperm and Sertoli cell plasma membranes. An acrosomal vesicles (Av) is also seen. e was fixed with osmium alone.

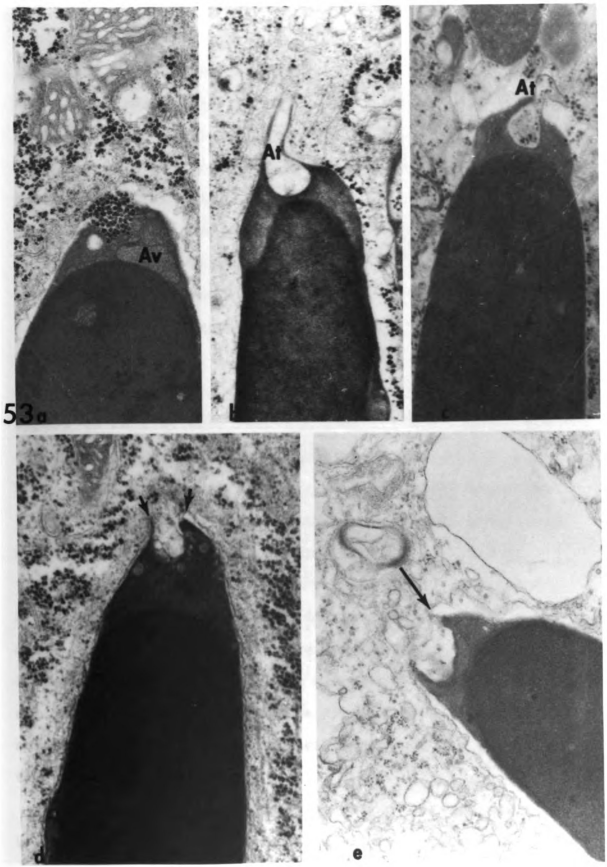
Av
Af
Af
53a
b
c
d
e

reported. However, Nicander (1967) showed extension of the sperm plasma membrane, similar to that shown in Figure 53b in an immature bull sperm. Burgos and Vitale-Calpe (1967) observed vesicles at the anterior portion of "late spermatids" in the toad. However no connection between the spermatids and Sertoli cell was mentioned. Once the granules migrate into the acrosome they appear to change configuration from α-type rosettes to highly ordered β-type particles.

Other structures seen in the acrosomes are the stacks of membranes. As many as six separate membranes have been observed in one acrosome (Figure 54a). These appear to be flattened membrane sacs and not tubules for nothing that would resemble tubular cross-sections has been observed. The sacs in the most compacted state are 7.0 to 9.0 nm apart. The distance between the continuous membranes of a single sac measure about 1.8 to 1.9 nm (Figure 54c). However, these distances vary considerably. After Karnovsky's fixation (post-fixed with osmium) a dense fiber is seen between the layers of the collapsed sacs (Figure 54b). The double membrane of the sac is similar to the nuclear membrane (Figure 54d). In fact the nuclear membrane is clearly visible only in the area of the stacks (Figure 54e).

Vesicles forming from the stacks or, alternatively, vesicles forming new stacks can be seen (Figure 54b).

Figure 54. Membranous stacks, R. pipiens.

a) x 33,000.

b) x 57,000.

c) x 33,000.

d) x 33,000.

e) x 33,000.

f) x 26,000.

Note the acrosomal membranous stacks (As), intranuclear inclusion (I). Arrows in b and c indicate vesicles forming from or forming new membranous stacks. c, d, and e were fixed with osmium alone.

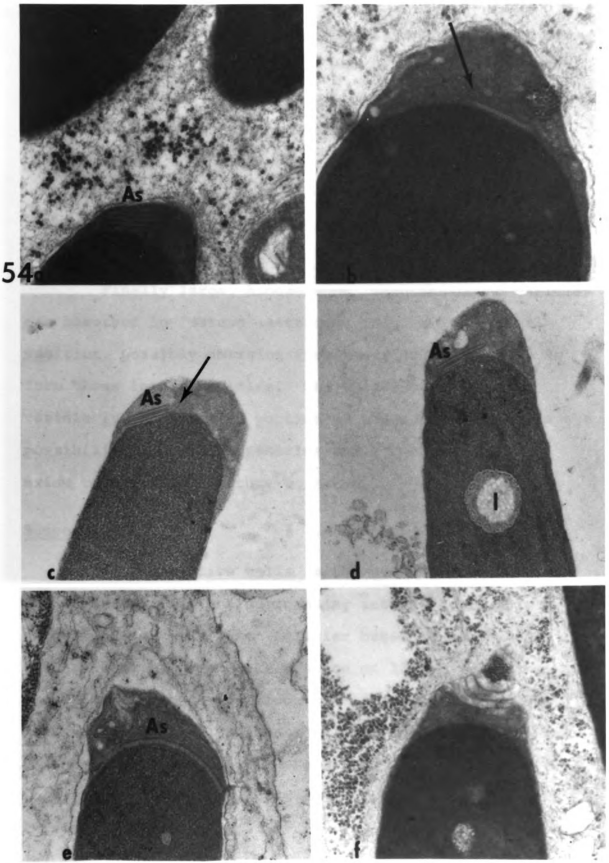
54
As
a
b
As
c
As
I
d
As
e
f

Membrane vesicles are also visible at the lateral aspects of fully formed stacks (Figure 54c).

An interesting micrograph (Figure 54f) shows what may be the formation of the stacks. These dilated sacs could collapse to form the densely packed stacks.

It should be pointed out that extensive membrane stacks are never seen in the same section as the acrosomal granule.

Finally large, homogeneous, membrane-bound vesicles are observed in "mature" acrosomes (Figure 55). Small vesicles, possibly emerging from the stacks, may fuse to form these larger vesicles. The existence of a large vesicle in the anterior portion of the acrosome negates the possibility that these vesicles and acrosomal granules exist together in a mature acrosome.

Supportive Cells

The supportive cells in the seminiferous tubule are separated from the surrounding interstitial cells by a thin (60 nm thick), non-cellular basement membrane (Figure 56a, b, c and d). A space of 30 to 120 nm separates the cells of the seminiferous tubule from the basement membrane. Although the basement membrane is known to be PAS positive in the toad (Burgos and Vitale-Calpe, 1967A), in R. pipiens (Cavazos and Melampy, 1954) and in mammals (Wislocki, 1949), no indication of any positive reaction

Figure 55. Acrosomal vesicles, R. pipiens.

a) x 33,000.

b) x 42,000.

c) x 33,000.

Note the large acrosomal vesicles (AV).

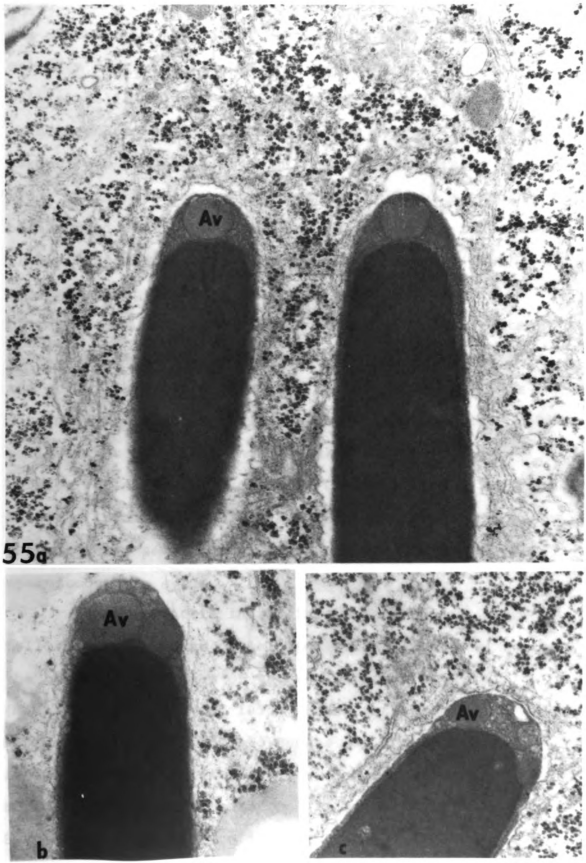
Av
55a
Av
b
Av
c

was observed in this study (see Figure 66b). A layer of collagen separates the basement membrane from the interstitial cells (Figure 56c). No additional layer of spindle-shaped cells, as described by Burgos (1960) and Gardner and Holyoke (1964) in mammals, is visible.

The basement membrane generally forms a smooth base around the tubule: however in some cases it becomes highly irregular and branchings occur. Burgos (1960) suggests that the branchings may indicate areas of pinocytosis. They also may aid in anchoring the sustentacular cells to the basement membrane. Half-desmosomes are occasionally seen which may also function for this purpose (Figure 56d). Burgos and Vitale-Calpe (1967 A&B) believe that the infoldings may also supply a larger surface for metabolic exchange. Clermont (1958) suggests that the infoldings provide a mechanism for changes in the volume of the seminiferous tubules that occur during the spermatogenetic cycle.

Spermiogenesis in amphibians takes place within follicular structures called spermatocysts that rest on the basement membranes of the seminiferous tubules (Houssay, 1954; Burgos, 1955; Burgos and Fawcett, 1956; Burgos and Ladman, 1957 and Burgos and Vitale-Calpe, 1967A). A spermatocyst consists of germinal cell(s) surrounded by sustentacular cells, either follicle or Sertoli cells, which are different stages of the same

Figure 56. Follicle cells and basement membranes.

a) R. clamitans. x 6,000.

b) R. pipiens. x 5,100.

c) R. clamitans. x 17,400.

d) R. pipiens. x 20,700.

Note the basement membrane (BM), follicle cells (Fc), desmosomes (De), spermatogonia (Sa), spermatocytes (Se), microtubule (MT), Sertoli cell cytoplasm (Sc), collagen (C) and half-desmosome (Hde). Arrows indicate apposing follicle cell plasma membranes.

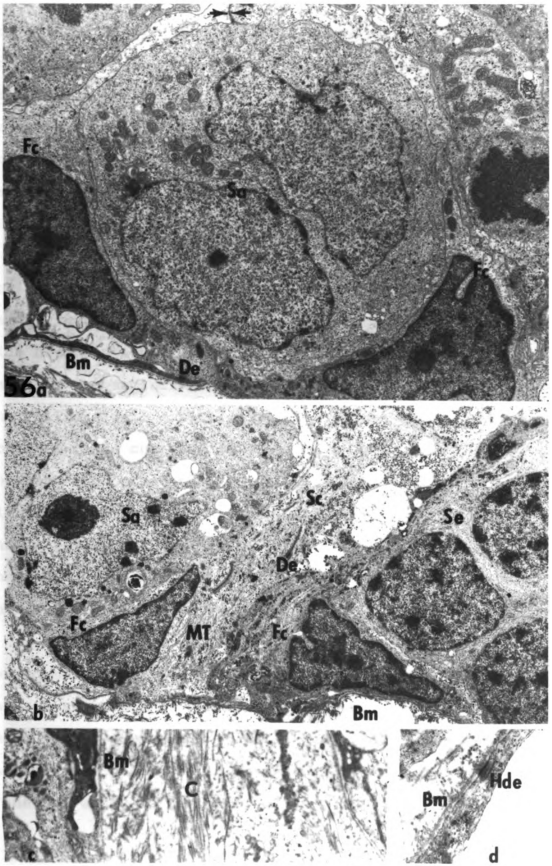
Fc
Sa
Fc
Bm
De
56a
Sa
Sc
Se
De
Fc
MT
Fc
b
Bm
Bm
C
c
Bm
Hde
d

sustentacular cell type. In all stages of spermatogenesis the germinal cells are separated from the blood supply, which is in the interstitial area, by the basement membrane and supportive cells. This is different from what is observed in mammals where spermatogonia and primary spermatocytes are in direct contact with the basement membrane (Elftman, 1963).

Spermatogonia are surrounded by at least two follicle cells and all the products of spermatogenesis remain in the cyst. With nuclear elongation, the spermatids become associated in clusters perpendicular to the walls of the seminiferous tubule, each cluster related to one follicle cell. With maturation of the sperm, the follicle cells change from a flattened cell into a large columnar type cell, the Sertoli cell. With this transformation the spermatocyst breaks down (Burgos and Fawcett, 1956 and Burgos and Vitale-Calpe, 1967A). The elongating spermatids complete their development not surrounded by but interdigitating with the cytoplasm of the Sertoli cells.

Figure 57 is a diagramatic representation of the development of the follicle to a Sertoli cell. Figure 57a shows a spermatocyst containing a primary spermatogonium surrounded by two follicle cells (also see Figure 56a). The follicle cells are in contact with the basement membrane and encircle the germ cell. There is, at the base

Figure 57. Diagramatic representation of follicle cell to Sertoli cell development.

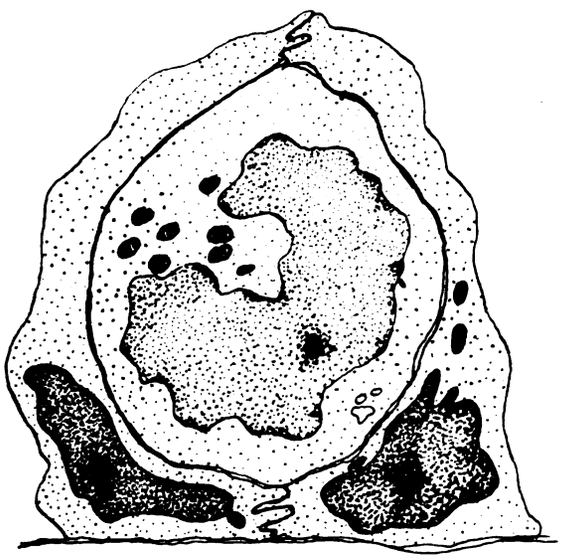

57a

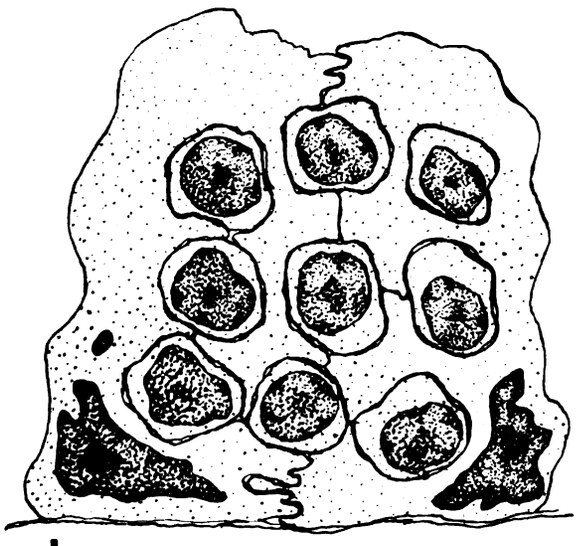

b

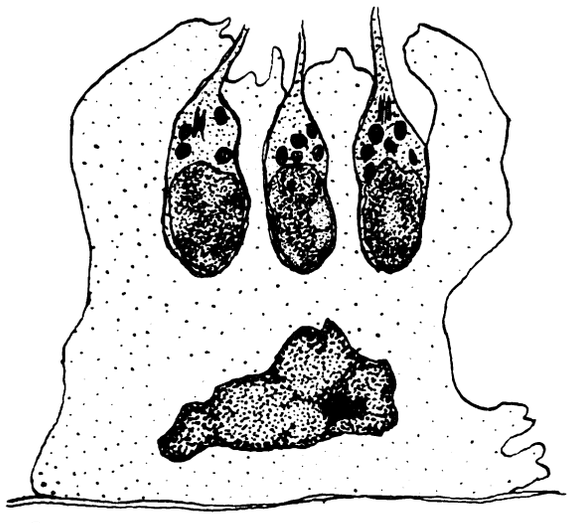

c

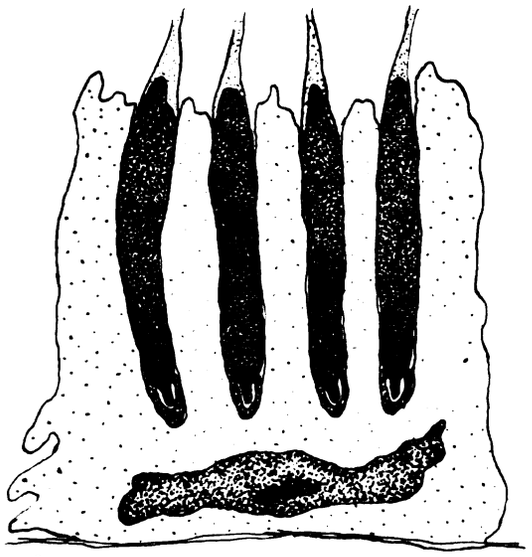

d

of the cyst, interdigitation of the follicle cell plasma membranes, often with desmosomes.

With meiosis, the follicle cells increase in size and become less dense, filling the spaces between cells of the cyst (Figure 57b). During nuclear elongation cells separate. The spermatids at this point (Figure 57c) are no longer surrounded by the follicle cells. The follicle cell cytoplasm invades the cluster of spermatids and the spermatids now interdigitate with the supportive cell cytoplasm. This is the transition stage from follicle to Sertoli cell. By the time the spermatozoa have matured, the Sertoli cells have fully elongated (Figure 57d). The sperm will remain embedded in the Sertoli cell until spermiation the following spring.

Follicle Cells--Figure 56a shows a portion of a spermatocyst containing two follicle cells surrounding a type 2 primary spermatogonium. The nuclei of the follicle cells are dense with small lobes. Chromatin has condensed along the nuclear periphery. Some condensation is visible in the interior of the nucleus and a single nucleolus is evident. The cytoplasm is very dense along the basement membrane but fades to an almost artifactual-like clearness at the apical end. Arrows indicate the apposing plasma membranes in the apical region.

Figure 56b shows a similar arrangement around a spermatogonium on one side of the micrograph and

spermatocytes on the other. These cysts are separated by a portion of Sertoli cell cytoplasm, characterized by microtubules and desmosomes. Notice that all three cells are in contact with the basement membrane.

The cytoplasm of the follicle cell often becomes very thin in areas around the cluster (Figure 58a). Often, finger-like projections are seen extending into the adjacent follicle or Sertoli cell cytoplasm and into the areas between the germinal cells. Glycogen particles are visible and can often be used as an aid for distinguishing follicle cell cytoplasm. Mitochondria are oblong and slightly larger than those of the germinal cells; the internal structure, however, is similar. Many free ribosomes, often in clusters, and a small amount of rough endoplasmic reticulam (RER) are seen (Figure 58b). In the elongating Sertoli cells a peculiar type of RER associated with mitochondria is present, the ribosomes being present only on the mitochondrial side of the reticulum.

As the Sertoli cell invades the spermatid cluster microtubules become apparent and the cytoplasm has lost much of its density (Figure 58c). A small amount of RER is still visible. The microtubules may be responsible for changing the shape from the flattened follicle cell to the elongated Sertoli cell.

Figure 58. Follicle-Sertoli cell development.

a) R. pipiens. x 16,200.

b) R. clamitans. x 10,200.

c) R. clamitans. x 15,300.

Note the follicle cells (Fc), desmosome (De), glycogen particle (G), mitochondria (M), spermatogonium (Sa), Sertoli cell cytoplasm (Sc), spermatocyte (Se), spermatid (St), rough endoplasmic reticulum (RER) and microtubules (MT).

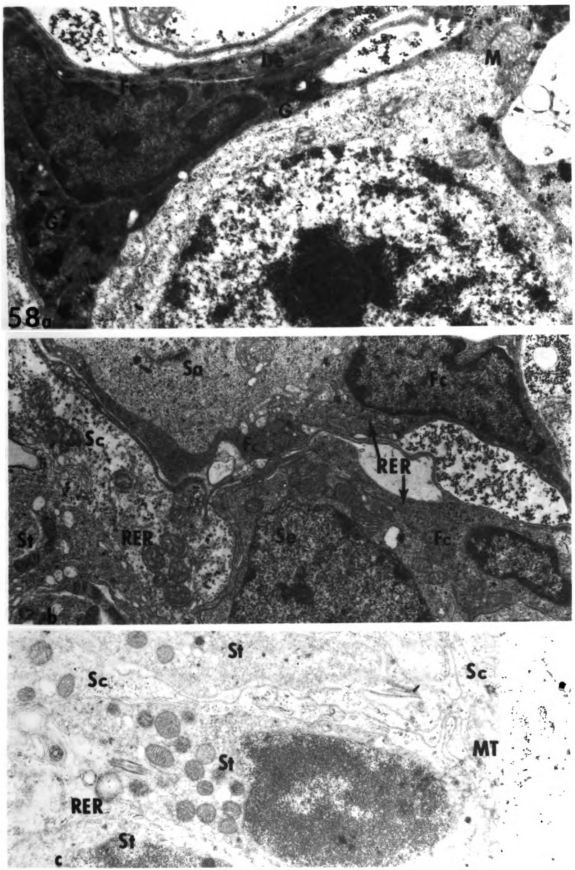
M
G
G
58a
Sa
Fc
Sc
Fc
RER
St
RER
Sb
Fc
St
Sc
Sc
St
MT
RER
St
c

Sertoli Cells--The mature Sertoli cell is a highly developed, complex structure. It was once claimed that the Sertoli cells exist as a syncytium. However, electron microscopic observations showed that each cell is bounded by its own plasma membrane (Fawcett and Burgos, 1956). The Sertoli cells provide support and protection for the sperm and may also supply nutrients; however, this has not been clearly established (Bloom and Fawcett, 1968).

The Sertoli cell nuclei are large with an irregular scalloped outline (Figure 59a and b). Chromatin is condensed along the nuclear periphery. This is more evident in Sertoli cell nuclei of R. pipiens than in those of R. clamitans. The nucleoplasm of both species has a fine granular appearance. In R. pipiens occasional clumps of chromatin are dispersed throughout the nucleoplasm. A single nucleolus is present.

The cytoplasm can be divided into two areas; the basal and apical portions. The basal portion in contact with the basement membrane contains most of the cellular organelles, including the nucleus, mitochondria, lipid droplets, Golgi elements, lysosome-like structures, microtubules, tonofibrils, glycogen, endoplasmic reticulum and microtubules. The sperm heads lie in the area of transition between these two areas. The acrosomes lie near the Sertoli cell nuclei and the sperm tails extend into the lumen.

Figure 59. Sertoli cells.

a) R. clamitans. x 5,000.

b) R. pipiens. x 6,000.

c) R. clamitans. x 10,200.

Note the Sertoli cell nuclei (Scn), glycogen particles (G), lipid vacuoles (Li), mitochondria (M), Sertoli cell plasma membrane interdigitations (In), microtubules (MT), rough (RER) and smooth (SER) endoplasmic reticulum and a lysosome-like body (Ly).

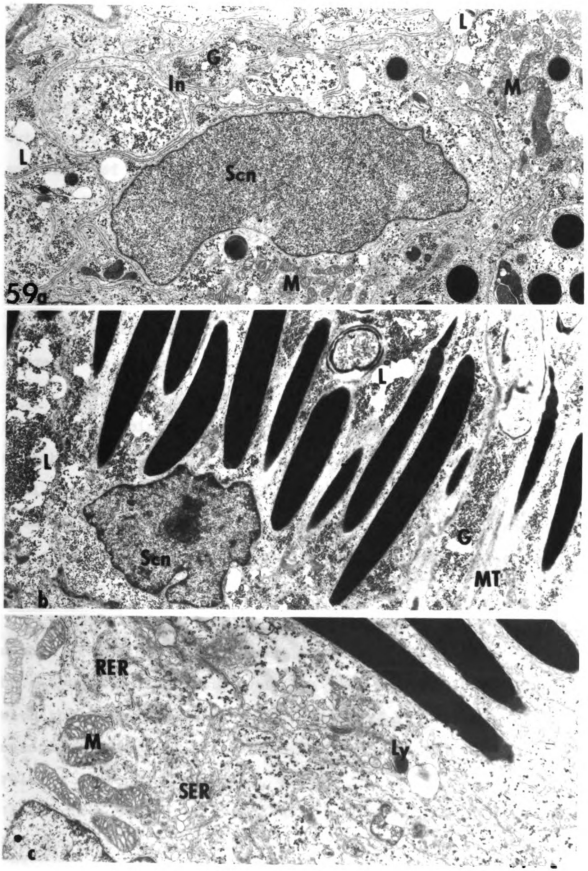
L
G
In
M
L
Scn
M
59a
L
L
Scn
G
MT
b
RER
M
Ly
SER
c

The intercellular spaces between the sperm and Sertoli cells are generally irregular without any associated specialization of the plasma membranes or adjacent cytoplasm, except possibly the connection noted in forming acrosomes of R. pipiens (see Figure 53d and 3). In mammals Brökelmann (1963) and Nicander (1967) described peculiar surface modifications of the Sertoli cell plasma membrane in the area in association with the acrosome which appears as a sheath of higher electron density than the rest of the Sertoli cell cytoplasm. Brökelmann (1963) suggests it may play a role in sperm release.

Rough endoplasmic reticulum is scarce and usually found in association with the mitochondria (Figure 59c). Smooth endoplasmic reticulum is found throughout the whole cell (Figures 59c and 61b). In the toad (Burgos and Vitale-Calpe, 1967A) a large amount of smooth endoplasmic reticulum is responsible for the "spongy-like" appearance of the basal portion of the cell.

Golgi elements are usually found between the nuclei of the Sertoli cell and acrosomes (Figure 60a and b). Lysosome-like structures are seen both in association with the Golgi-elements (Figure 60b) and free in the cytoplasm (Figure 61d). Lysosomes may function in sperm release (Burgos and Mancini, 1948). Nieni and Kormano (1965) have described a high acid phosphatase activity in the apical portion of rat Sertoli cells at the time of

Figure 60. Sertoli cell, basal region 1.

a) R. pipiens. x 17,400.

b) R. clamitans. x 42,000.

c) R. clamitans. x 42,000.

Note the Golgi elements (GE), acrosomes (A), Sertoli cell nuclei (Scn), glycogen (G), mitochondria (M), inclusion body (Ib) and lysosome-like bodies (Ly).

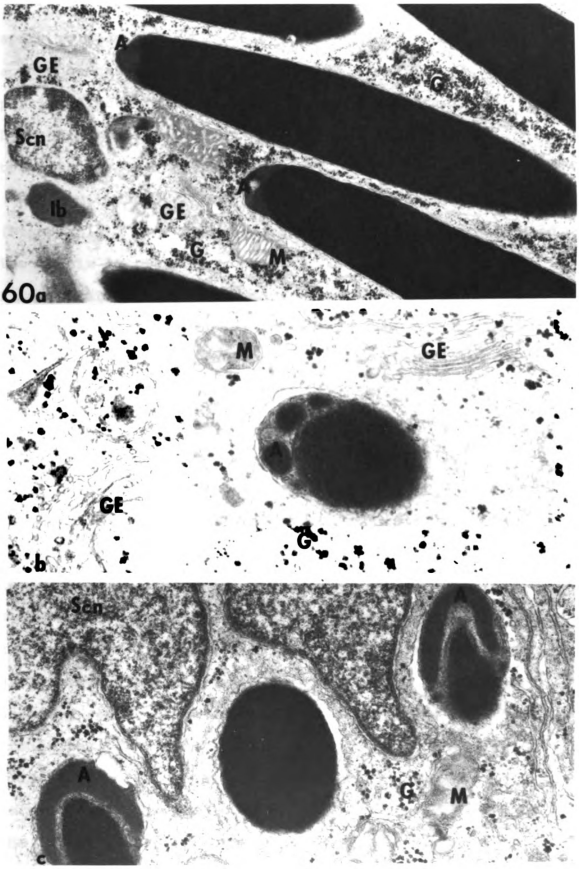

rosomes (A),
gen (G),
(Ib) and

sperm release. Burgos (1955) finds that the amounts of acid phosphatase in R. pipiens Sertoli cells vary with pituitary activity and thus with the spermatogenetic cycle. Lysosomes may also be involved in degrading residual cytoplasm or degenerating germinal cells.

Mitochondria are oblong and up to 2 μm in length (Figure 61a). The cristae are tubular and highly branched. The matrix is clear. Brökelmann (1964) finds in R. temporaria that mitochondria tend to clump around the nucleus, especially during the mating season. Similar clumping was noted in R. clamitans (Figure 59a) but not in R. pipiens Sertoli cells (Figure 59b).

Lipid vacuoles in various stages of degradation by fixation procedures are seen in the basal portion and lower portion of the apical region in the Sertoli cells in both species (Figure 61a and b). Lofts (1964) and Lofts and Boswell (1960) have described cyclic changes in the amounts of lipids in R. esculenta and R. temporaria Sertoli cells. These authors find very little lipid in the testes of frogs actively engaged in spermatogenesis or in hibernating animals. However, just prior to the breeding season, a sharp rise in the amount of lipids is visualized. These lipids are released into the lumen at spermiation. In the mammalian Sertoli cell, Nieni and Kormano (1965) (also see Mann, 1964) have evidence that the lipids accompany developing spermatids to the apical

Figure 61. Sertoli cell, basal region 2.

a) R. pipiens. x 26,100.

b) R. clamitans. x 26,100.

c) R. pipiens. x 57,000.

d) R. pipiens. x 26,100.

Note the inclusion bodies (Ib), lipid vacuoles (Li), acrosomes (A), smooth endoplasmic reticulum (SER), microtubules (MT), tonofibrils (T), and a lysosome-like body (Ly).

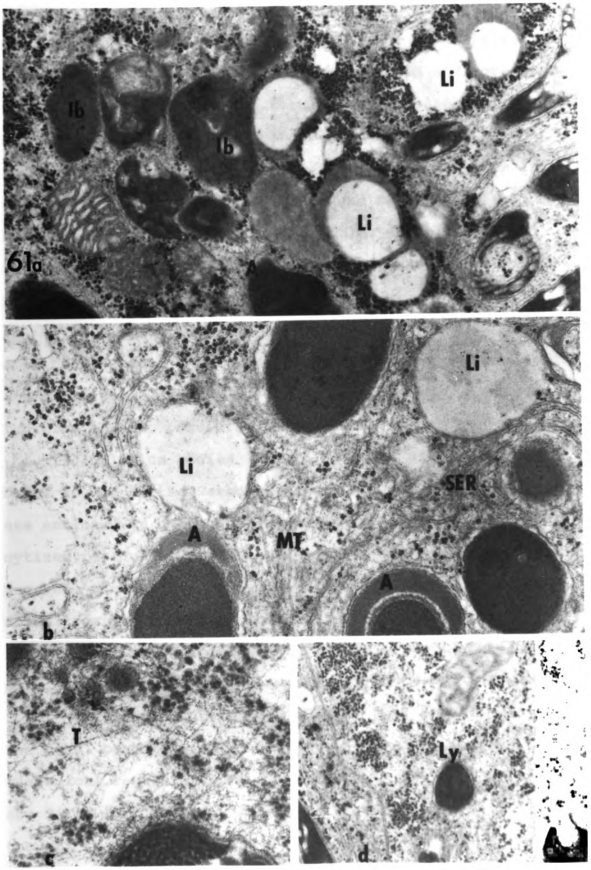
Ib
Ib
Li
Li
61a
Li
Li
SER
A
MT
A
b
T
c
Ly
d

portion of the Sertoli cell. These lipids are released into the lumen. Later some are phagocytized and move back toward the periphery of the tubule. Lacy (1960), Brökelmann (1963) and Lynch and Scott (1951) suggest that in mammals at least some of these lipids may function in steroid hormone production. Bloom and Fawcett (1968) suggests that the presence of agranular endoplasmic reticulum in the Sertoli cell may be evidence for steroid production.

A similar proposal may be made for the lipids in amphibian Sertoli cells. However, since most of the lipids are eliminated into the lumen with spermiation, a nutrient function is also possible (Burgos, 1955).

Inclusion bodies (Figure 61a) are visible in the basal region of the Sertoli cells. Some of these inclusions are enclosed in membranes and may be portions of phagocytized residual cytoplasm or degenerating germinal cells. However, since these bodies have not been observed in the apical portion of the Sertoli cell where phagocytosis of residual cytoplasm should occur, it is believed they are portions of degenerating germinal cells.

Although microtubules (Figure 61b) are present in the basal portion of the cell, they are more apparent in the apical region (Figure 62b and c). Since microtubules are first seen in the elongating Sertoli cell, they are thought to function in the extension of and, later, for

Figure 62. Sertoli cell, apical region.

a) R. clamitans. x 4,000.

b) R. pipiens. x 17,400.

c) R. pipiens. x 15,300.

Note the sections through four levels (1, 2, 3, 4) of the apical region of Sertoli cells. Also note in b and c the direction of the microtubules (MT).

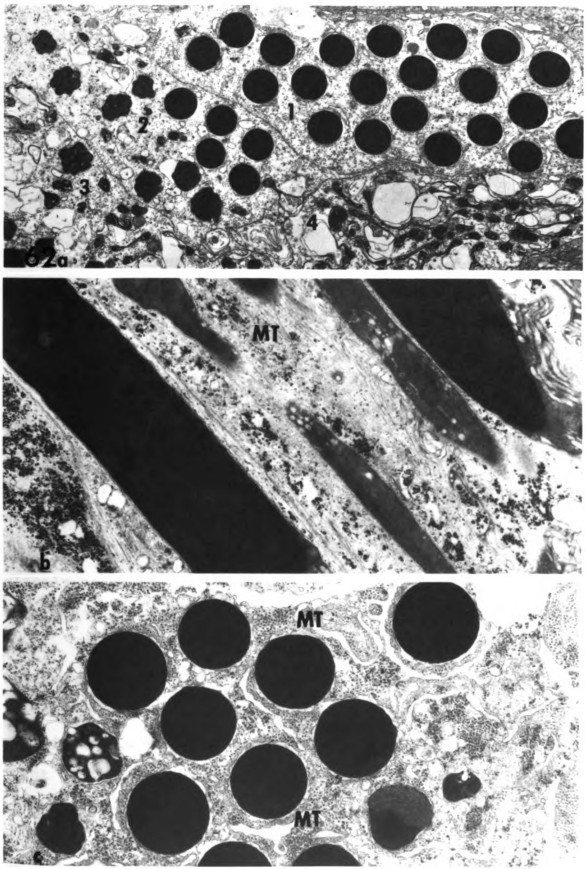
1
2
3
4
a
MT
b
MT
MT
c

the maintenance of the columnar type Sertoli cell. Tonofibrils, approximately 5.0 nm in diameter, are also seen in the basal region (Figure 61c).

The apical portion of the Sertoli cells is considerably less dense than the basal portion due its lack of organelles. Figure 62a shows the apical region of four Sertoli cells in cross section at various distances from the base (1) being the most basal and (4) the most apical region.

Microtubules lie in a plane parallel to the long axis of the sperm and in cross section appear to encircle the sperm cells (Figure 62c). A small amount of smooth endoplasmic reticulum is present, often with dilated sacs attached.

Glycogen is dispersed through out the cytoplasm of the Sertoli cells. No intranuclear glycogen as described by Brökelmann (1964) was seen. Glycogen is often closely associated with lipid vacuoles (Figure 61a) and outlines the sperm embedded in the Sertoli cell.

Sustentacular cells maintain a close relationship with each other. Interdigitations of plasma membranes (Figure 59a) of neighboring cells and specialized attachment devices such as desmosomes (macula adherens) and tight junctions are visible (Figure 63) at the basal region of the cells. Tight junctions are more common in

Figure 63. Attachment devices.

a) R. pipiens. x 81,000.

b) R. clamitans. x 57,000.

Noted in (a) the dense border of the desmosomes (Db), plasma membranes (PM), the two sets of fibrils (1 + 2) and the fusion (f) of the two outer sets of fibrils. Arrows indicate areas between desmosomes.

In (b) note the tight junctions (TJ), plasma membranes (PM), microtubules (MT) and glycogen particles (G).

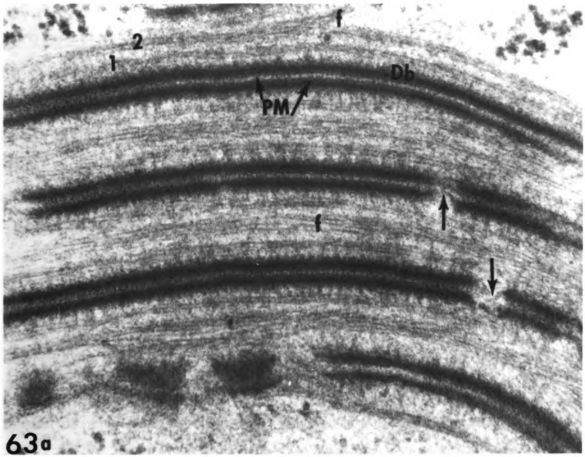
1
2
f
Db
PM
f
6.3a

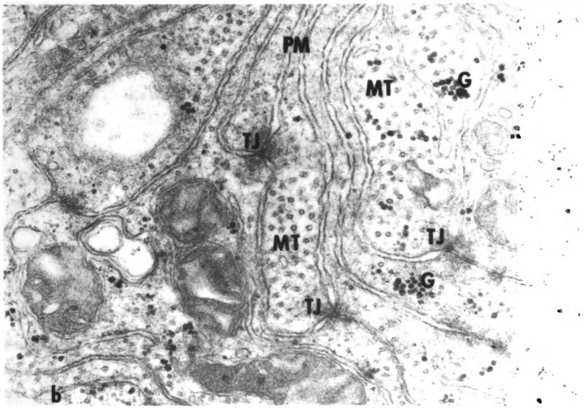
PM
MT
G
TJ
MT
TJ
G
TJ
b

R. clamitans testes while desmosomes are more prominent in R. pipiens.

In both species the space between apposing cell membranes measures 15 to 22 nm wide. In the area of the tight junction (Figure 63b) the space narrows to 7.0 nm. Densely staining cytoplasm is closely applied to the tight junction.

Desmosomes vary in length from 0.25 to 2.0 μm (Figure 63a) and separate the membranes by a space 20 to 22 nm wide. However, between linearly arranged desmosomes the plasma membranes seem to touch (arrows). Dense fibrous-like material fills the intercellular spaces in areas of the desmosomes. An extremely dense border lines the inner portion of the cell membranes. Adjacent to the dense border of the desmosomes are two sets of fibrils (1 + 2). The outer set fuses in areas of closely packed desmosomes. Each fibril is approximately 90 nm in diameter.

Intranuclear Inclusions

Intranuclear inclusions of various types have been described at the ultrastructural level in numerous plant and animal cells in both normal and pathological states (Caramia et al., 1967; Krishan et al., 1967; Jones and Fawcett, 1966; Popoff and Stewart, 1968 and Brökelmann, 1964). At the electromicroscopic level inclusions are

seen in the spermatozoa both of invertebrates (Longo and Anderson, 1969 A&B; Phillips, 1966; Kessel, 1967) and vertebrates (Baker, 1966; Hadek, 1969 A&B; Anberg, 1957). Inclusions appear with such regularity in published pictures of spermatozoa that they are seldom labeled. In most cases they appear as homogeneous, small electron-transparent areas. Fawcett (1958) called them chromatin defects. Unlike cytoplasmic vacuoles they are not bounded by a membrane but appear as cavities in the condensed chromatin.

The significance of these inclusions is not known. Gatenby and Beams (1935) considered them as possible hydrostatic organs or respiratory vacuoles. Shnall (1952) observed vacuoles opening at the surface of the head and suggested that they may be eliminating gaseous end products of metabolism. Vacuoles do occur in the spermatozoa of normal males of proved fertility (Fawcett, 1958). Thus it may be that these vacuoles arise through mishaps in chromatin consensation and have no function per se.

Intranuclear inclusions of varying substructure, size, density and shape are observed in some spermatids and spermatozoa of both species studied there. Some inclusions are characterized by electron-transparent matrices speckled with material of higher density (Figure 64a and b). Other types of inclusions include glycogen particles (Figure 64g), tubules (Figure 64e),

Figure 64. Intranuclear inclusions, spermatids.

a) R. clamitans. x 26,100.

b) R. clamitans. x 26,100.

c) R. clamitans. x 15,300.

d) R. pipiens. x 30,000.

e) R. pipiens. x 26,100.

f) R. pipiens. x 63,000.

g) R. pipiens. x 10,200.

rmatids.

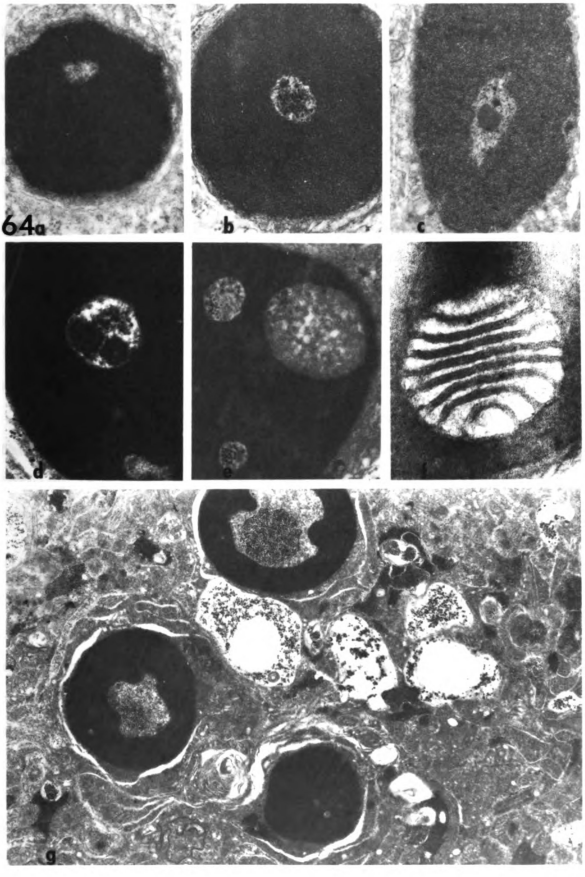

Figure 64. Intranuclear inclusions, spermatids.

a) R. clamitans. x 26,100.

b) R. clamitans. x 26,100.

c) R. clamitans. x 15,300.

d) R. pipiens. x 30,000.

e) R. pipiens. x 26,100.

f) R. pipiens. x 63,000.

g) R. pipiens. x 10,200.

ermatids.

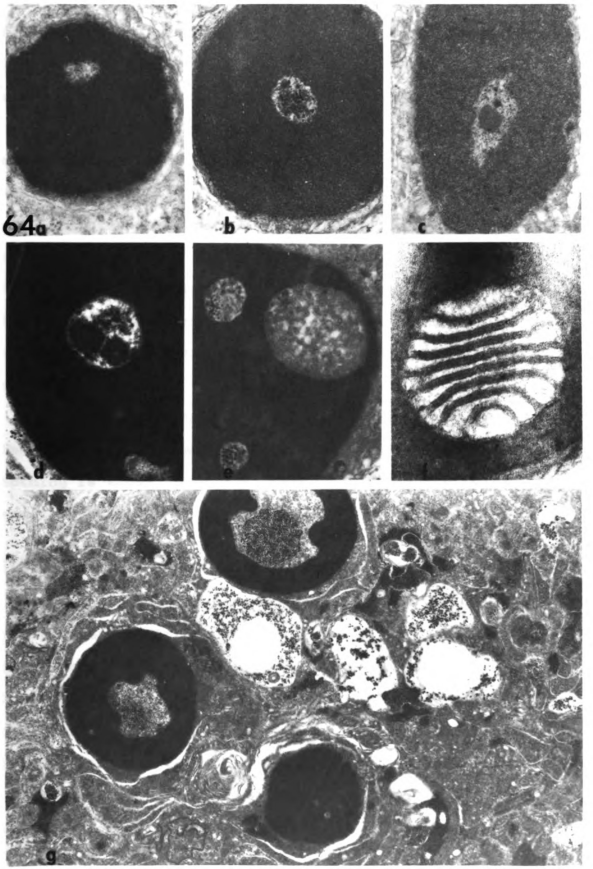

homogeneous bodies (Figure 64c and d) and mitochondrial-like bodies (Figure 64f). Hadek (1969B) reported tubular whorls in normal appearing nuclei of hamster spermatids.

With the elongation of spermatid nuclei the small areas of incomplete compaction are still visible (Figure 65a and b). The glycogen may have condensed into small tightly-dense packets (Figure 65d and e). With osmium fixation the glycogen has a "washed out" appearance (Figure 65e). Notice that there is no membrane surrounding the glycogen packets. Areas of tightly packed fibrils (Figure 65b) and heterogeneous inclusions (Figure 65c) are still visible.

Other than the fact that some inclusions are in fact glycogen (see section entitled "Histochemistry") nothing is known about how these inclusions are formed or how they function.

Histochemistry

Glycogen--Burgos (1955) described glycogen (PAS-positive material) in R. pipiens testes as granules in the apical region of the Sertoli cell, as globules in the tubular lumen and in minute traces on the surface of the spermatocytes. Cavazos and Melampy (1959), trying to trace acrosome formation in R. pipiens by the PAS technique, described a heavy concentration of glycogen localized within the tubules and "dispersed throughout all cell

Figure 65. Intranuclear inclusions, spermatozoa.

a) R. clamitans. x 7,500.

b) R. clamitans. x 25,000.

c) R. pipiens. x 33,000.

d) R. pipiens. x 33,000.

e) R. pipiens. x 33,000 (osmium fixed).

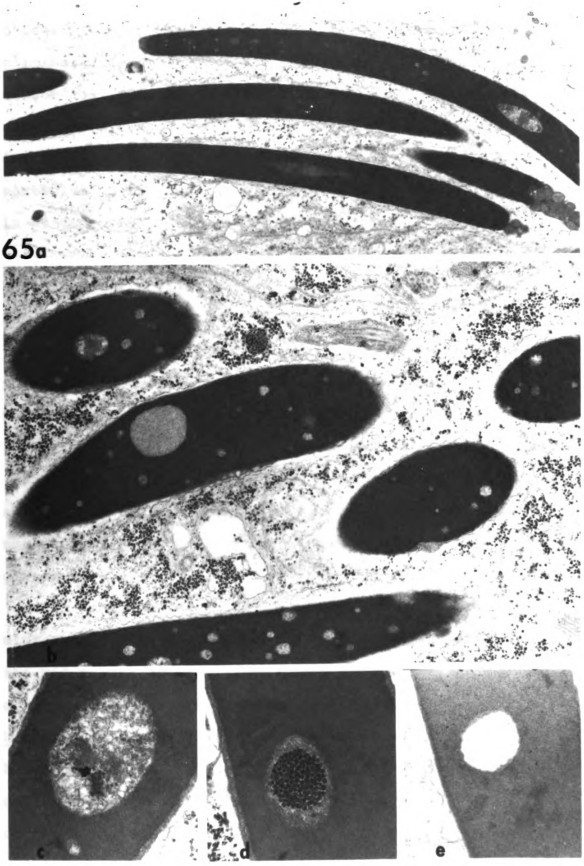

rmatozoa.

ım fixed).

types." They showed PAS-positive beads, which were eliminated by amylase treatment, in the acrosomal portion of the cell and one to three such beads in linear array along the sides of the sperm heads. Brökelmann (1964) described at the ultrastructural level glycogen-like particles in the nucleus and cytoplasm of Sertoli cells in R. temporaria.

The toad is said to have PAS-positive mucoprotein in the Sertoli cells, rather than glycogen (Mancini and Burgos, 1948).

Glycogen has been described in the seminiferous tubules of deer (Wislocki, 1961), man (Montagna and Hamilton, 1952) and rats and guinea pigs (Vilar et al., 1962). Clermont and Leblond (1955) and Cavazos and Melampy (1959) have described PAS-positive material in the forming acrosomes of a large number of mammals. This material is not sensitive to amylase and is thus not thought to be glycogen.

Anderson and Personne (1969) have, at the electron microscopic level, been able to show glycogen particles in the mid-pieces and tails of mature spermatozoa in a number of phyla from Plathyhelminthes to the Chordates. R. pipiens, one of the two amphibians used in this study, had perimitochondrial glycogen deposits. Amongst the other Chordates no spermatozoal glycogen was found in any of the reptiles, birds, or mammals studied.

Restivo and Reverberi (1957) showed by biochemical analysis the presence of 1.5 to 3.0% glycogen, on a dry weight basis, in the sperm of two ascidians, Ciona and Phallusia.

With PAS technique at the light microscopic level and the PA-TSG-SP technique at the ultrastructural level, glycogen has been located in the Sertoli cells, spermatids, spermatozoa, residual cytoplasm and tubular lumen of both species studied here.

Figure 66a and b are light micrographs of PAS-positive material in the seminiferous tubules. At the electron microscopic level, Figure 67 shows portions of Sertoli cells treated with PA-TSC-SP. The glycogen particles are deeply stained. Positive material is visible throughout the Sertoli cell cytoplasm as various sized clumps. It is also visible in the mid-piece and at the sperm plasma membrane (Figure 67b). Positive material is also visible as intranuclear inclusions (Figure 68a), in the acrosome of R. pipiens spermatozoa (Figure 68b) and in the residual cytoplasm (Figure 68c).

Amylase-PA-TSC-SP-treated controls (Figure 69) show lack of staining of the intranuclear, residual cytoplasmic and Sertoli cell glycogen. Figure 70 are TSC-SP controls showing the lack of contrast of the glycogen particles.

Figure 66. Light micrographs, PAS-positive material.

a) R. pipiens. x 1,500.

b) R. clamitans. x 400.

Note pinkish PAS-positive material. Arrow indicates acrosomal granule. a was counter-stained with toluidine blue.

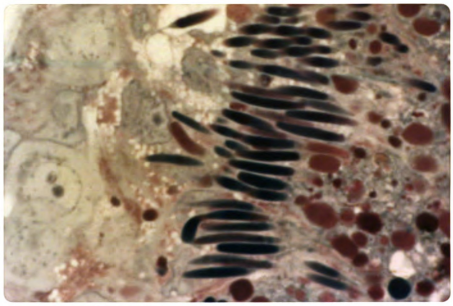

66a

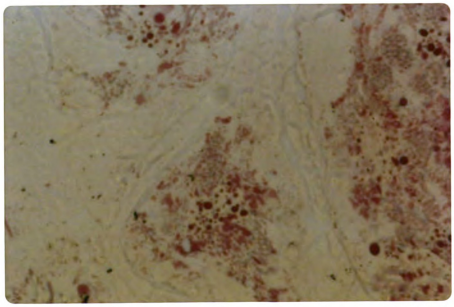

b

Figure 67. Sertoli cell glycogen.

a) R. pipiens. x 17,400.

b) R. clamitans. x 17,400.

Note the glycogen (G) scattered throughout the Sertoli cell cytoplasm, in portions of the mid-piece (MP), tail (T) and at the sperm plasma membrane (arrows). Spermatozoa nuclei (N) are also visible.

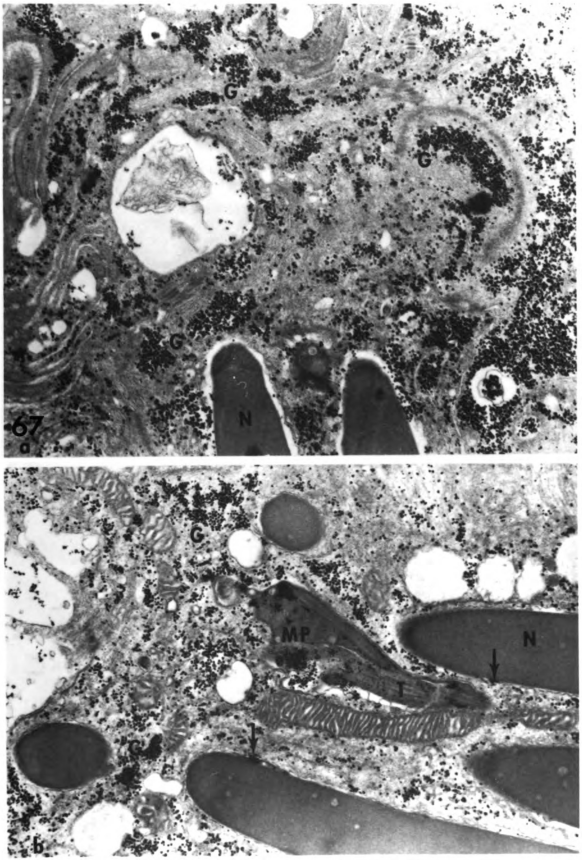
G
G
G
N
67
a
G
MP
T
N
b

Figure 68. Intranuclear, acrosomal and residual cytoplasmic glycogen.

a) R. clamitans. x 22,200.

b) R. pipiens. x 33,000.

c) R. pipiens. x 10,200.

Note the glycogen in the acrosome (A) of a R. pipiens spermatozoon, in the residual cytoplasm (Rc), Sertoli cell cytoplasm (Sc) and as inclusion bodies (I) in the sperm nuclei (N).

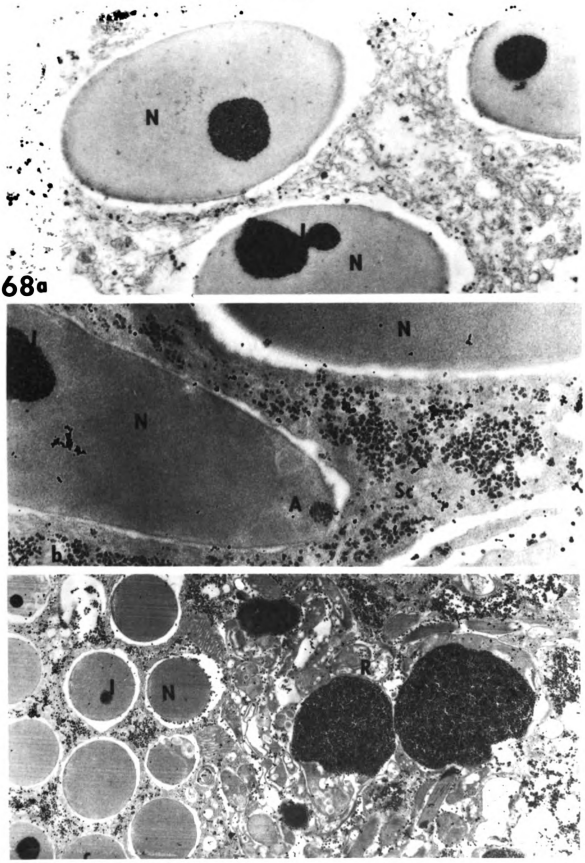
N
N
68a
N
N
A
Sc
b
N
R

Figure 69. Amaylase-PA-TSC-SP controls.

a) R. clamitans. x 17,400.

b) R. pipiens. x 10,200.

Note the lack of staining in the Sertoli cell cytoplasm (Sc), residual cytoplasm (Rc) and the intranuclear inclusions (I).

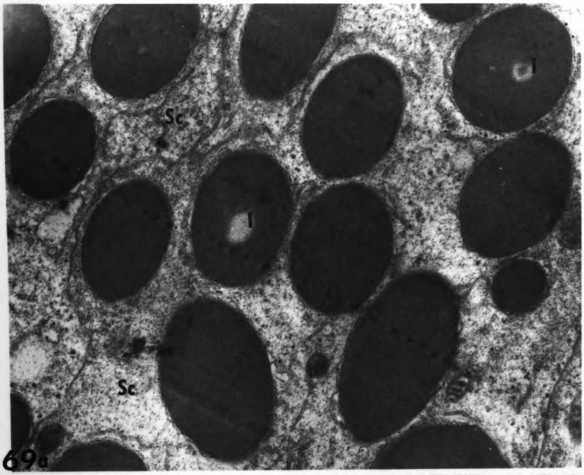

69a

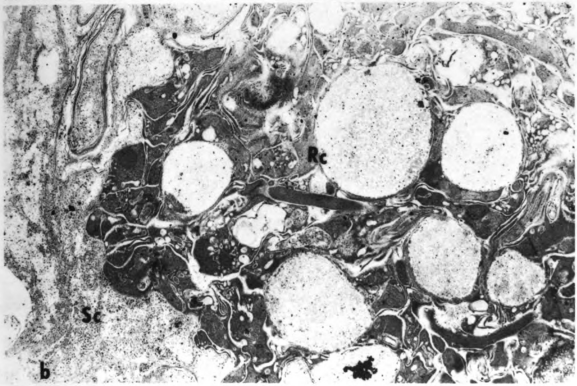

b

Sertoli cell
(Rc) and

Figure 70. TSC-SP controls.

a) R. pipiens. x 10,200.

b) R. clamitans. x 22,200.

c) R. pipiens. x 10,200.

Note the lack of contrast in the glycogen particles in the residual cytoplasm (Rc), in the inclusions (I) in the nucleus (N) and in the Sertoli cell cytoplasm (Sc).

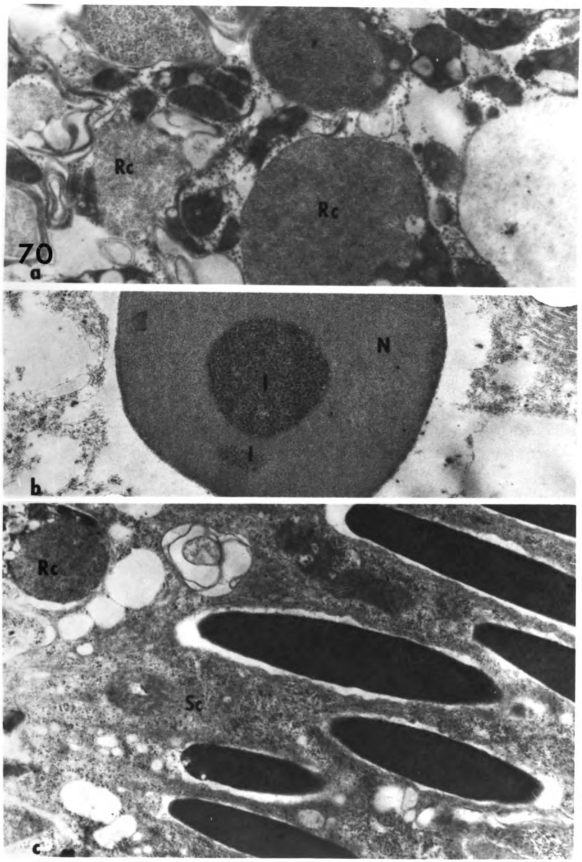

n the glycogen
ytoplasm (Rc), in
ucleus (N) and in
Sc).

There seems to be little doubt, due to the staining characteristics, size, appearance, and reaction to specific inhibitors, that the material described here is, in fact, glycogen.

Significance of Testicular Glycogen--The glycogen in the acrosome of R. pipiens spermatozoa may indicate an immature state of development. It is well known that a PAS-positive material, although not believed to be glycogen, is present in the forming mammalian acrosome (Clermont and Leblond, 1955 and Cavazos and Melampy, 1959). Since R. pipiens acrosome formation appears to take place on compacted, elongated nuclei, a dissolution of this PAS-positive material may take place before final maturation (see section entitled "Acrosomes of R. pipiens Spermatozoa" p. 145). The difference in chemical composition of the PAS-positive material in mammals and that in R. pipiens acrosomes may well be due only to species variation.

Glycogen in the sperm nucleus has not been previously described. However Brökelmann (1964) has described a pocket of glycogen-like material in the Sertoli cell nuclei of R. temporaria. Caramia et al. (1967) described intranuclear glycogen in liver cells from patients with diabetes. No specific function, other than storage, can be suggested at this time for the dense pocket of intranuclear glycogen in the sperm cells.

The glycogen in the mid-piece of mature spermatozoa may function as a source of energy for metabolism and mobility since frog sperm are ejaculated into an aqueous medium presumably lacking in metabolic substances. Evidence of an active phosphorylase and the presence of glycogen in the mid-pieces of the Gastropod (Helix) sperm (Personne and Anderson, 1969) and of glucose-6-phosphatase in glycogen-containing mitochondria (Anderson, 1968) of sea urchin sperm suggests that these enzymes may, at least in these species, be utilized in glycogen metabolism.

Anderson and Personne (1969) point out that since survival time of spermatozoa in storage organs varies among species, spermatozoa must be capable of surviving under conditions of high sperm density and low oxygen tensions. These conditions are what one would expect in the seminiferous tubules of hibernating frogs. These authors suggest that spermatozoal survival under these conditions may depend on anaerobic utilization of energy-rich substances. This may be the reason why frog spermatids make, package and eliminate into the lumen large quantities of glycogen. These "stores" of glycogen may then be used during hibernation. The fact that "stored" glycogen swells (see Figure 44) may indicate a hydrolysis of the glycogen into glucose. The glucose may then be used in anaerobic glycolysis as is fructose in mammalian

seminal fluid. However, no studies on the seasonal variations of glycogen have been done to substantiate such a suggestion.

Sertoli cell glycogen increases during active spermatogenesis (Brökelmann, 1964) and may function as an energy source for the Sertoli cell during the winter months. In amphibians, at spermiation, the whole (Burgos and Ladman, 1957 and Loft, 1964) or portions of (Burgos and Vitale-Calpe, 1967B and van Oordt et al., 1954) the Sertoli cell, and thus the remaining glycogen, are eliminated with the sperm. This glycogen, along with any remaining tubular glycogen, may make up a portion of the seminal plasma and be a source of metabolities while the sperm are in the seminal vesicles. It is in these vesicles, in some species that the spermatozoa are briefly stored prior to amplexus (Rugh, 1951).

Non-specific acid and alkaline phosphatases have been localized in R. clamitan spermatozoa.

Acid Phosphatase--Although the preparation leaves much to be desired in its technical aspects, certain characteristics are apparent. Acid phosphatase activity is associated with the inner and outer acrosomal membranes (Figure 71a and b). The acrosome proper, however, shows no activity. The sperm plasma membrane, nuclear membranes, mid-pieces and tails also show no activity under the

Figure 71. Acid phosphatase, R. clamitans.

a) experimental. x 33,000.

b) experimental. x 33,000.

c) experimental. x 26,100.

d) control. x 26,100.

Note in a and b the deposits on the inner aspects of the acrosomal (A) membranes and the lack of specific localized deposits in the nucleus (N), mid-piece (MP) and tail (T). A control (d) shows no deposits in the acrosome (A) or nucleus (N).

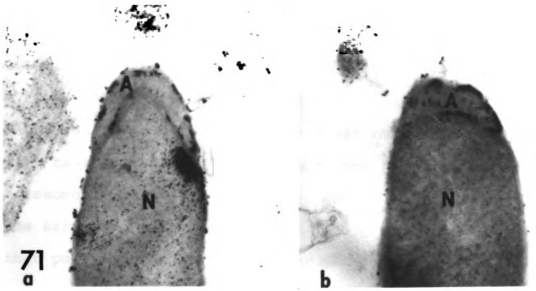
A
N
71
a
A
N
b

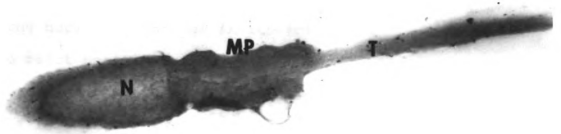
MP
T
N
c


N
d

conditions used in this study (Figure 71c). No specific localizations were observed in the control (Figure 71d).

Alkaline Phosphatase--Most of the alkaline phosphatase activity in the acrosomal region is associated with that part of the nuclear membrane in proximity to the acrosome (Figure 72a, b and c). Activity is also found in the acrosomal membranes (Figure 72a, b and c) and possibly that portion of the sperm plasma membrane covering the acrosome (Figure 72a).

In the mid-piece region the centrioles and the tubules of the axial filaments show activity (Figure 72d and e). The outer mitochondrial membrane and that portion of the nuclear membranes in contact with the mid-piece also react positively.

No specific localization was observed in the controls (Figure 72f and g).

Gordon and Barrnett (1967) described in the rat and guinea pig spermatozoa both alkaline and neutral phosphatases on the outer mitochondrial membrane. Anderson (1968), studying sea urchin sperm, finds alkaline phosphatase activity in the mitochondria of the mid-piece. Anderson suggests an autolytic role for the phosphatases, serving to break down endogenous nutritional reserves, phospholipids and proteins, for energy production. He also suggests that these enzymes may function in autolysis of the mitochondria after fertilization.

Figure 72. Alkaline phosphatase, R. clamitans.

a) experimental. x 42,000.

b) experimental. x 42,000.

c) experimental. x 42,000.

d) experimental. x 22,000.

e) experimental. x 33,000.

f) control. x 42,000.

Note the deposits on the acrosomal membrane (AM) and nuclear membrane (NM) in (a), (b), and (c). The sperm plasma membrane shows signs (arrow) of activity. Activity (d + e) is also present on the centrioles (C) and axial filament (AF) and on the outer mitochondrial membranes (MM). The controls (f + g) show no deposits.

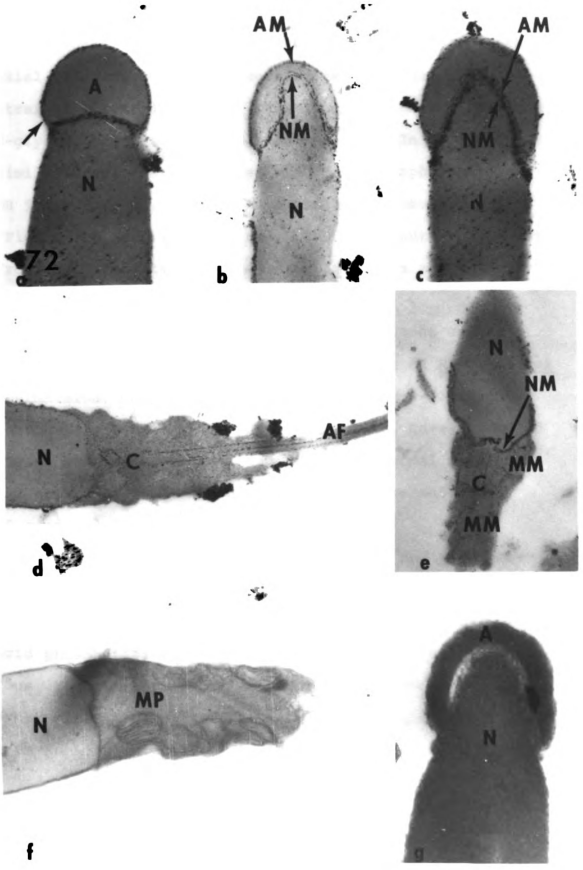
A
N
a
AM
NM
N
b
AM
NM
N
c
N
C
AF
d
N
NM
MM
C
MM
e
N
MP
f
A
N
g

Gordon and Barrnett (1967) found, on the peripheral axial filament doublets, reaction products deposited "as straight linear densities" when reacted with ATP (but not β-glycerolphosphate) and Mg++ at pH 7.0. In R. clamitans similar results are obtained with β-glycerophosphate at pH 9.0. However, in this case the inner tubules (Figure 72d) are also stained. The above authors suggest from their results that the outer filaments are actively involved in the bending of the flagellum.

There exist on the acrosomal membranes and at least on portions of the nuclear membranes of R. clamitans spermatozoa, enzymes capable of catalyzing β-glycerol-phosphate at an alkaline pH. An alkaline, Ca++-activated ATPase has been located on the inner acrosomal membrane and sperm plasma membrane of guinea pig spermatozoa (Gordon and Barrnett, 1967).

In sea urchin sperm both alkaline and acid phosphatases were found in intact and reacted acrosomes and on the plasma membrane (Anderson, 1968). In R. clamitans acid phosphatase is limited to the acrosomal membranes. Thus, the similarity of lysosomes and acrosomes noted in other material (Novikoff, 1961 and Allison, 1967) is also seen in R. clamitans.

DISCUSSION

Spermatocytogenesis and that portion of the meiotic cycle studied here are identical in the two species at the ultrastructural level. These processes also appear to conform with the published descriptions of observations at the light microscopic level (Champy, 1913; Sharma and Sekhri, 1955; Sharma and Dhindsa, 1955; Burgos and Ladman, 1955 and Glass and Rugh, 1943). Undoubtedly differences could be distinguished by other means of investigation, such as isotopic labeling studies or histochemical techniques. Since there is such a meager literature on the comparative ultrastructural aspects of these stages, their unique morphological characteristics may only become obvious after more species have been investigated.

Some structural differences do exist between the stages of spermatocytogenesis in mammals and those in the two species of Rana described here. The most obvious is the large increase in size of the type 2 primary spermatogonia. No such increase was noted in any mammalian spermatogonia studied (Gardner and Holyoke, 1964 and Nicander and Plöem, 1969A). Clermont (1970) did measure

a 3 mμ increase in the nuclear diameter of type A2 spermatogonia in the monkey. The lobed shape of the nucleus of type 2 spermatogonia is a feature common to amphibians (Champy, 1913) but is not observed in mammalian spermatogonia. It is in this stage where mitochondrial multiplication takes place, a process that seems to be associated with the dense intermitochondrial dense material. Johnson and Hammond (1963) find a 7-fold increase in the number of mitochondria in mouse spermatocytes during the first meiotic prophase. It is interesting to note that the dense intermitochondrial material is most evident in this stage of mammalian spermatogenesis.

Mammalian spermatogonia make contact with the basement membrane (Gardner and Holyoke, 1964 and Nicander and Plöem, 1969A). In these two species of Rana all germinal cells are separated from the basement membranes by follicle or Sertoli cell cytoplasm. This, however, may be an inherent difference between the cystic and non-cystic type of spermatogenesis.

Nicander and Plöem (1969A) suggest that the growth and differentiation of cytoplasmic organelles in mammalian primary spermatocytes are important introductory events in the process of spermiogenesis. These changes include increase in the number of mitochondria (Johnson and Hammond, 1963), the activity of the Golgi apparatus in the apparent formation of proacrosomal granules (Gresson and Zlotnik,

1945), the production of messenger RNA required for spermatid differentiation (Monesi, 1965) and the formation of the chromatoid body (Sud, 1961). Although some of the above phenomena occur in similar stages in these two species of Rana, evidence at the present time is too scanty to extend the suggestion of Nicander and Plöem to them.

The early stages of spermiogenesis are similar in both species studied here, but differences are encountered in acrosome formation. In R. clamitans spermatids, acrosomes are formed by the fusion of vesicles. These vesicles appear to be products of a Golgi-like cisternal element present at the anterior portion of the spermatid. This occurs before elongation and compaction of the nuclear material. In R. pipiens, acrosome formation seems to occur as a result of a series of complicated interactions (not yet completely understood) which occur in association with fully elongated, compacted nuclei. There is no indication that Golgi elements participate in acrosomal formation. It is recognized that this is contrary to the frequently cited association of the Golgi elements with acrosome formation but no other conclusion could be reached from the data available.

Burgos and Fawcett (1956) observed no conspicuous Golgi complex in the toad spermatid. They state that the Golgi material is represented by one or more small

aggregations of spherical vesicles. In differentiation of the acrosome these vesicles coalesce to form a large vesicle which later forms the acrosome.

Baker (1967) showed, at the electron microscopic level, that acrosomal formation in the salamander Amphiuma tridactylum occurs in a manner similar to that found in mammals. That is, a typical Golgi element gives rise to the acrosome.

At the light microscopic level the Golgi elements in R. tigrina spermatids appear as deeply stained granules scattered "here and there" throughout the cytoplasm (Sharma and Sekhri, 1955). Some of these granules coalesce to form a proacrosome which migrates to the anterior portion of the nucleus. The proacrosome then differentiates into the acrosome. Similar observations were made of acrosomal formation in the toad, Bufo stomaticus (Sharma and Dhindsa, 1955) except that the proacrosome forms at the anterior end of the spermatid nucleus. Champy (1913) believed that acrosomes of all amphibians are formed from an anterior group of central corpuscles. He did not suggest a Golgi-acrosome relationship.

Considering both the light and electron microscopic observations of amphibian acrosomal formation it is evident that no common mechanism exists.

Morphologically the two species have completely different acrosomes. The acrosomes of R. clamitans

spermatozoa consist of homogeneous bag-like structures, overlapping the anterior portion of the nucleus, with typical inner and outer acrosomal membranes. They are somewhat similar to the acrosomes of chicken spermatozoa (Nagano, 1962). The acrosomes of R. clamitans spermatozoa, when viewed in the light microscope, appear as a small bulge at the anterior portion of the nucleus.

In R. pipiens spermatozoa the acrosomes are situated at the most anterior portion of the nucleus with no overlap. There exists some doubt as to the structure of the mature acrosome. A large PAS- and PA-TSC-SP-positive acrosomal granule, membranous stacks and vesicles of various sizes and densities have been observed. No typical inner and outer acrosomal membranes are visible, but the membranous stacks or vesicles may be homologous to them. The acrosomes of R. pipiens spermatozoa are not clearly visible in living preparations when viewed in the light microscope.

R. pipiens spermatozoa are not the only amphibian spermatozoa with an acrosomal granule. Hirschler (see Nath, 1965) described an acrosomal "bead" in Triton spermatozoa as did McGregor (1899) for Amphiuma. Sharma and Sekhri (1955) described, using phase optics, a clear acrosomal granule in the acrosomes of living R. tigrina spermatozoa. Nath (1965) suggests that it is doubtful that such spermatozoa are fully mature.

It is interesting to note that Cavazos and Melampy (1954) did not observe a PAS-positive granule in the acrosomes of R. pipiens testicular spermatozoa. These investigators did describe one to three Schiff-positive granules in linear arrangement along side of the sperm head. In the present study, PAS- and PA-TSC-SP-positive materials are demonstrated in the acrosomes of R. pipiens spermatozoa and in the nuclei and inside the sperm plasma membrane of the spermatozoa of both species (see section entitled "Histochemistry" p. 186).

Only one published report on the ultrastructural features of anuran amphibian (Bufo arenarum) acrosomes (Burgos and Fawcett, 1956) is available. Brökelmann (1964) published a single micrograph of R. temporaria acrosomes in his study of the Sertoli cells in that species. In both of these species the acrosome appears as a flattened vesicle extending well down the elongated nucleus. Toad spermatozoa also have a perforatorium located between the acrosome and the nucleus. No such structure is visible in R. temporaria spermatozoa or in those of the two species studied here. At the light microscopic level the acrosomes of Bufo stomaticus spermatozoa resemble those of Bufo arenarum and those of R. tigrina are somewhat similar to the acrosomes of R. pipiens spermatozoa. Without ultrastructural investigations no meaningful comparison can be made. If a relationship exists between the structure of

anuran amphibian acrosomes and their taxonomic status, it is not clear from the available evidence.

The spermatozoa of both species studied here have "primitive" mid-pieces. That is, the mitochondria and centrioles are positioned close to the posterior end of the nucleus with no neck or separating juncture. The mid-pieces are inconspicuous when viewed in the light microscope. Most anuran amphibian spermatozoa have similar looking mid-pieces (Nath, 1965). Two centrioles are present and the distal one is continuous with the axial filament. The entire tail region of both species consists of the typical 9 + 2 axial filament arrangement throughout their entire length. No undulating membranes are present. The mitochondria are not fused but exist as individual organelles. The mitochondria in the mid-pieces of R. clamitans spermatozoa have many well defined cristae. In R. pipiens spermatozoa the cristae are poorly developed and scarce. This difference is interpreted as a true species variation, since the samples observed were taken from approximately the same stages in their respective spermatogenetic cycles.

A primitive type of connecting piece is present in the mid-pieces of R. clamitans spermatozoa. No similar structure is seen in R. pipiens spermatozoa. Connecting pieces have been observed in the spermatozoa of both reptilian (Austin, 1965 and Hamilton and Fawcett, 1968)

and mammalian (Fawcett, 1965) species in which they are a much more complicated structure.

The following is a summary of the differences observed between the two species of Rana and mammalian spermatogenesis.

COMPARISON OF SPERMATOGENESIS OF TWO SPECIES OF *RANA* AND MAMMALS

	R. clamitans	*R. pipiens*	Mammals
Type of spermatogenesis	cystic	cystic	non-cystic
Spermatocytogenesis			
1) largest germinal cells in tubule	type 2 primary spermatogonia	type 2 primary spermatogonia	primary spermatocytes
2) stage of mitochondrial multiplication	type 2 primary spermatogonia	type 2 primary spermatogonia	primary spermatocytes
3) intermitochondrial "cement" best developed	type 2 primary spermatogonia	type 2 primary spermatogonia	primary spermatocytes
4) polymorphic nuclei	type 2 primary spermatogonia	type 2 primary spermatogonia	primary spermatocytes
5) cytoplasmic crystalloid bodies	none observed	none observed	in human spermatogonia
6) spermatogonial cell associations	surrounded by sustentacular cells	surrounded by sustentacular cells	rests on basement membrane

continued

	R. clamitans	R. pipiens	Mammals
Premeiotic prophase			
1) sex vesicles	none observed	none observed	present
2) intercellular bridges	present	present	debate as to when they first appear
Spermiogenesis			
1) acrosome forms from	cisternal elements	?	Golgi
2) time of spermatid cluster break up	mid-spermiogenesis	late spermiogenesis	not applicable
3) elimination of the residual cytoplasm	separately from each spermatid	"en masse"	separately from each spermatid
4) fate of residual cytoplasm	eliminated into lumen	eliminated into lumen	phagocytized by Sertoli cell
5) basal plate	present	absent	present
6) first appearance of spermatid glycogen	late spermiogenesis	mid-spermiogenesis	?
7) place of final sperm maturation	testes	testes	epipidymis

continued

	R. clamitans	R. pipiens	Mammals
Mature spermatozoa			
1) structure of acrosome	homogeneous "bag"	not determined (granule, stacks or vesicles)	homogeneous "bag"
2) position of acrosome	overlaps nucleus	confined to tip of nucleus	overlaps nucleus
3) subacrosomal space	present	absent	present
4) shape of nucleus	cylindrical	cylindrical	flattened
5) mid-piece type	"primitive"	"primitive"	"elongated"
6) glycogen in mid-piece	present	present	absent
7) mitochondria	individual organelles	individual organelles	fused organelles, forming helix
8) mitochondrial cristae	many, parrallel to each other	scarce	species variations
9) connecting piece	present	absent	present
10) centrioles	proximal + distal	proximal + distal	proximal only
11) tail	9 + 2	9 + 2	9 + 9 + 2
12) annulus	absent	absent	present

SUMMARY

1) The ultrastructural aspects of spermatogenesis were studied in two species of Rana.
2) Spermatocytogenesis, that portion of the meiotic cycle studied here and the early phases of spermiogenesis are similar in the two species. These processes were compared to the similar stages described in mammals.
3) Acrosomal formation and the final structure of the acrosomes and mid-pieces are different in the two species. These variations were compared with similar published accounts of amphibian material.
4) Sustentacular cell development was studied.
5) Histochemical localization of glycogen and acid and alkaline phosphatases was carried out.

LITERATURE CITED

LITERATURE CITED

Adams, E. C. and Hertig, A. T. (1964). Studies on guinea pig oocytes. I. Electron microscopic observations on the development of cytoplasmic organelles in oocytes of primordial and primary follicles. J. Cell Biol. 21, 396-427.

Allison, A. (1967). Lysosomes and disease. Sci. Amer. 217, 62-73.

Ånberg, Å. (1957). The ultrastructure of the human spermatozoon. Acta Obst. Gynecol. Scand. 36, Suppl. 2, 1-133.

Anderson, W. A. (1968). Cytochemistry of sea urchin gametes. III. Acid and alkaline phosphatase activity of spermatozoa and fertilization. J. Ultrast. Res. 25, 1-14.

Anderson, W. A., Weissman, A. and Ellis, R. A. (1967). Cytodifferentiation during spermiogenesis in Lumbricus terrestris. J. Cell Biol. 32, 11-26.

Anderson, W. A. and Personne, P. (1970). The localization of glycogen in the spermatozoa of various invertebrate and vertebrate species. J. Cell Biol. 44, 29-51.

André, J. (1962). Contribution á la connaissance du chondrione. Etude de ses modifications ultrastructurales pendant la spermatogénèse. J. Ultrastruct. Res. Suppl. 3, 1-185.

André, J. (1963). Specializations in sperm. In "General Physiology of Cell Specialization" (D. Mazia and A. Tyler, eds.), Chap. 7 pp. 91-115. McGraw-Hill Co., New York.

Aoki, A., Vitale-Calpe, R. and Pisano, A. (1969). The testicular interstitial tissue of amphibian Physalaemus fucumaculatus. Z. Zellforsch. Mikroskop. Anat. 98, 9-17.

Austin, C. R. (1965). Fine structure of the snake sperm tail. J. Ultrast. Res. 12, 452-462.

Austin, C. R. (1968). "Ultrastructure of Fertilization." Holt, Rinehart and Winston, New York.

Baccetti, B., Dallai, R. and Rosati, F. (1970). The spermatozoa of arthropoda. J. Ultrast. Res. 31, 212-228.

Baker, C. L. (1962). Spermatozoa of Amphiuma: spermatellosis, helical motility and reversibility. J. Tenn. Acad. Sci. 37, 23-37.

Baker, C. L. (1963). Spermatozoa and spermateleosis in Cryptobranchus and Necturus. J. Tenn. Acad. Sci. 38, 1-11.

Baker, C. L. (1965). The male urogenetal system of the Salamandridae. J. Tenn. Acad. Sci. 40, 1-17.

Baker, C. L. (1966). Spermatozoa and spermateleosis in the Salamandridae with electron microscopy of Diemictylus. J. Tenn. Acad. Sci. 41, 2-25.

Baker, C. L. (1967). Spermateleosis of a salamander, Amphiuma tridactylum. Cuvier. La Cellule. 67, 92-120.

Barch, S. and Shaver, J. R. (1963). Regional antigenic differences in frog oviduct in relation to fertilization. Am. Zool. 3, 157-165.

Berg, W. A. (1950). Lytic effects of sperm extracts on the eggs of Mytilus edulis. Biol. Bull. 98, 128-138.

Blom, E. and Birch-Anderson, A. (1965). The ultrastructure of the bull sperm. Nord. Vet.-Med. 17, 193-212.

Bloom, W. and Fawcett, D. W. (1968). "A Textbook of Histology." W. Saunders Company, Philadelphia.

Bloom, G. and Nicander, L. (1961). On the ultrastructure and development of protoplasmic droplet of spermatozoa. Z. Zellforsch. Mikroskop. Anat. 55, 833-844.

Bowen, R. H. (1920). Studies on insect spermatogenesis I. The history of the cytoplasmic components of the sperm in Hemiptera. Biol. Bull. 39, 316-363.

Brökelmann, J. (1963). Fine structure of germ cells and Sertoli cells during the cycle of the seminiferous epithelium in the rat. Z. Zellforsch. Mikroskop. Anat. 59, 820-850.

Brökelmann, J. (1964). Uber die Stütz-und Zwischenzellen des Froschhodens während des Spermatogenetischen Zyklus. Z. Zellforsch. Mikroskop. Anat. 64, 429-461.

Burgos, M. H. (1955). Histochemistry of the testes in normal and experimental treated frogs (Rana pipiens). J. Morph. 96, 283-299.

Burgos, M. H. (1960). Fine structure of the basement membrane of the human seminiferous tubules. Anat. Rec. 136, 312.

Burgos, M. H. and Fawcett, D. W. (1955). Studies on the fine structure of the mammalian testes. I. Differentiation of the spermatids in the cat (Felis domestica). J. Biophys. Biochem. Cytol. 1, 287-300.

Burgos, M. H. and Fawcett, D. W. (1956). An electron microscope study of spermatid differentiation in the toad, Bufo arenarum Hensel. J. Biophys. Biochem. Cytol. 2, 223-240.

Burgos, M. H. and Ladman, A. J. (1957). The effects of purified gonadotrophins on the morphology of the testes and thumb pads of the normal and hypophysectomized autumn frog (Rana pipiens). Endocrinology. 61, 20-34.

Burgos, M. H. and Mancini, R. E. (1948). Ciclo espermatogenico anual del Bufo arenarum Hensel. Rev. Soc. Argent. Biol. 24, 328-336.

Burgos, M. H. and Vitale-Calpe, R. (1967A). The fine structure of the Sertoli cell--spermatozoan relationship in the toad. J. Ultrastruct. Res. 19, 221-237.

Burgos, M. H. and Vitale-Calpe, R. (1967B). The mechanism of spermiation in the toad. Am. J. Anat. 120, 227-252.

Caramia F., Ghergo, G. F. and Menghini, G. (1967). A glycogen body in liver nuclei. J. Ultrast. Res. 19, 573-585.

Cavazos, L. A. and Melampy, R. M. (1954). A comparative study of periodic acid-reactive carbohydrates in vertebrate testes. Am. J. Anat. 95, 467-496.

Champy, C. (1913). Recherches sur la spermatogenese des Batraciens. Arch. de Zool. 52, 13-304.

Clark, A. W. (1967). Some aspects of spermiogenesis in a lizard. Amer. J. Anat. 121, 369-400.

Clermont, Y. (1958). Contractile elements in limiting membrane of the seminiferous tubules of the rat. Exptl. Cell Res. 15, 438-440.

Clermont, Y. (1967). Cinétique de la spermatogenèse chez lez mammiferes. Arch. d'Anat. Micro. 56, 7-60.

Clermont, Y. (1970). Two class of spermatogonial stem cells in the monkey (Cercopithecus aethiops). Am. J. Anat. (in press).

Clermont, Y. and Bustos-Orbegon, E. (1968). Rexaminatron of spermatogonial renewal in the rat by means of seminiferous tubules mounted "in toto." Am. J. Anat. 122, 237-248.

Clermont, Y. and Leblond, C. P. (1955). Spermiogenesis of man, monkey, ram and other mammals as shown by the "periodic acid-shiff" technique. Am. J. Anat. 96, 229-254.

Clermont, Y. and Leblond, C. P. (1959). Differentiation and renewal of spermatogonia in the monkey, Macacus chesus. Am. J. Anat. 104, 237-274.

Clérot, J. C. (1968). Mise en evidence par cytochimie ultrastructurale de l'emission de protein par le noyaw d'auxocytes de bactraciens. J. Microscopie 7, 973-992.

Cole, F. J. (1930). "Early Theories of Sexual Generation." Oxford Univ. Press, London and New York.

Coimbra, A. and Leblond, C. P. (1966). Sites of glycogen synthesis in rat liver cells as shown by electron microscope radioautography after administration of glucose H-3. J. Cell Biol. 30, 151-175.

Dan, J. C. (1967). Acrosome reaction and lysins. In "Fertilization" (C. B. Metz and A. Monroy, eds.), Chap. 6, pp. 237-293. Academic Press, New York and London.

Daoust, R. and Clermont, Y. (1955). Distribution of nucleic acids in germ cells during the cycle of the seminiferous epithelium in the rat. Am. J. Anat. 96, 255-279.

Davenport, H. A. (1960). "Histological and Histochemical Technics." W. B. Saunders Company, Philadelphia.

DeRobertis, E. D. P., Nowinski, W. W. and Saez, F. A. (1960). "General Cytology." W. B. Saunders Company, Philadelphia.

Dietert, S. E. (1966). Fine structure of the fate of the residual bodies of mouse spermatozoa with evidence for the participation of lysosomes. J. of Morph. 120, 317-346.

Eddy, E. M. (1969). Structure and composition of the chromatoid body in spermiogenesis. Anat. Rec. 163, 181-182.

Eddy, E. M. (1970). Cytochemical observations on the chromatoid body of the male germ cells. Biol. Reprod. 2, 114-128.

Elftman, H. (1963). Sertoli cells and testes structure. Amer. J. Anat. 113, 25-33.

Fawcett, D. W. (1958). The structure of the mammalian spermatozoon. Int. Rev. Cytol. 7, 195-235.

Fawcett, D. W. (1961). Intercellular bridges. Exptl. Cell Res., Suppl. 8, 174-187.

Fawcett, D. W. (1965). The anatomy of the mammalian spermatozoon with particular reference to the guinea pig. Z. Zellforsch. Mikroskop. Anat. 67, 279-296.

Fawcett, D. (1966). "The Cell." W. B. Saunders Company, Philadelphia and London.

Fawcett, D. W. (1970). A comparative view of sperm ultrastructure. Biol. of Reprod. 2, 90-127.

Fawcett, D. W. and Burgos, M. H. (1956). The fine structure of Sertoli cells in the human testes. Anat. Rec. 124, 401.

Fawcett, D. W., Eddy, E. M. and Phillips, D. M. (1970). Observations on the fine structure and relationships of the chromatoid body in mammalian spermatogenesis. Biol. Reprod. 2, 129-153.

Fawcett, D. W. and Philips, D. M. (1967). Further observations on mammalian spermiogenesis. J. Cell Biol. 35, 152A.

Feder, N. and O'Brien, T. P. (1968). Plant microtechnique: some principles and new methods. Amer. J. Bot. 55, 123-142.

Firlet, C. F. and Davis, J. R. (1965). Morphogenesis of the residual body of the mouse testis. Quart. J. Microscop. Sci. 106, 93-98.

Flemming, W. (1880). Investigation of other materials (amphibians, mammals, plants) as regards the ubiquitous occurrence of indirect nuclear division. (as translated in--J. Cell Biol. 1965. 25, 1-69.

Franklin, L. E. (1968). Formation of the redundant nuclear envelope in monkey spermatids. Anat. Rec. 161, 149-162.

Gardner, P. J. and Holyoke, E. A. (1964). Fine structure of the seminiferous tubule of the Swiss mouse. I. The limiting membrane, Sertoli cell, spermatogonia, and spermatocytes. Anat. Rec. 150, 391-404.

Gatenby, J. B. and Beams, H. W. (1935). The cytoplasmic inclusions in the spermatogenesis of man. Quart. J. Micr. Sci. 78, 1-29.

Glass, F. M. and Rugh, R. (1944). Seasonal study of the normal and pituitary stimulated frog (Rana pipiens). I. Testis and thumb pad. J. Morph. 74, 409-428.

Gomori, G. (1956). Histochemical methods for acid phosphatase. J. Histochem. Cytochem. 4, 453-461.

Gordon, M. and Barrnett, R. J. (1967). Fine structural cytochemical localizations of phosphatase activities of rat and guinea pig. Exptl. Cell Res. 48, 395-412.

Gresson, R. A. R. and Zlotnik, I. (1945). A comparative study of cytoplasmic components of the male germ cells of certain mammals. Proc. roy. Soc. Edinb. B62, 139-161.

Hadek, R. (1969A). "Mammalian Fertilization." Academic Press, New York and London.

Hadek, R. (1969B). Intranuclear whorls in the hamster spermatid. J. Ultrast. Res. 27, 396-401.

Hamilton, D. W. and Fawcett, D. W. (1968). Unusual features of the neck and middle-piece of snake spermatozoa. J. Ultrast. Res. 23, 81-97.

Hope, J. (1965). The fine structure of the developing follicle of the rhesus ovary. J. Ultrast. Res. 12, 592-610.

Horstmann, E. (1961). Elektronenmikroskopische Untersuchungen zur Spermiohistogenese beim Menschen. Z. Zellforsch. Mikroskop. Anat. 54, 68-98.

Houssay, B. A. (1954). Hormonal regulation of the sexual function of the male toad. Acta Physiol. Latinoamer. 4, 1-41.

Johnson, H. A. and Hammond, H. D. (1963). The rate of mitochondrial increase in the murine spermatocyte. Exptl. Cell Res. 31, 608-610.

Jones, A. L. and Fawcett, D. W. (1966). Hypertrophy on the agranular endoplasmic reticulum in hamster liver induced by phenobarbital. J. Histochem. Cytochem. 14, 215-232.

Karnovsky, M. J. (1965). A formaldehyde-gluteraldehyde fixative of high osmolarity for use in electron microscopy. J. Cell Biol. 27, 137A.

Kessel, R. G. (1966). The association between microtubules and nuclei during spermiogenesis in the dragon fly. J. Ultrast. Res. 16, 293-304.

Kessel, R. G. (1966). An electron microscope study of nuclear-cytoplasmic exchange in oocytes of Ciona intestinalis. J. Ultrastruct. Res. 15, 181-196.

Kessel, R. G. (1967). An electron microscope study of spermiogenesis to the development of microtubular systems during differentiation. J. Ultrast. Res. 18, 677-694.

King, H. D. (1907). The spermatogenesis of Bufo lentiginosus. Am. J. Anat. 7, 345-387.

Kingsbury, B. F. (1902). The spermatogenesis of Desmognathus fusca. Am. J. Anat. 1, 99-135.

Krishan, A., Uzman, B. G. and Hedley-White, E. T. (1967). Nuclear bodies: a component of cell nuclei in hamster tissue and human tumors. J. Ultras. Res. 19, 563-572.

Lacy, D. (1960). Light and electron microscopy and its use in the study of factors influencing spermatogenesis in the rat. J. Rog. Microscop. Soc. 79, 209-225.

Leblond, C. P. and Clermont, Y. (1952). Definition of the stages of the cycle of the seminiferous epithelium in the rat. Ann. N. Y. Acad. Sci. 55, 548-573.

Lofts, B. (1964). Seasonal changes in the functional activity of the interstitial and spermatogenetic tissues of the green frog, Rana esculenta. Gen. Comp. End. 4, 550-562.

Lofts, B. (1969). Patterns of testicular activity. In "Perspectives in Endocrinology" (E. J. W. Barrington and C. Barker Jorgensen, eds.), pp. 239-304. Academic Press, New York and London.

Lofts, B. and Boswell, C. (1960). Cyclic changes in the distribution of testis lipids in the common frog, Rana temporaria. Nature. 187, 708-709.

Longo, F. J. and Anderson, E. (1969A). Spermiogenesis in the surf clam Spisula solidissima with special reference to the formation of the acrosomal vesicle. J. Ultrast. Res. 27, 435-443.

Longo, F. J. and Anderson, E. (1969B). Sperm differentiation in the sea urchins Arbacia punctulata and Strongylocentrotus purpuratus. J. Ultrast. Res. 27, 486-509.

Longo, F. J. and Dornfeld, E. J. (1967). The fine structure of spermatid differentiation in the mussel, Mytilus edulis. J. Ultrast. Res. 20, 462-480.

Lynch, K. M. and Scott, W. W. (1951). Lipid distribution in the Sertoli cell and Leydig cell of the rat testis as related to experimental alterations of the pituitary-gonad system. Endo. 49, 8-14.

Mann, T. (1964). "The Biochemistry of Semen and of the Male Reproductive Tract." Methuen and Co., London.

McGregor, J. H. (1899). Spermatogenesis of Amphiuma. J. Morph. 15, Suppl., 57-104.

McIntosch, J. R. and Porter, K. R. (1967). Microtubules in the spermatids of the domestic fowl. J. Cell Biol. 35, 153-173.

Metz, C. B. (1967). Gamete surface components and their role in fertilization. In "Fertilization" (C. B. Metz and A. Monroy, eds.), Chap. 5, pp. 163-263. Academic Press, New York and London.

Millonig, G. and Porter, K. R. (1960). Proc. European Regional Conf. Electron Micr., Delft, 655.

Monesi, V. (1965). Synthetic activities during spermatogenesis in the mouse. Exptl. Cell Res. 39, 197-224.

Montagna, W. and Hamliton, J. B. (1952). Histological studies of human testes. Anat. Rec. 112, 237-250.

Nagano, T. (1962). Observations on the fine structure of the developing spermatid in the domestic chicken. J. Cell Biol. 14, 193-205.

Nagano, T. (1969). The crystalloid of Lubarsch in the human spermatogonium. Z. Zellforsch. Mikroskop. Anat. 97, 491-501.

Nath, V. (1956). Cytology of spermatogenesis. Int. Rev. Cyto. 5, 394-453.

Nath, V. (1965). "Animal Gametes (Male)." Asia Publishing House, New York.

Nicander, L. (1967). An electron microspocical study of cell contacts in the seminiferous tubules of some mammals. Z. Zellforsch. Mikroskop. Anat. 83, 375-397.

Nicander, L. and Bane, A. (1966). Fine structure of the sperm head in some mammals, with particular reference to the acrosome and subacrosomal substance. Z. Zellforsch. Mikroskop. Anat. 72, 496-515.

Nicander, L. and Plöem, L. (1969A). Fine structure of spermatogonia and primary spermatocytes in rabbits. Z. Zellforsch. Mikroskop. Anat. 99, 221-234.

Nicander, L. and Plöem, L. (1969B). The chromatoid body and the "ring centriole" in mammalian spermatogenesis. J. Ultrastruct. Res. 29, 576.

Niemi, M. and Kormano, M. (1965). Cyclical changes in and significance of lipids and acid phosphatase activity in the seminiferous tubules of the rat testis. Anat. Rec. 151, 159-170.

Novikoff, A. (1960). Lysosomes and related particles. In "The Cell (J. Brachet and A. E. Mirsky, eds.) Vol. 2. Academic Press, New York.

Odor, D. J. (1965). The ultrastructure of unilaminar follicles of the hamster ovary. Amer. J. Anat. 116, 493-522.

van Oordt, G. J., Beenakkers, A. M. Th., van Oordt, P. G. W. J. and Stadhouders, A. M. On the mechanism of the initial stages of spermiation in the grass frog, Rana temporaria. Acta Endoc. 17, 294-301.

van Oordt, P. G. W. J. (1960). The influences of internal and external factors in the regulation of the spermatogenetic cycle in amphibia. In "Symposia of the Zoological Society of London No. 2" (E. J. W. Barrington, ed.) pp. 29-52. Zoological Society of London, London.

Phillips, D. M. (1966). Observations on spermiogenesis in the fungus gnat Sciara coprophila. J. Cell Biol. 30, 477-517.

Popoff, D. and Stewart, S. (1968). The fine structure of nuclear inclusions in the brain of experimental golden hamsters. J. Ultrast. Res. 23, 347-361.

Regaud, C. (1901). Etudes sur la structure des seminiferes et sur la spermatogenese chez des mammiferes. Arch. d'Anat. Microscop. 4, 101-156.

Reger, J. F. (1963). Spermiogenesis in the tick, Amblyomma dissimili, as revealed by electron microscopy. J. Ultrast. Res. 8, 607-621.

Reger, J. F. (1967). A study of the fine structure of developing spermatozoa from the oligochaete Enchytraeus albidus. Z. Zellsforsch Mikroskop. Anat. 82, 257-269.

Restivo, F. and Reverberi, G. (1957). Ricerce sugli spermi di Ciona e di Patella. Localizzazione della citochromo-ossidasi, della succino-deidrogenasi e del glicogeno. Acta Embrol. Morphol. Exp. 1, 164-170.

Reynolds, E. S. (1963). The use of lead citrate at high pH as an electron-opaque stain in electron microscopy. J. Cell Biol. 17, 208-212.

Robison, W. G. (1966). Microtubules in relation to the motility of a sperm syncytium in an armored scale insect. J. Cell Biol. 29, 251-265.

Roosen-Runge, E. C. (1962). The process of spermatogenesis in mammals. Biol. Rev. 37, 343-377.

Rugh, R. (1951). "The Frog." The Blakiston Company, Philadelphia.

Schnall, M. D. (1952). Electronmicroscopic study of human spermatozoa. Fert. and Ster. 3, 62-82.

Shaver, J. R. (1966). Immunobiological studies on the jelly coats of anuran eggs. Am. Zool. 65, 75-87.

Sharma, G. P. and Dhindsa, K. S. (1955). Amphibian spermatogenesis. II. The sperm of toad. Res. Bull. Panj. Uni. 82, 175-187.

Sharma, G. P. and Ram Parshad (1955). The morphology of chromosomes in Laccotrephes maculatus. Res. Bull. Panj. Uni. 72, 67-72.

Sharma, G. P. and Sekhri, K. K. (1955). Amphibian spermatogenesis. I. The sperm of frog. Res. Bull. Panj. Uni. 79, 145-158.

Smith, B. V. K. and Lacy, D. (1959). Residual bodies of seminiferous tubules of the rat. Nature 184, 249-251.

Solari, A. J. (1969). The evolution of the ultrastructure of the sex chromosomes (sex vesicles) during meiotic prophase in mouse spermatocytes. J. Ultrastruct. Res. 27, 289-305.

Solari, A. J. and Tres, L. A. (1970). The three-dimensional reconstruction of the XY chromosomal pair in human spermatocytes. J. Cell Biol. 45, 43-53.

Srivastava, P. N., Adams, C. E. and Hartree, E. F. (1965). Enzymatic action of lipoglycoprotein preparations from sperm acrosomes on rabbit ova. Nature 205, 498.

Sud, B. N. (1961). Morphological and histochemical studies of the chromatoid body and related elements in the spermatogenesis of the rat. Quart. J. Micro. Sci. 102, 495-505.

Sutton, W. S. (1902). On the morphology of the chromosome group in Brachystola magna. Biol. Bull. 4, 24-39.

Sutton, W. S. (1903). The chromosomes in heredity. Biol. Bull. 4, 231-251.

Swierstra, E. E. and Foote, R. H. (1963). Cytology and kinetics of spermatogenesis in the rabbit. J. Repr. Fertil. 5, 309-322.

Thiéry, J. P. (1967). Mise en évidence des polysaccharides sur coupes fines en microscopie électronique. J. Microsc. 6, 987-990.

Tres, L. L. and Solari, A. J. (1968). The ultrastructure of the nuclei and the behavior of sex chromosomes of human spermatogonia. Z. Zellforsch. Mikroskop. Anat. 91, 75-89.

Tyler, A. (1939). Extraction of an egg membrane lysin from sperm of the giant keyhole limpet (Megathura crenulata). Proc. Natl. Acad. Sci. U.S. 25, 317-323.

Tyler, A. (1967). Problems and procedures of comparative gametology and syngamy. In "Fertilization" (C. B. Metz and A. Monroy, eds.), Chap. 1, pp. 1-26. Academic Press, New York and London.

Vilar, O., Perez del Cerro, M. I. and Mancini, R. E. (1962). The Sertoli cell as a "bridge cell" between the basal membrane and the germinal cells. Histochemical and electron microscope observations. Exptl. Cell Res. 158-161.

Wada, S. K., Collier, J. R. and Dan, J. C. (1956). Studies on the acrosome. V. An egg-membrane lysin from the acrosomes of Mytilus edulis spermatozoa. Exptl. Cell Res. 10, 168-180.

Watson, M. L. (1952). Spermatogenesis in the albino rat as reveled by electron micrscopy. Biochim. et Biophys. Acta. 8, 369-374.

Weakley, B. S. (1966). Electron microscopy of the oocyte and granulosa cells in the developing ovarian follicles of the golden hamster (Mesocricetus auratus). J. Anat. 100, 503-534.

Wilson, E. B. (1925). "The Cell in Development and Heredity." Macmillan, New York.

Wimsatt, W. A., Krutzsch, P. H. and Napolitano, L. Studies on sperm survival mechanisms in the female reproductive tract of hibernating bats. Am. J. Anat. 119, 25-60.

Wislocki, G. B. (1949). Seasonal changes in the testes, epididymis and seminal vesicles of deer investigated by histochemical methods. Endo. 44, 167-189.

Zahnd, J. P. and Porte, A. (1966). Signes morphologigues de transfert de matérial nucléaire dans le cytoplasme des ovocytes de certain especes de Poissons. C. R. Acad. Sci (Paris) 262, 1977-1978.